DEFENSE DOCUMENTATION CENTER

FOR

SCIENTIFIC AND TECHNICAL INFORMATION

CAMERON STATION, ALEXANDRIA, VIRGINIA

64-12

A Final Report

A Study of Ultrasonics

for Flaw Detection in Turbojet Engines

Nondestructive Testing Study
Contract AF 34(601) — 14090
Order Number 63-2
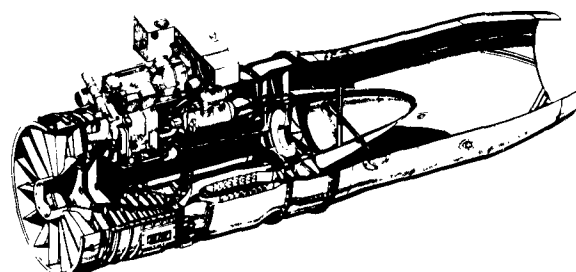
Prepared for:

Oklahoma City Air Materiel Area
Tinker Air Force Base, Oklahoma

ENGINEERING RESEARCH
OKLAHOMA STATE UNIVERSITY

Ultrasonics Laboratory
School of Mechanical Engineering
OKLAHOMA STATE UNIVERSITY
Stillwater, Oklahoma

A STUDY OF ULTRASONICS

FOR

FLAW DETECTION IN TURBOJET ENGINES

FOREWORD

The following report documents the progress made in developing ultrasonic inspection methods for compressor blades of turbojet engines. The main emphasis was placed on the development of transducers for the inspection of the compressor blades of the J-79 and J-71 engines.
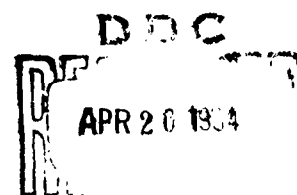
Much of the work done was concerned with the development of a usable surface wave standardization system. A unique type of calibration block was developed making possible the accurate calibration of transducers and the calibration of the reject level and gain settings of the pulse-echo system.

One section of the report deals with the effects of protective paint coatings on the efficiency of ultrasonic flaw detection of compressor blades. The remainder of the report is composed of ultrasonic cleaning studies of turbojet engine components.

PROJECT PERSONNEL

Project Leader . . . . Dr. R. L. Lowery

Faculty Associate. . . . . O'Neill J. Burchett

Research Assistants. . . . . James A. Daniel

Phillip W. Randles

James D. Simpson

James Townsend

Phillip R. Wilcox

Project Assistants . . . . Kenneth Barrett

John A. Brammer

James Earl Gray

Franklin Kay

Donald Lumadue

Jesse McIlhaney

Robert Rumbaugh

Alvin York

TABLE OF CONTENTS

THE EFFECTS OF COMPRESSOR PAINTING ON THE EFFICIENCY

OF ULTRASONIC FLAW DETECTION OF COMPRESSOR BLADES

1

PROJECT PERSONNEL

Principal Investigator   James D. Simpson

INTRODUCTION

In the future, the first few rows of compressor blades in many of the turbojet engines used by the Air Force will be painted with some type of protective high-temperature paint. This paint is expected to eliminate the oil spray procedure which is commonly being used to protect the blades from corrosive atmospheres. The paint coating will be applied approximately .001 of an inch thick, being sprayed on in most cases.

One of the types of paints which will be in common usage is manu- factured by the Glidden Company under the trade name Nubelon S. This paint is very successful in resisting ambients encountered up to 600°F, and has been documented in a test program administered by the Navy.

Along with the protective effects of the paint, it is expected that some difficulty might ensue in the ultrasonic inspection of these blades since it may be possible that the paint will attenuate surface waves to a degree as to make the ultrasonic tests insensitive. Also, it is possible that any scratch or void in the paint may have the effect of reflecting the ultrasonic wave, thus presenting the indication of a flaw where none actually exists.

The object of this study was to determine whether the Nubelon S paint, as applied according to the factory directions and specifications, will have a detrimental effect on the ultrasonic inspection of compressor blades primarily from the General Electric and Allison engines.

CONCLUSIONS

It is concluded that the painting of the forward stages of turbojet compressor blades with Nubelon S paint will cause no serious effects in the ultrasonic inspection routine. If the paint were applied to a thicker base than recommended by the manufacturer, it is possible that the surface waves would be attenuated to a degree. This is especially true of the higher frequencies, such as five megacycles or higher. However, since the most commonly used inspection frequency is 2.25 megacycles, it is thought, in general, that no difficulty of any sort should arise. Specifically, the findings of this study are as follows:

1. The addition of the Nubelon S in the recommended thickness will not seriously hinder ultrasonic inspection by surface wave pulse echo.

2. Scratches and voids in the paint will not cause serious extraneous flaw indications.

3. It is entirely unlikely that the paint coating can cover flaws in a blade to the extent that they could not be detected by ultrasonics.

EXPERIMENTAL PROCEDURE

The first set of measurements was run for the purpose of determining the effects of varying thicknesses of painted coatings on surface wave signal attenuation. Fig. 1 demonstrates the pattern used for applying the paint to a sheet of stainless steel. It must be noted that it is impossible to attain precisely the same thickness of coating for each of these tests, but it is assumed that if the same amount of vehicle is used each time in the paint and the same spray pressure, that the coats would be somewhat reproducible. It is also thought that the method used here of applying the paint corresponds very closely to the method which would be used in actual field practice.

From this installation, it might be assumed that the paint has approximately .001 inch thickness for each coat. Therefore, the three increments are .001 inch, .002 inch, and .003 inch. The bare sections on the test plate were for the purpose of comparing the response with the sections which had paint. In all cases, the readings were taken 1½ inches from an edge of the plate. The edges of the plate were ground to a reasonably true perpendicular edge, although it is possible there could have been slight variations.

1 Coat	Clean	2 Coats	Clean	3 Coats

Fig. 1. Painted Test Specimen.

The data taken from this experimental setup are shown in Table 1. The distance shown in the first column is the distance between the transducer and the edge of the plate. The readings shown correspond to averages of a large number of readings (30 to 60). From these readings, it can be seen that there is an increasing amount of attenuation with the double and triple coat plates, but that there is very little difference between and bare plate and the plate with only one coat. It can be concluded from these readings that there probably would be very little effect on the accuracy of the readings resulting from only one thin coat of paint.

Another set of experiments was taken to determine the attenuation as a function of distance of transmission. The test specimen which was used for these tests is shown in Fig. 2. This consists of a clean stainless steel plate, one side was covered with two coats of the Nubelon S paint. The signal attenuation versus distance was then determined for each of the two sides. This is shown in Fig. 3. It may be seen from these curves that the attenuation rate is reasonably linear for the untreated surface, whereas, the attenuation increases with distance for the painted surface. This indicates that the application of a thick coat of paint might cause difficulties on long range ultrasonic pulse echo detection.

TABLE I

ATTENUATION DATA

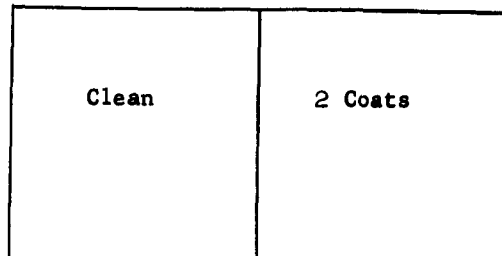| Distance	Coats of Paint	Average Amplitude of Echo Pulse
1.5"	0	2.135
1.5	1	2.157
1.5	2	1.194
1.5	3	.664

6

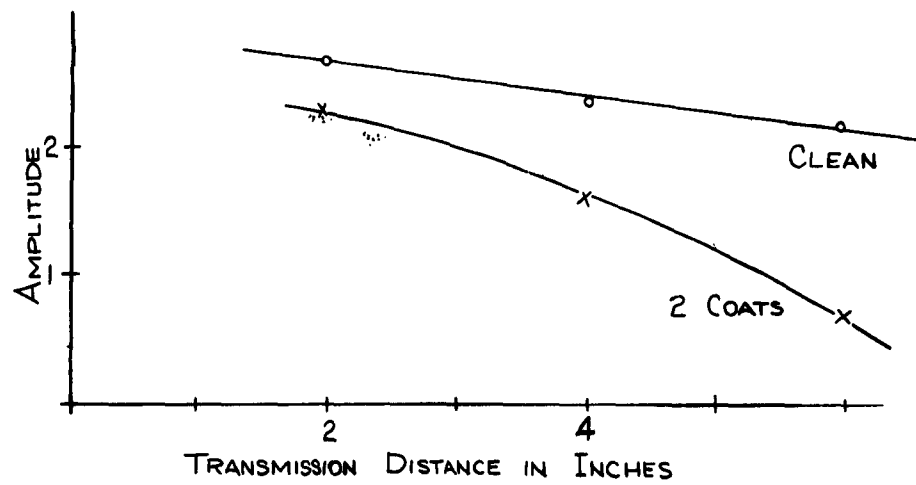Fig. 2. Test Specimen for Attenuation
Measurements.

Fig. 3. Response Vs. Distance for Two Coats of Nubelon S.

In the third set of experiments, several known flaws were tested with a clean surface and then retested following the painting of the surface with a very thin layer of Nubelon S. In every case, there was very little difference in the results between the two tests. It is considered that it would be impossible for a large flaw to go undetected, and it is also thought that it would be impossible for the paint to seep into an extremely fine fatigue crack. Even in the remote possibility that the paint could fill a void, there still would be a strong reflection due to the fact that the mechanical impedance of the paint is very much dissimilar to that of the surrounding steel; therefore, it would still be a discontinuity which could be easily detected.

In several other miscellaneous tests, scratches and defects in the paint coating were tested, using ultrasonic surface waves, with sensitivity levels normally used in testing compressor blades having bare surfaces. It was found in all cases that the test scratches in the paint, produced by a scribe or sharp instrument, produced no reflections that could be detected under these normal gain settings. It should be noted also that generally it is difficult to detect shallow scratches in the metal itself using 2.25 megacycle surface wave inspection.

The question of whether fatigue cracks produced after the painting will cause the paint to crack would be difficult to answer without sufficient field tests. The field test would be necessary to make available cracked blades for which the entire service history was known. It is not possible to produce in the laboratory the exact conditions encountered in the operation of a turbojet engine.

However, several other tests were run in which compressor blades were artificially fatigued by an electromagnetic driver; and in each

8

case, the cracks were visible in the paint with the use of a stereo-
microscope. However, even if the cracks did not come through the paint,
they could still be detected by ultrasonics, as shown by the previously
mentioned experiments.

In considering all the tests which have been run, it must be noted
that in each case the effects of the normally encountered variables such
as transducer, contact pressure, quantity and location of the coupling
oil, the fine tune of the instrument itself, the condition of the sur-
face, and numerous other qualities all have more effect on the quality
of the reflected signal than does the addition of one coat of paint.
Therefore, it is concluded from these tests that a thin coating of
Nubelon S paint or similar paint will cause no serious difficulties
with the ultrasonic surface wave testing technique currently under devel-
opment at the Nondestructive Testing Laboratory at Oklahoma State
University.

Further tests are going to be run in which the difficulties encoun-
tered in removing the paint will be explored. However, at this time, it
is thought there should be no difficulties in effectively removing the
paint from the surface, prior to overhaul, although the existing chemical
cleaning solutions and processes may not be adequate. At the worst, the
most extensive revision in the cleaning system for these types of parts
would be the institution of some strong type of paint remover. This is
thought to be of little consequence at the present time.

SURFACE WAVE CALIBRATION STANDARDS

PROJECT PERSONNEL

Principal Investigator   James D. Simpson

Project Associates   James A. Daniel

                                                    Phillip W. Randles

INTRODUCTION

The development and application of ultrasonics to nondestructive testing of materials and parts has proceeded very rapidly in the past few years. Standards have been developed which are useful for comparison and evaluation of instruments, and in some cases, for estimation of flaw sizes. For the most part, these standards have been developed for longitudinal waves or perhaps in a few cases for shear waves; but very little work has been done with standards for surface waves. Evaluation and comparison of surface wave transducers requires appropriate standards which are not available at this time. Estimation of the flaw size or determination of maximum allowable flaw signal requires standards compatible with the type of waves being implemented.

The object of this study is to develop means of inspecting compressor blades from jet engines with ultrasonic techniques. Fatigue flaws on the surface of the blades are of primary interest which leads quite naturally to the use of Rayleigh surface waves to perform the inspection. Surface wave standards become necessary for evaluation and comparison of specialized transducers, and as aids in the calibration of sensitivity and reject control levels for assembly line testing.

The standards studied were the hole, the edge slot, and the variable edge angle. Also, experiments were run on several other possible standards systems.

12

SUMMARY AND CONCLUSIONS

A thorough investigation has been made of several types of possible surface wave standards. Several of these, the variable diameter hole, the variable slot width, and the variable edge angle have been the more successful.

From these analyses, the following conclusions are made:

1. The variable edge angle standard is superior to all others tested in that the range of angle from 10 degrees to 80 degrees produces an extremely wide range of echo strengths. This standard is easy to manufacture and is easy to use. It is recommended for general purpose use.

2. A second standard consisting of a small hole in the blade to be tested can be used when a special purpose transducer is needed. A transducer shoe fitting a curved blade would not fit the prismatical angle-bar and could not be tested by that means. The small circular hole can be normalized with a variable edge angle, thus using the edge angle as a primary standard and the hole as a secondary standard.

3. The varible width edge slot produces a linear variation of echo width and could be useful for calibrating a system for larger flaw indications.

BASIC CONSIDERATIONS

A research group working under the supervision of Dr. R. L. Lowery at Oklahoma State University has been doing research and development work on procedures for ultrasonic inspection of jet engine components. Primary interest has been in inspection of compressor blades. One problem which has been encountered is the question of standards. The development of adequate standards does indeed seem to be prerequisite to development of successful and practical testing procedures.

During the past few years, a great deal of work has been done in the field of ultrasonic testing. Several standards have been developed for longitudinal testing, of which the best known and most frequently used are the Alcoa Series "A" test blocks. Surface wave testing has not been used as often as longitudinal testing, and to date there are no surface wave standards being widely used.

After a considerable amount of study on the theory of surface waves and after actually using surface wave techniques for testing parts, certain requirements that a standard must meet to be of benefit can be specified.

It is found that there are two general parameters in ultrasonic testing -- those controlled by the operator and those controlled by the specific inspection problem. These parameters are listed as follows:

A. Operator Controlled Parameters

    1. Equipment selection

      a.   Instrument type

      b.   Transducer type (crystal, case and wedge)

  2. Operation of Equipment

      a.   Technique

          (1) Coupling method

          (2) Scanning procedure

          (3) Maximum indication procedure

      b.   Control Settings

          (1) Reject level

          (2) Sensitivity

          (3) Delay time

          (4) Pulse rate

B. Inspection Controlled Parameters

  1. Specimen properties

      a.   Wave velocity

      b.   Attenuation

      c.   Geometry

          (1) Transducer size and shape

          (2) Transducer type (longitudinal, shear, or surface)

      d.   Transducer frequency

      e.   Surface condition

      f.   Noise level

  2. Flaw properties

      a.   Transducer type (longitudinal, shear, or surface)

      b.   Depth

      c.   Width

      d.   Shape

e. Impedance

f. Orientation.

A standard should be designed so as to assist the operator in adjusting his control parameters to measure the Inspection Controlled Parameters. It should also serve as a means by which the operator can select the proper equipment for the inspection problem at hand. For an example of the first case, if a certain size flaw could be tolerated, then the maximum indication of any flaw would be the standards indication corresponding to the flaw specified. In the second case, the standard must be used as the means by which the response of instruments and transducers can be compared.

The logical type standard would be one which gives proportional indication amplitudes for different size standard reflectors. As explained before, a standard must of necessity be a secondary standard since it would be very difficult to produce a standard flaw. On the other hand, standards which are made up of reflectors of different sizes could be thought of as an idealized flaw. A slot machined in a steel plate might , for example, be considered an idealized flaw. Since the interface would be air, the reflection would be very high. The reflecting surface would be perpendicular to the direction of wave travel, so there would be no loss of energy due to angle of incidence at an angle to the reflector. A flaw, say a fatigue crack, of the same size as a slot would probably give a lower indication than the corresponding interface which would allow more energy to pass through than if it had been air alone. Also, the interface of the fatigue crack would probably be jagged, thus allowing more energy to be deflected away from the transducer. These effects are demonstrated in Figure 1.
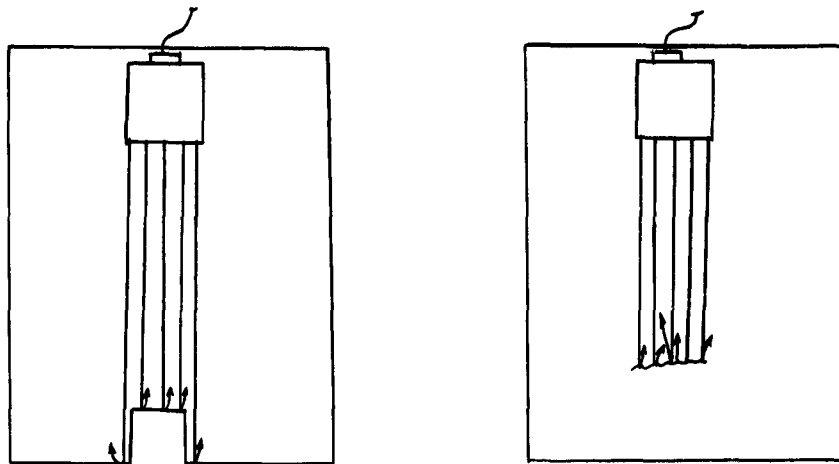
Figure 1. Reflection from Regular and Irregular Surfaces.

Some sort of surface wave standards appear to be necessary in setting up procedures for ultrasonic testing of compressor blades. Specific reasons can be listed as follows:

(1) testing and comparison of transducers

(2) testing and comparison of the pulser-receiver units

(3) analysis of flaws

(4) specifying flaw tolerances

(5) aid in adjusting controls for actual testing.

This last reason points out the demanding need of surface wave standards to be used in the testing procedures. One of the problems of surface wave testing of compressor blades is adjusting the sensitivity and reject level controls to obtain optimum results. These

17

control settings must allow the operator to detect small flaws and must also limit the noise level so that noise signals are not confused with flaw indications any more than necessary.

The desirable characteristics of a surface wave standard include:

(1) The signal response should be reproducible to a high degree of accuracy.

(2) It would be preferable for the signal amplitude to vary linearly with some parameter of the standard.

(3) The standard should be capable of producing very small echo signals of the same order of magnitude as those arising from actual small fatigue flaws.

(4) The standard should be compatible with the actual part to be tested so that a comparison can be made, preferably with the same transducer.

Several possible surface wave standards have been investigated during the past year as a part of the development of a procedure for ultrasonic testing of compressor blades. A list of the more practical ideas which have been investigated is given below, and a detailed discussion of the results obtained from each possible standard follows.

Tentative surface wave standards:

(1) adoption of conventional longitudinal standards.

(2) variable width flat faced slots.

(3) variable diameter round holes.

(4) variable impedance mismatch.

(5) variable damping of a standard echo signal

(6) variable edge angle

(7) standardized flaws in compressor blades identical with those to be tested.

18

These studies indicated that these types of standards might prove to be very valuable for ascertaining and testing the capabilities of ultrasonic testing equipment but would be of no use as surface wave standards. Various manufacturers of ultrasonic testing equipment were contacted to determine if they had any knowledge of existing surface wave standards. These companies agreed there were no existing surface wave standards. They also agreed there was considerable need for surface wave standards of some sort.

STANDARDS DEVELOPMENT

I. Variable Width Flat Faced Slots

A trial standard was designed and tested which consisted of a
circular steel plate with varying width slots machined along the edge.
By varying the width of the slots, it was believed that a linear varia-
tion in the ultrasonic indication could be obtained.

The slots were used because: (1) It was believed that the theo-
retical considerations would be simple since the reflectors would con-
sist of a secondary rectangular piston source, and (2) it was believed
that the indication would be directly proportional to the width of
the slots. To determine the amounts of energy returned to the trans-
ducer from a slot, a theoretical investigation of the ultrasonic reflec-
tions from a slot must be made.

If the radiation patterns from the rectangular piston source, or
for simplification a line source, were independent of length and fre-
quency, the energy reflected to the transducer should be proportional
to the length of the line source. Since the radiation patterns depend
upon the length of the reflector and frequency (which determines wave
length in a particular medium), one of the main factors which determine
the pressure received by the transducer is the radiation pattern effect.

Suppose the width of the piezoelectric crystal is one inch and the
width of a slot is one-half inch. The maximum radiation the slot could
possibly reflect would be one-half of the total energy sent out by the
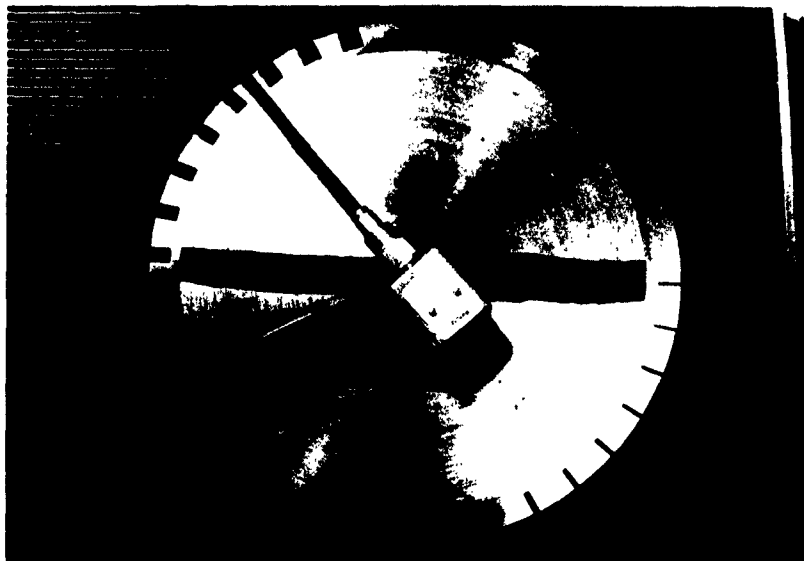transducer. Due to the varying radiation patterns formed by different

Figure 2. Circular Plate with Slots.

width slots at a given frequency, the energy received by the transducer will be less than the ideal case.

The radiation patterns from any source can be approximated by a number of point sources aligned in the same geometrical shape and of the same phase relationship as the actual radiator. The radiation pattern can then be obtained by summing the contributions of each point source at any angle to an arbitrary axis of radiation. This process is sufficient for the main beam of the reflection pattern but is not sufficient for the secondary maxima since the relative intensity of the secondary maxima rises to unity which is the same as for the main beam. For this reason, the source must be analyzed as a continuous line source. As a line source, secondary maxima of the pattern become

21

progressively smaller instead of rising to unity. This is due to the fact that for directions other than the normal to the line, all the radiation from all points can never be in phase; whereas, in the source consisting of point sources, secondary maxima equal in intensity to the radiation straight ahead appear at angles inclined to the normal when radiation from all points are in phase. In the case of the continuous line source, the secondary maxima are much smaller, although not necessarily so small as to exercise a disturbing influence.

The equation for the relative pressure of the straight line source is derived by Irving Wolff and Louis Malter (5) by taking the equation for (n) point sources a distance (d) apart and allowing (n) to approach infinity and (d) to approach zero in such a way that nd = L. Therefore, the line source is the limiting case. The equation so derived is

$$R_\alpha = \frac{\sin(\frac{\pi \ell}{\lambda} \sin\alpha)}{\frac{\pi \ell}{\lambda} \sin\alpha} \tag{1}$$

where R = relative pressure,

α = angle between the normal (to the line source),

L = length of the line source, and

λ = wave length.

The amount of energy intercepted by a slot will be proportional to its width compared to the width of the beam sent out by the transducer. The slot widths which would be of any value, therefore, would be those of width equal to or less than the width of the transducer beam. For the ideal case, all the energy intercepted by a slot would be reflected to the transducer. Because of the radiation patterns as described by Equation 1, all the energy reflected from the slots will

not be picked up by the transducer. Since the maximum voltage output of the transducer will be proportional to the amplitude of the pressure reflected to the crystal, the effect of the energy being spread over a large area will reduce the indication.

The average pressure on the face of the crystal must be found to accurately predict the indication returning from a slot. The intensity of the reflected wave is proportional to the square of the pressure. The area under the intensity curve divided into the area that intercepts a slot gives the portion of the total intensity that was incident on the transducer. The square root of this value is the average pressure incident on the crystal. To find these values, Equation 1 must be solved for various values of L. To predict the indications, the following values must be computed:

1. Area under R_α^2 curve for different values of L.

2. Area of R_α^2 curve that intersects the transducer.

3. Ratio of total R_α^2 curve to the part that returns to the transducer.

4. Portion of total energy from the transducer that intersects the slot.

The area of the R_α^2 curve represents the total intensity reflected by the slot. The area of the R_α^2 curve inside the angle that intersects the transducer represents the intensity received by the transducer. This is shown in Figure 3.

The value obtained from dividing the total area into the intercepted area gives the portion of the total that is received by the transducer. Since the computations would be long and tedious, a digital computer was used to compute the needed quantities. The results are shown in Table 1.

23

Once the four values have been computed, the theoretical percentage of the total energy that leaves the transducer and is reflected back to the transducer can be found as follows:

A = size of slot compared to size of crystal

B = portion of area of R_α^2 that returns to transducer

C = percentage of total indication

by knowing A and B

$$C = AB \times 100$$

TOTAL INTENSITY

INTENSITY INTERCEPTED
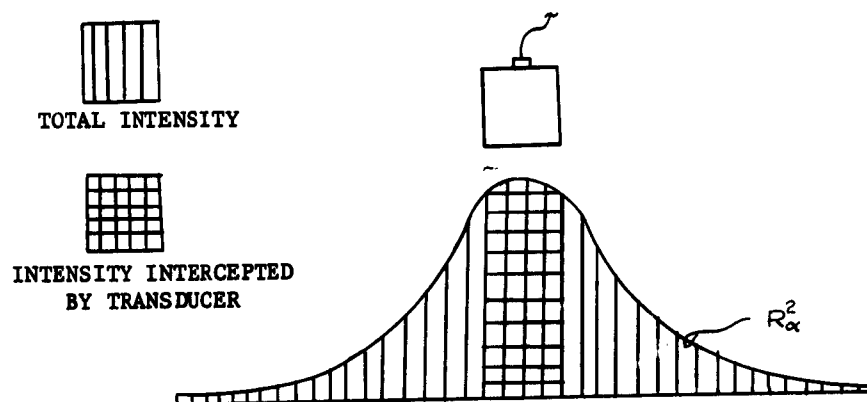BY TRANSDUCER

R_α^2

Figure 3.   Portion of Intensity Intercepted by Transducer.

From the values computed, a theoretical curve can be drawn for any set of slot widths. To determine if the radiation patterns are the main controlling factors in the indications as seen by the transducer, the theoretical curve should be compared with an experimental curve.

To test the feasibility of using machined slots as a surface wave testing standard, a theoretical curve for transducer indication for various size slots is needed. The usual size of transducers ranges between one-fourth inch and one inch. For the reflections to be of value, they must be smaller than the beam width of crystal. The range selected to analyze was from 0.03125 to 0.5 of an inch.

For the theoretical consideration, the sizes of the slots started at 0.03125 inch and went to 0.5 inch in 0.015625-inch increments. To obtain values for the transducer indications, Equations 1 and 2 must be solved for each slot width. Equation 1 was solved for the area of R_α^2 for each slot width and for various frequency transducers with a digital computer. To compute the value of A in Equation 2, the transducer beam width was divided into the slot width. The value B in Equation 2 was found by dividing the total area of the R_α^2 curve into the area of R_α^2 that intercepts the receiver crystal and taking the square root of this value. The value of C in Equation 2 was found by multiplying A by B. This gives the portion of the total pressure response that is returned to the transducer. The following is a sample calculation:

Slot width = .3125 inch

Transducer frequency = 2.25 mc   Transducer width = 1 inch

Portion of R intercepted by transducer = 12°

A = .3125 ÷ 1 = .3125   B (by computer) = $(.89608937)^{\frac{1}{2}}$ = .9475

25

$$C = AB = .3125 \times .9475 = .296 = 29.6\%.$$

The results of these computations are shown in Table I and Figure 4. Also shown in the figure is the curve that would be obtained neglecting the radiation pattern.

It can be seen from the figure that the curves become more linear for higher crystal frequencies. Also the reflection becomes more directional for high frequencies. The reflection from a .265625-inch slot at 5 mc should give the same indication as a .28125-inch slot at 2.25 mc, or the same indication as a .375-inch slot at 1.0 mc. If the transducer were located closer to the slots, the curves would lie closer to the linear curve which is independent of frequency. If it were located further from the slots, it would intercept a smaller portion of the intensity curve, and the curves would lie further from the linear curve.

From these curves, it is evident that slots could be used as a testing standard. To see if experimental values are the same as the theoretical values, slots of different widths were machined in a steel plate.

The transducer used to test the plate was a 2.25 mc 1-inch by 0.5-inch transducer. The crystal width was one inch, but the beam width was measured and was found to be 0.6 inch. The transducer was placed so it would intercept a twelve degree arc of the radiation pattern. A Magnaflux ultrasonic testing instrument (shown in Figure 5) was used to take the data. Indications were read in centimeters. The actual portion of the total energy sent out by the transducer that was reflected to the transducer was found by dividing the indication of the total reflection from a boundary into the indication received from the

TABLE I

THEORETICAL REFLECTIONS FROM SLOTS

(Transducer Width = 1 inch)

| Slot Width (in.)	Percent of Total Reflection		
	Transducer Frequency		
	1 mc	2.25 mc	5 mc
.031250	.921	1.17	1.79
.046875	1.492	2.25	3.255
.062500	2.21	3.44	4.82
.078125	3.20	4.69	6.50
.093750	4.18	6.16	8.27
.109375	5.39	7.71	10.00
.125000	6.60	9.23	11.69
.140625	7.78	10.91	13.30
.156250	8.97	12.65	14.94
.171875	10.41	14.25	16.44
.187500	11.60	16.01	17.95
.203125	13.10	17.80	19.45
.218750	14.70	19.83	20.95
.234375	16.29	21.20	22.50
.250000	17.79	22.95	24.1
.265625	19.25	24.60	25.7
.281250	20.75	26.25	27.3
.296875	22.4	28.00	28.9
.312500	24.1	29.62	30.6
.328125	25.9	31.15	32.1
.343750	27.6	32.60	33.5
.359375	29.5	34.30	35.3
.375000	30.9	35.80	36.8
.390625	32.6	37.50	38.3
.406250	34.3	39.00	39.8
.421875	36.1	40.40	41.4
.437500	38.0	41.90	43.0
.453125	39.7	43.40	44.5
.468750	41.4	44.75	46.1
.484375	43.0	46.40	47.6
.500000	44.6	48.00	49.2
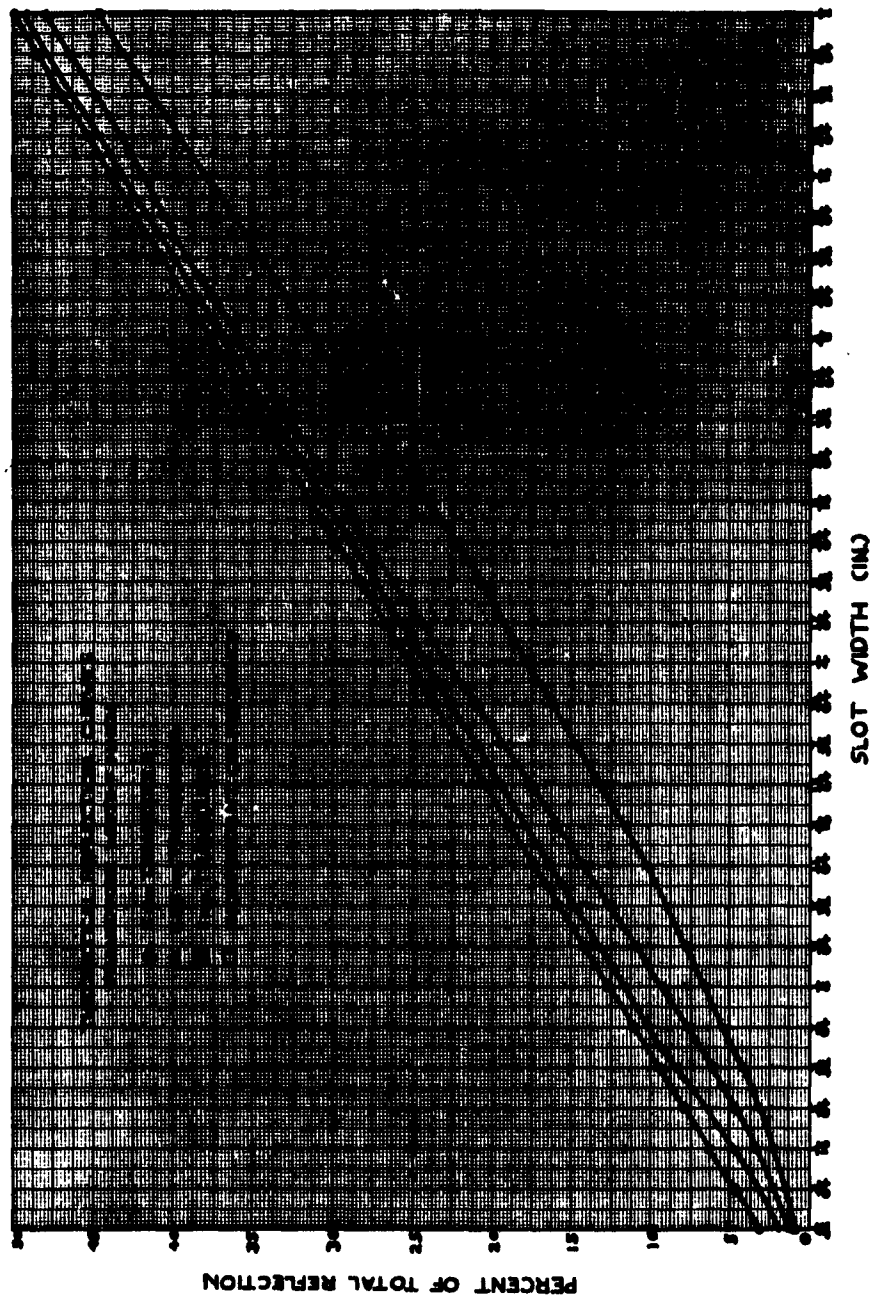
Figure 4. Theoretical Reflection Curves.
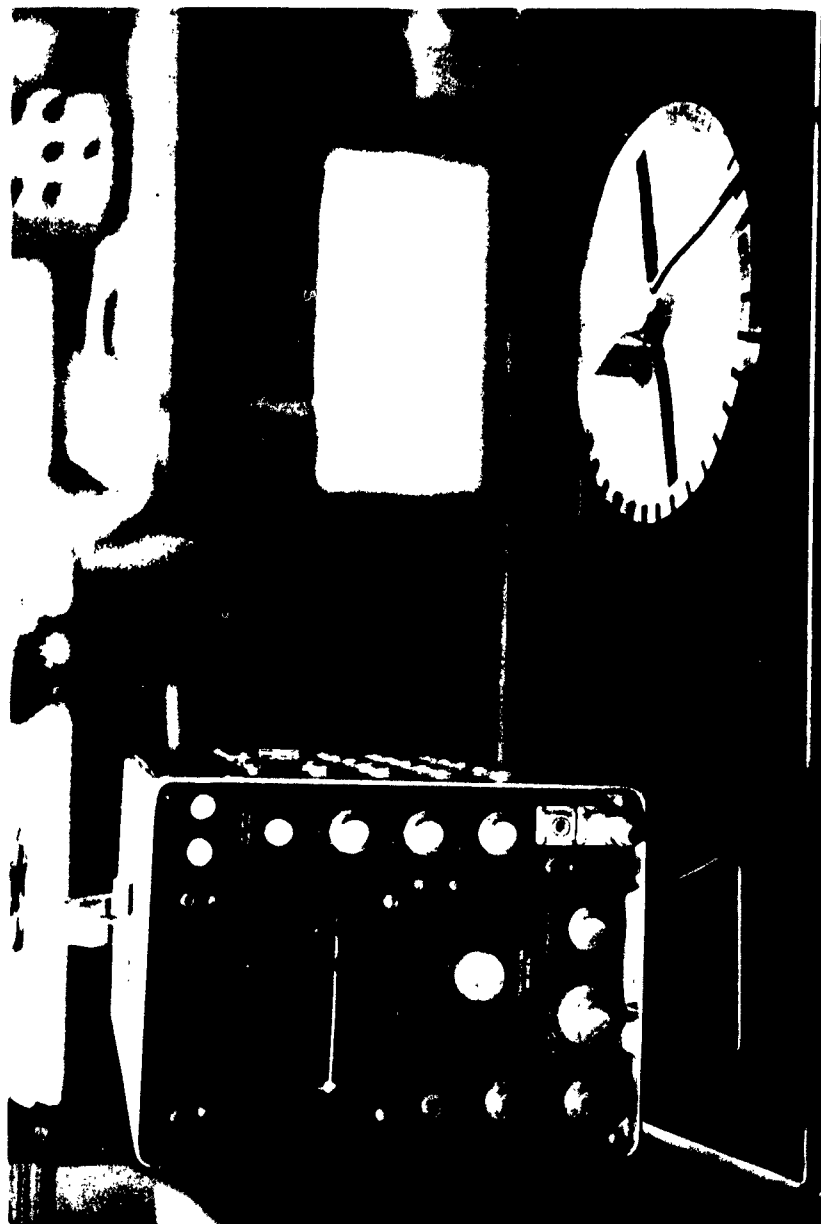
Fig. 5. Ultrasonic Testing Instrument Used.

slots. The theoretical percentage was computed as mentioned before. The data obtained are found in Table II. These data are plotted in Fig. 6. It is seen that the theoretical values and the experimental values agree within a few per cent.

The main difficulty in obtaining data from these slots was in getting the maximum indication possible. One of the factors that contributed to this problem was the fact that the transducer had to be placed so that the maximum intensity portion of the beam had to be incident on the slot while at the same time the crystal had to be perfectly parallel to the slot. Another main factor in this problem was the different indications that could be obtained with different oil film thicknesses under the transducer. If any air were between the transducer and the plate, that portion of the surface wave would not reach the crystal. If too much oil were used, the oil would damp out a portion of the surface wave before it reached the crystal, or it would reflect a portion of the returning wave. The first plate tried was a square steel plate with slots machined along the edges. It was very difficult to obtain data from this plate because the transducer was difficult to position. The circular plate proved to be better than the square one because positioning was achieved by varying only one coordinate. The best results were obtained when the portion of the plate over which the transducer would be moved was coated with a thin film of oil. The transducer was then placed on the plate and a weight was set on the transducer to keep a constant pressure applied to it. The transducer was moved by sliding it a short distance around the small radius of the center hole.

30

TABLE II

THEORETICAL AND EXPERIMENTAL REFLECTIONS FROM SLOTS

(Transducer Width = 0.6 inch)

(Transducer Frequency = 2.25 mc)

Slot Width (in.)	Percent of Total Reflection	
	Theoretical	Experimental
.031250	1.95	3.64
.046875	3.75	4.55
.062500	5.74	5.06
.081250	7.80	6.57
.093750	10.27	9.1
.109375	12.85	11.4
.125000	15.38	14.0
.140625	18.20	17.1
.15625	21.05	19.5
.171875	23.75	20.4
.187500	26.70	25.7
.203125	29.7	30.6
.218750	33.1	33.7
.234375	35.4	33.7
.250000	38.3	37.8
.265625	41.0	41.9
.281250	43.8	44.5
.296875	46.7	45.3
.312500	49.4	48.2
.328125	51.9	50.0
.343750	54.4	54.2
.359375	57.2	56.8
.375000	59.7	58.6
.437500	69.7	65.4
.468750	74.5	66.5
.500000	80.0	63.5
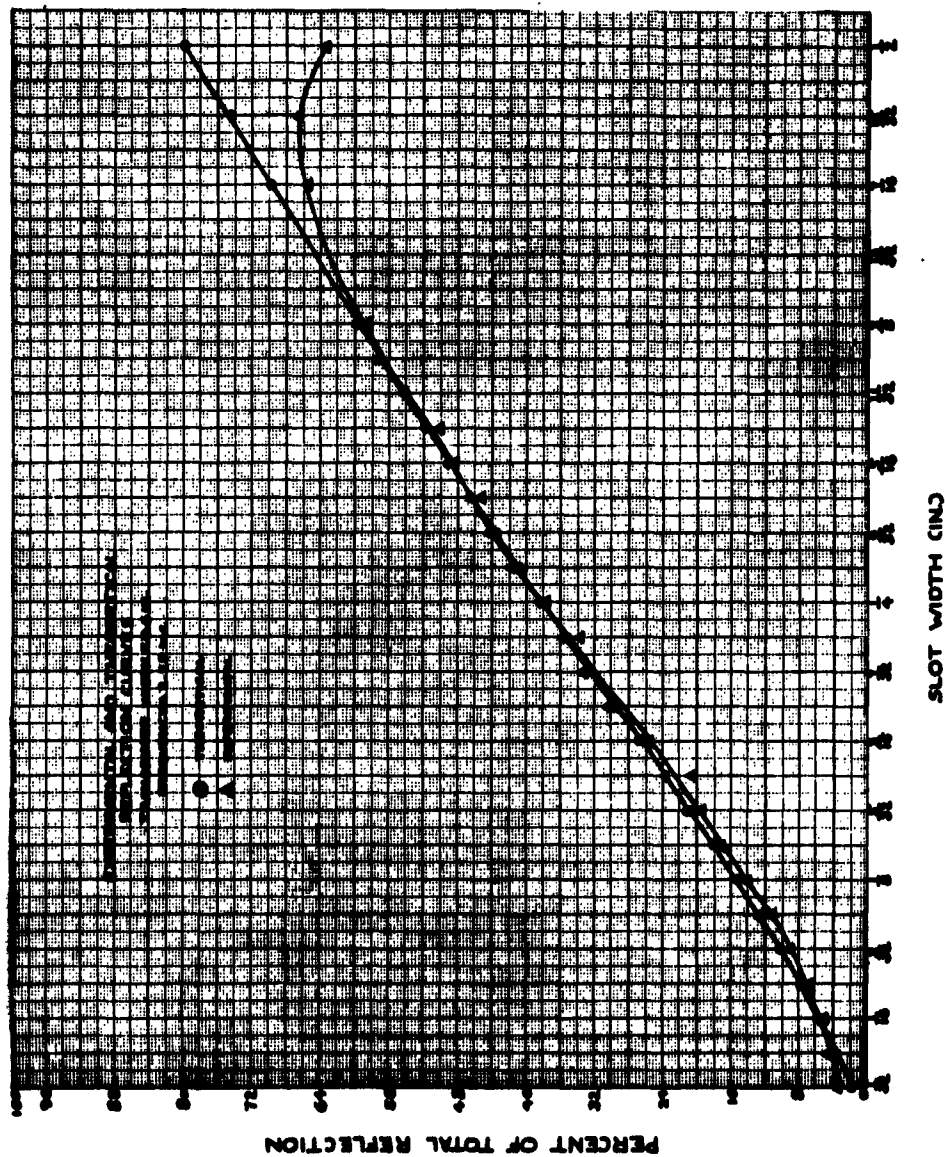
Figure 6. Experimental and Theoretical Reflection Curves.

To conclude the discussion of variable width slots as a possible standard, a listing of the advantages and disadvantages of the slots is in order. The construction of a circular steel plate with slots machined along the edges is simple to construct and reproduce accurately. The only variation that could occur using the same type of material would be in the machining tolerances. It cannot be said that this standard is easy to use. A wide variation of indications can be obtained by using slightly different methods of peaking procedure.

After working with surface wave techniques, it has been found that they are very sensitive to many variables. For this reason, it would be expected that a surface wave standard would be more difficult to use than a longitudinal wave standard.

From the theoretical curve, it was noted that the curve became more nonlinear as the frequency of the transducer decreased. If the slots were to be used as a standard, a standard curve would have to be drawn for each frequency. Although the curves were all constantly creasing with the slot width, the decrease was not the same for each frequency.

It has been stated that a standard should be used for specifying flaw tolerances, for comparing transducers and test machines, and to check wear or stability of transducers. The question is how the standard developed can be used to perform these tasks.

Probably the main use of the standard would be to set the reject level on the instrument. Once the maximum size flaw permissible is stated, the standard slot corresponding to this size flaw would be found; and with the instrument receiving the indication from the slot, the reject level could be set. Any part, in which a flaw gave an

33

indication equal to the standards indication, would be rejected. If

at any time the operator wanted to check his instrument, it would be

a simple matter to check the instrument on the standard slot.

The slots can be used to compare transducers by measuring the

beam width, by measuring the sensitivity and resolution, and by testing

the signal to noise ratio. For comparing test instruments, they could

be used to test the linearity of the receiver amplifier, to test the

linearity of the controls, and to check the signal to noise ratio using

the same transducer on different instruments.

To check the wear or stability of a transducer, the new transducer

would be tested on a specific instrument and a standard slot. The con-

trol settings of the instrument and the test slot would be recorded.

If at any time, the transducer was suspected of being defective because

of loss of resolution power or wear, it would be checked using the data

previously taken on it. The same type of test could be done on a testing

instrument. In general, it seems that a standard of varying size slots

is promising.

III. Variable Interface Impedance

Since it seems that the radiation pattern effect is a main factor

in analyzing a standard, it would be advantageous to develop a standard

which would give the same indication independent of frequency. It

would be advantageous to developed a standard which would not depend

upon different size reflectors. This would greatly reduce the maximum

indication problem. One way of doing this would be to change the

impedance match at the interface instead of changing the size of the

reflector. By using a plane interface of greater width than the trans-

ducer beam width being used, and by changing the interface from steel

34

to air, which caused one hundred per cent reflection to something
between the air and steel, the indications received would be independent
of frequency and reflector width. By using several materials at the
reflecting boundary, the desired type of curve could be achieved.

One disadvantage of this standard is the difficulty of obtaining
empirical results within a narrow tolerance. The peaking procedure is
very critical. The amount of couplant oil beneath the transducer and
the metal surface condition between the transducer and the slot have
great effects on results. The amount of pressure on the transducer
and the amount of couplant oil are variables which are particularly
difficult to control. Good experimental results, as shown in the curves
presented earlier, are obtainable only by taking averages of several
readings. Individual readings may often vary by ten per cent or more.

When a particular inspection problem involves detecting very small
flaws, it will probably not be possible to obtain echo indications
from slots which are of the same order of magnitude as echoes from
small flaws. It is thought that this problem arises principally from
the machining problem of producing flat faced slots of very small width.

III. Variable Diameter Round Holes

Another possible standard, consisting of holes of variable diameter
drilled in a flat steel plate was evaluated. Holes of small diameter
are much easier to produce accurately than very narrow slots. It was
also hoped that the holes would produce weaker echo signals than a slot
with width corresponding to hole diameter because of the predictable
scattering effects produced by curvature.

Obtaining consistently reproducible data from the round holes
proved to be even more difficult than with the slots. Variation in

35

couplant conditions, variation of the amount of pressure on the trans-
ducer, and the procedure used for peaking, again proved to be critical
parameters. Individual readings seemed to be distributed about a mean
value with about fifteen per cent variation. By taking averages of
a fairly large number of readings, it was possible to obtain a fairly
reproducible curve. Data were taken using the Branson Sonoray unit
and the Magnaflux unit. Although the curves obtained from data taken
on the different machines are not identical, they are very similar.
Plots of average data obtained using the Magnaflux and the Branson
units are given in Fig. 8. Fig. 7 is a photograph of the circular
plate containing the test holes with the transducer used for the testing.
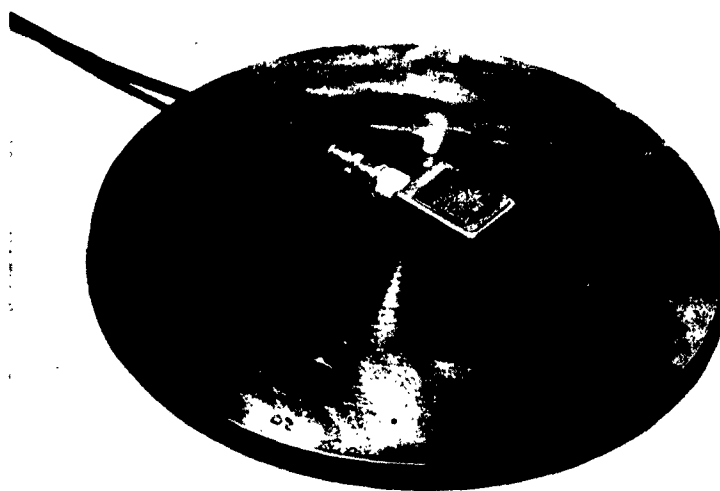
Fig. 7. Circular Plate with Holes.

36
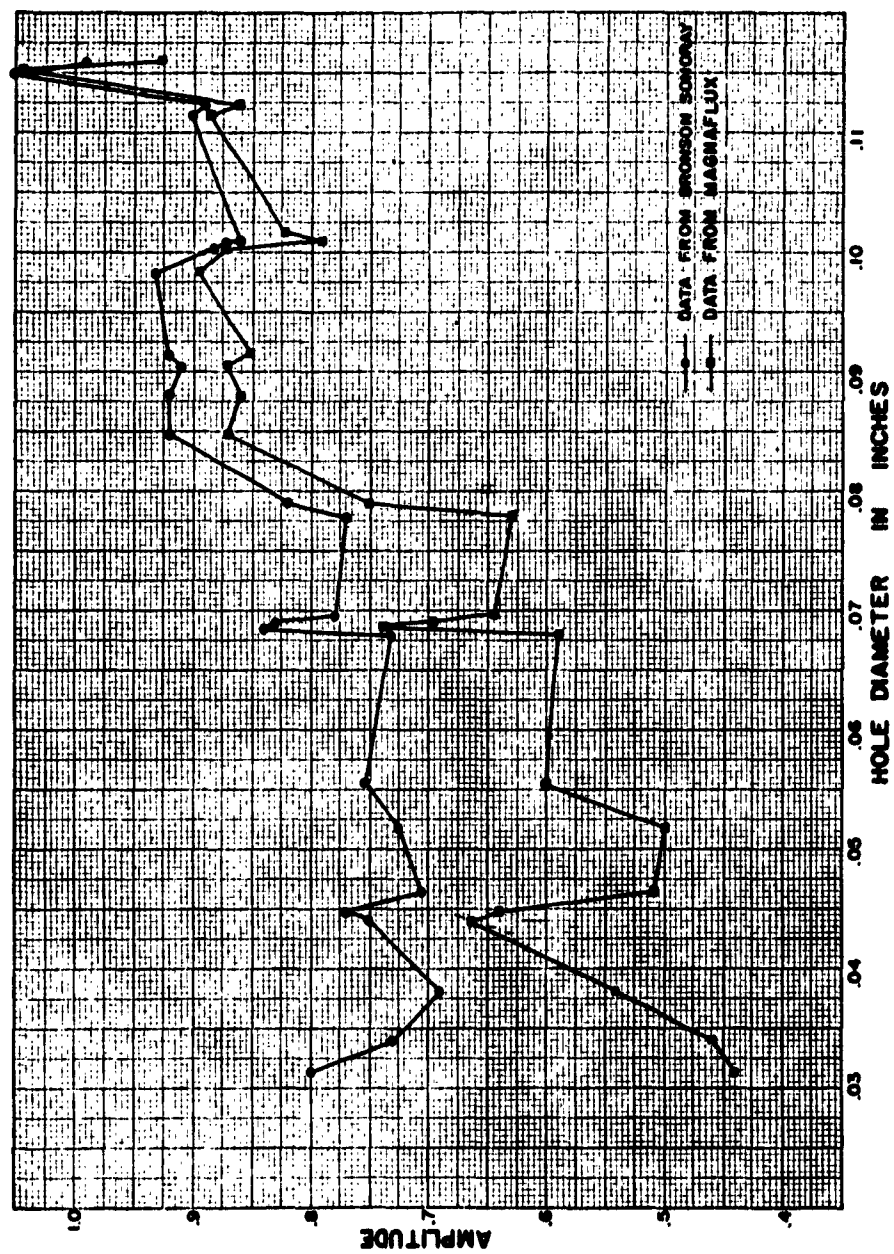
Fig. 8. Reflected Signal Amplitude Versus Hole Diameter.

At first glance, the data presented seem to be a hopelessly erratic collection or random points. It can be seen at once that the response echoes are not a linear function of diameter or even a monotomically increasing function of diameter. However, if the data points can be fitted to a theoretical or empirical curve; then it might be possible to judiciously select diameters so as to produce a standard for which response would be monotomically increasing with diameter. Fig. 9 illustrates how this procedure might be applied.

Looking back at Fig. 8, it can be seen that maxima and minima of the empirical data occur at multiples of the wave length. The wave length for Rayleigh surface waves of 2.25 mc in steel lies in the range of .048 to .050 inches. This periodic relation of echo amplitude with hole diameter indicates that interference phenomena may be the mechanism principally responsible for the oscillatory nature of the curve.

If the interference phenomenon is assumed to be the dominant mechanism influencing the response curve, a semi-theoretical curve can be developed as described in the following paragraphs.

The hole is assumed to be made up of a large number of incremental elements acting as sources of reflected radiation, as shown in Figure 10. Several assumptions might be made as to how reflection takes place at the incremental elements.

Case (1) Assume a perfect reflector -- any incident radiation which does not strike the surface perpendicularly will not be reflected back to the transducer.

Case (2) Assume perfect absorption and reradiation.

Case (3) The actual case will be somewhere between cases (1) and (2). One possible assumption might be that absorption and consequent
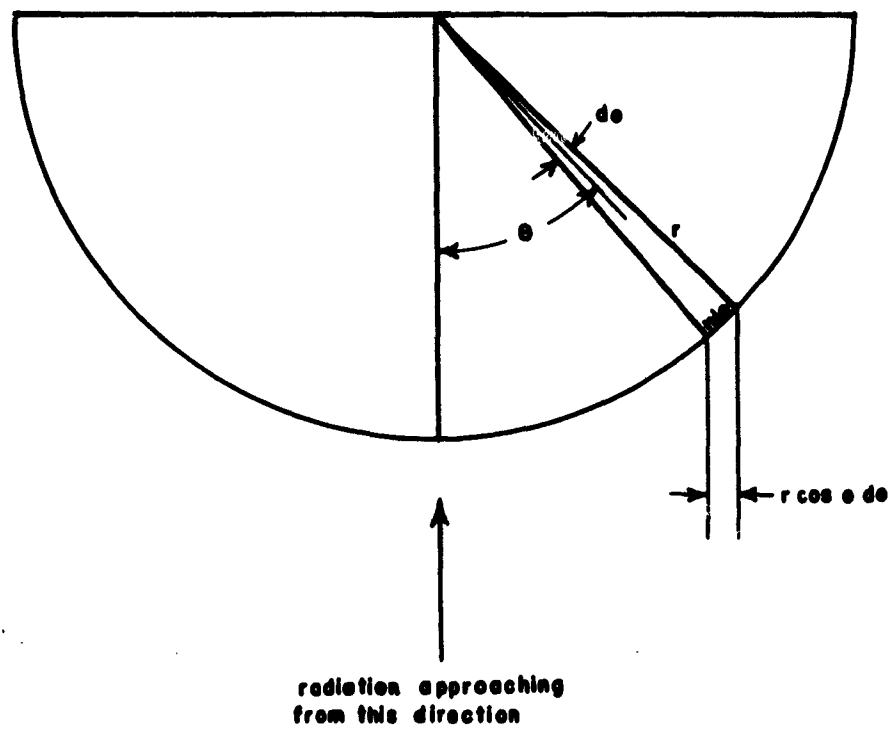
38
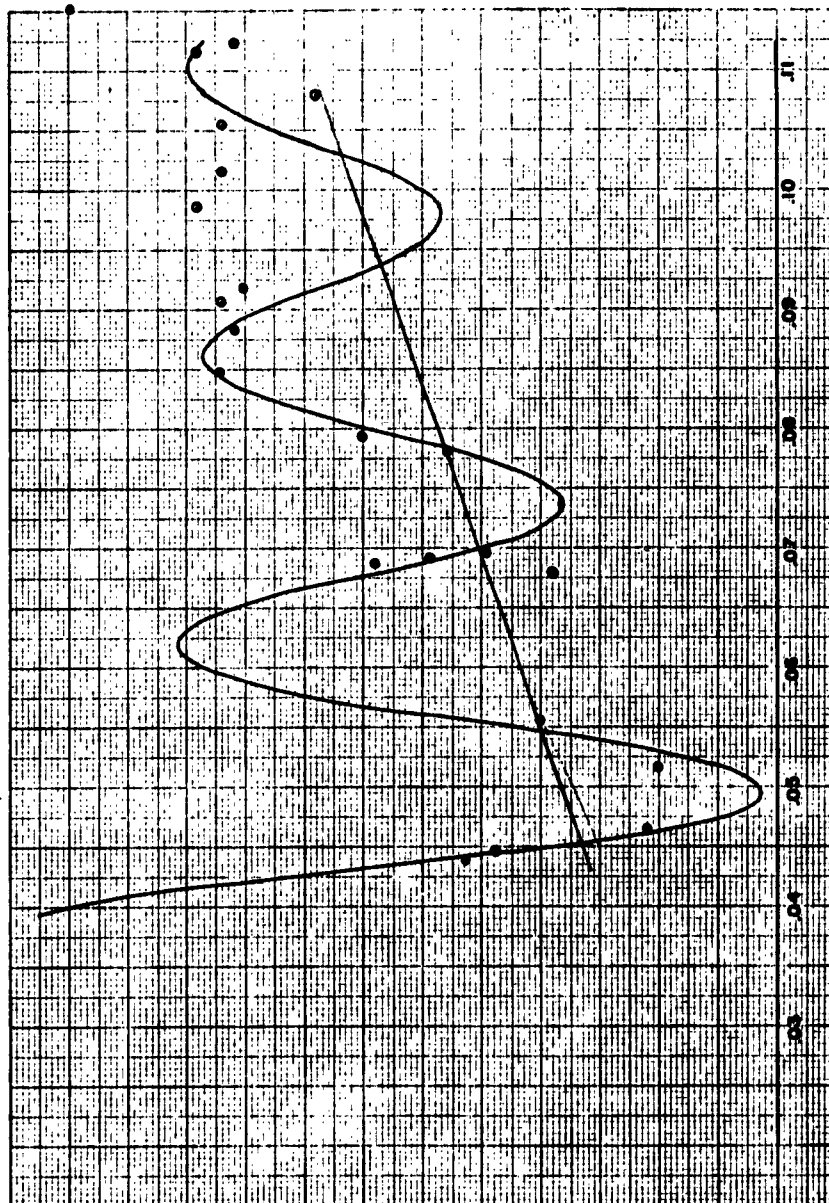
FIGURE 10

Model for Theoretical Analysis of Round Hole Reflection.

reradiation is proportional to the cosine of Θ. The strength of an incremental source then becomes $n = rd\Theta \cos^2\Theta_n$. Many assumptions similar to this one are possible.

<u>Case (4)</u> The assumption which has yielded results that are the most compatible with the experimental data to date is Case (2) with the additive factor proportional to diameter.

Making the assumption of perfect absorption and reradiation, the strength of elemental sources distributed around the half circumference facing the direction of source radiation is seen to be

$$An = C (r\cos\Theta d\Theta)^{\frac{1}{2}}$$

where the amplitude of vibrations is assumed proportional to the square root of intensity.

The equation of propagation of Rayleigh surface waves is

$$A = A\cos(pt + fx).$$

For increments of Δx and Δt, this equation becomes

$$A = A\cos[p(t+\Delta t) + f(x+\Delta x)]$$

Which can be written as

$$A = A\cos(pt+fx)\cos(p\Delta t+f\Delta x) - \sin(pt+fx)\sin(p\Delta t+f\Delta x).$$

This can be written

$$A = A(\cos\alpha\cos\beta - \sin\alpha\sin\beta)$$

where $\alpha = pt + fx$ and $\beta = p\Delta t + f\Delta x.$

The total amplitude is given by the sum of the contributions of the individual elements.

$$Amp = \Sigma_n(A_n\cos\alpha\cos\beta_n - A_n\sin\alpha\sin\beta_n)$$

$$= \Sigma_n A_n\sin(\beta_n + \psi).$$

The angle ψ is of no consequence and may be omitted so that

41

$$\text{Amp} = \Sigma_n A_n \sin\beta_n.$$

The angle β may be evaluated as follows:

$$\beta = p\Delta t + f\Delta x$$

with $p = \dfrac{2\pi c}{\lambda}$; $f = \dfrac{2\pi}{\lambda}$

where c is the velocity of propagation and λ is the wave length.

Setting $\Delta x = c\Delta t$ leads to $p\Delta t = f\Delta x$ or

$$\beta = 2f\Delta x.$$

Δx can be evaluated from Fig. 10 as $D(1-\cos\theta)$.

Making this substitution leads to the result,

$$\text{Amp} = \Sigma_n A_n \sin[\frac{4\pi D}{\lambda} (1-\cos\theta_n)].$$

The above presented results can be used to obtain a curve which fits the actual data with a fair degree of accuracy. A digital computer was used in making the summation indicated above. The curve plotted in Fig. 9 is

$$y = C_1\Sigma_n A_n \sin[\frac{4\pi D}{\lambda} (1-\cos\theta_n)] + C_2 D$$

where C_1 and C_2 are constants chosen to obtain a good curve. Obviously, if this investigation were to be carried any further it would be desirable to obtain a plot of response versus hole diameter for very small increments of diameter. There should be no large gaps wherein the curve is not defined by actual data points. Although the research would be interesting and probably yield fruitful results, it was decided that the difficulty in constructing this standard outweighs its usefulness.

IV. Variable Damping of a Standard Echo Signal

Since Rayleigh waves travel along the surface of the material, they are very easily damped. Damping can be produced by applying a weight to some sort of resilient pad placed between the transducer and the echo source. Such an arrangement is shown in Fig. 11. Pressure on the pad can be applied in several ways. The most obvious methods seemed to be use of ordinary weights or a mercury column.

Experimentation verified that it was possible to obtain a varying signal by this procedure, but that control conditions were very difficult to maintain. Individual data points were again very erratic, but it was possible to obtain a monotomic curve of echo amplitude versus applied damping force.
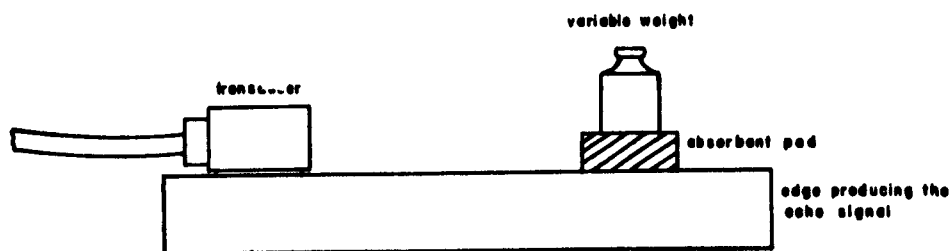
Fig. 11. Variable Damping Standard.

V. Variable Edge Angle

In many experimental sessions in the laboratory, it has been noted that the condition of the edges of a discontinuity has more effect on the magnitude of the reflection than possibly any other consideration. For example, compressor blades having large nicks and

43

dents caused by the ingestion of foreign objects into the engine often produce small reflections in comparison with small fatigue cracks. Also, on some laboratory specimens, it is possible to send a surface wave around at least two corners of a block if the edges are slightly rounded.

This led to the belief that the variation of the angle at the edge of a plate might be used as a standard. An investigation reported by Knopff and Tangi in Geophysics, December 1960, gives a theoretical correlation of the reflected and transmitted energy of a variable angle wedge. Also, de Bremaecker, Geophysics, 1958, deals with the transmission and reflection of Rayleigh waves around corners.

The experimental standards were first made by milling faces of varying angle around the periphery of a mild steel round plate, one-half inch in thickness and about 14 inches in diameter as shown in Fig. 12. Since this plate later proved to be unwieldy, another set of standards was made by milling the angled faces on 1" x 2" bar stock as shown in Fig. 13. In this way, a single bar will give four readings.

Several methods of taking data from these blocks were tried. It was found, generally, that the most reproducible results were produced by manually positioning the block until the reflection from the edge peaked at a preset location on the time axis of the screen. As in all other methods, extreme care was taken to remove excess oil from the path of the transducer since this can damp a considerable amount of energy.

Fig. 14 is a plot of reflection amplitude, in decibels, as measured by a Krautkramer USIP-10 instrument, using a barium titanate 2.25 mc transducer. The two curves, representing two different tests, were
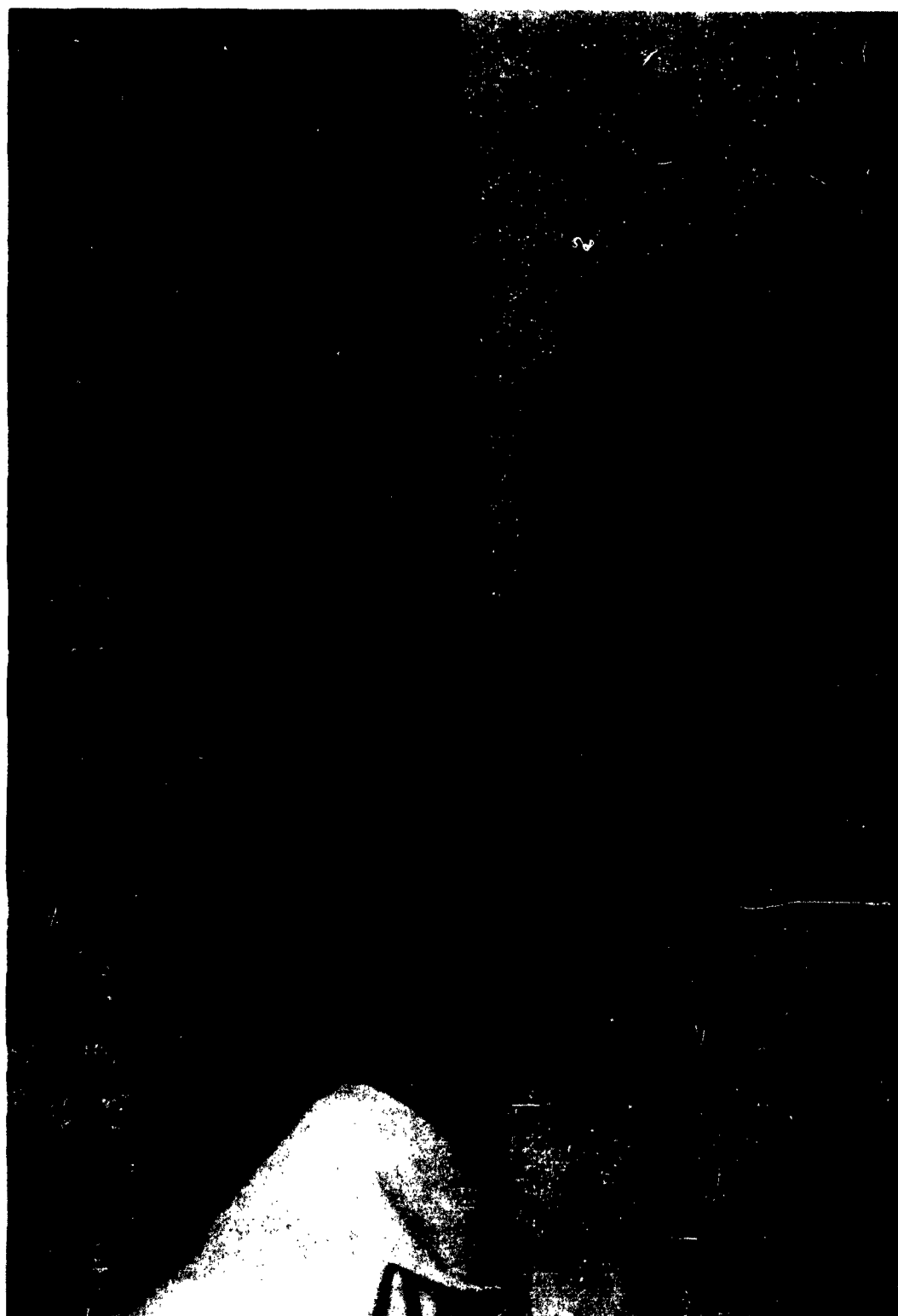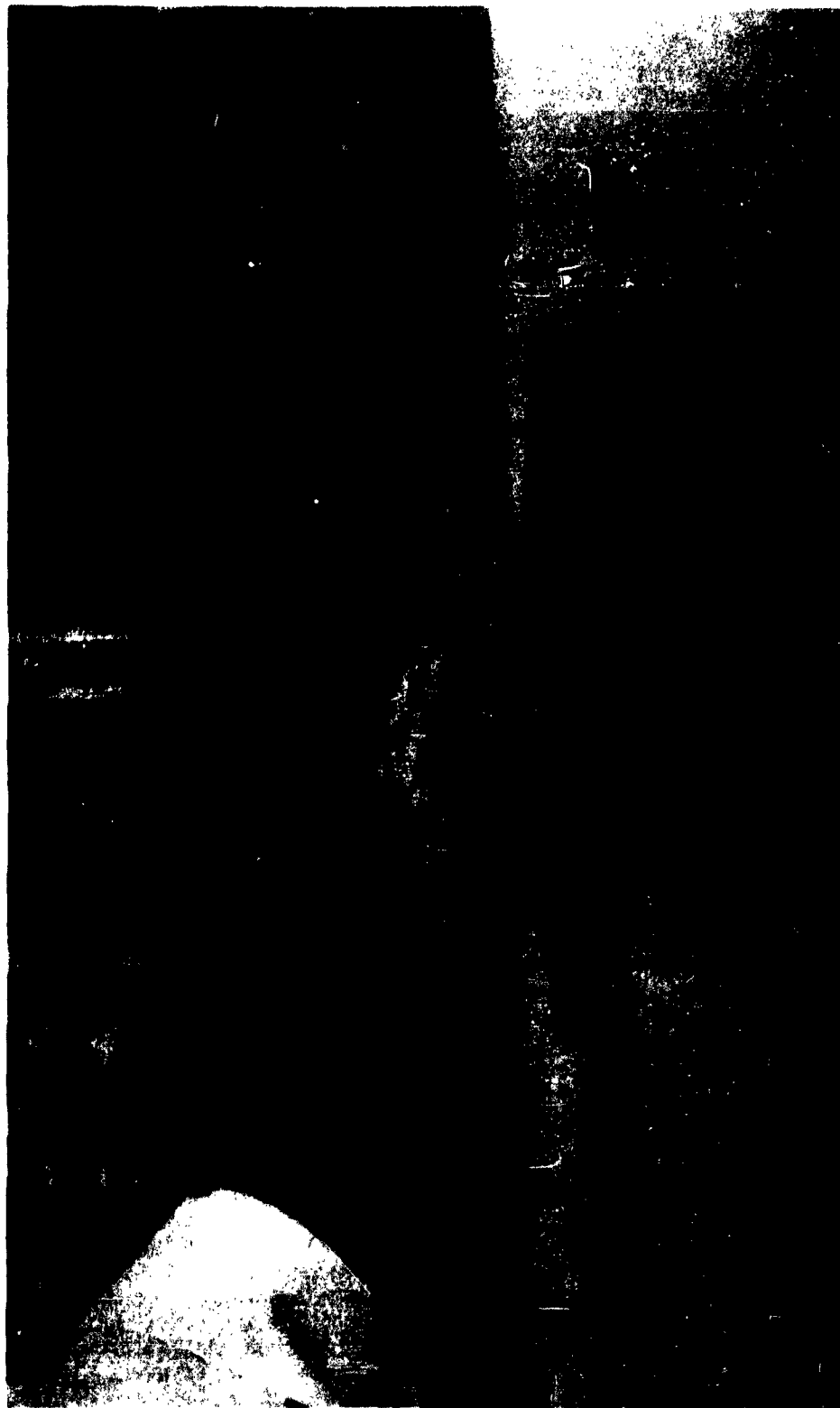
Fig. 12. Variable Wedge Angle Standard.

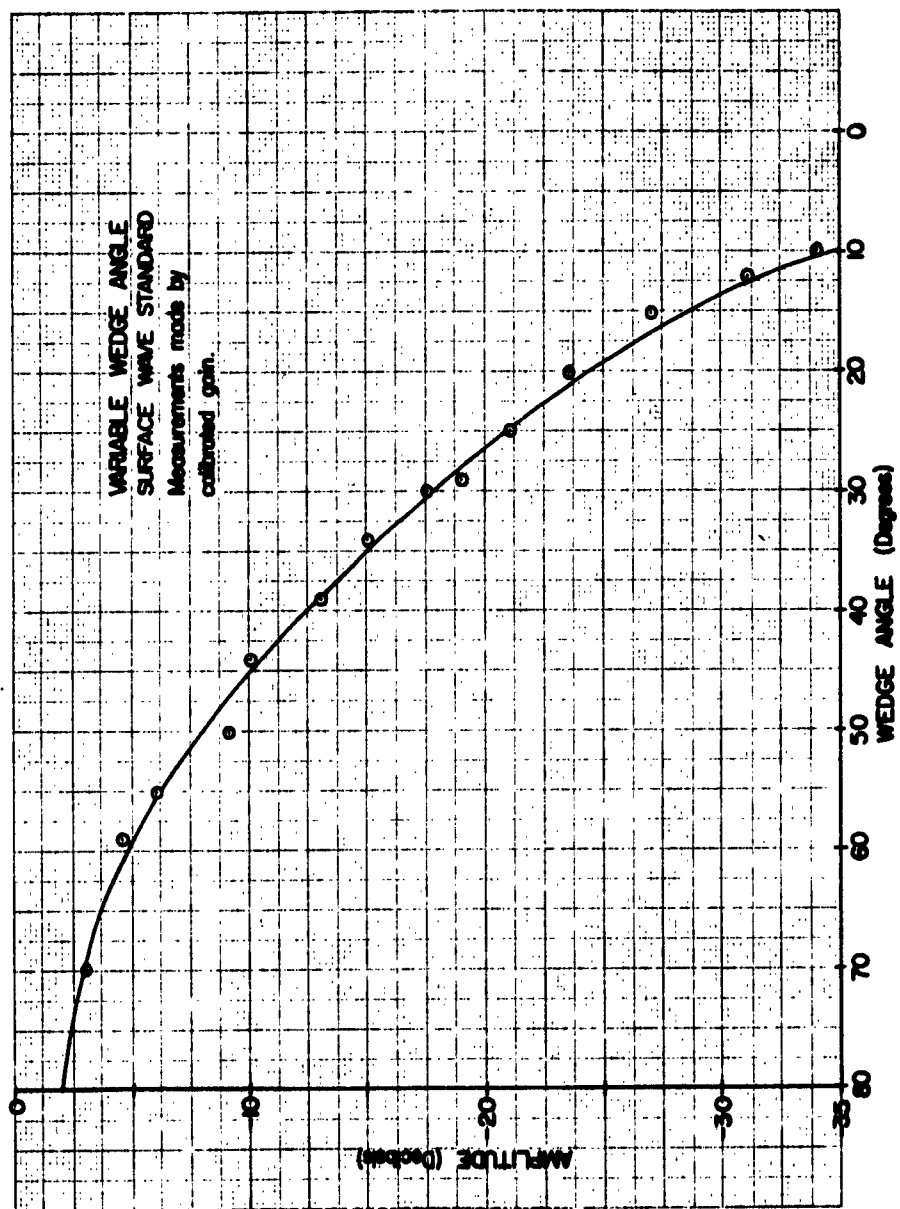Fig. 13. Variable Wedge Angle Blocks.

Fig. 14.

VARIABLE WEDGE ANGLE
SURFACE WAVE STANDARD
Measurements made by
calibrated gain.

WEDGE ANGLE (Degrees)

AMPLITUDE (Decibel)

obtained by adjusting the calibrated gain control until the reflection
was centered around "0DB" on the screen, and then reaching the gain
level.

There is little variation between these two successive tests.
Measurements made on other machines show the same trend and, in general,
prove that the readings are reproducible. The reflection is a maximum
at 80° and drops off at 90° as predicted by Knopff and Tangi.

Figs. 15 and 16 are plots of linear reflection response for two
different ranges of angles. Each curve represents an average of many
tests. The measurements were taken directly from the screen without
adjusting the gain during a given test.

A point of interest is that if the gain is adjusted to give full
scale deflection for the 80 degree edge angle, the reflection from the
angles below 30 degrees is difficult to discriminate from the noise
level in most pulse-echo systems. Similarly, if the reflection for
the 30 degree edge is adjusted for full scale deflection the signals
for angles below 10 degrees are difficult to measure. The reflections
from the angles below 10 degrees are comparable with those of extremely
fine fatigue cracks in .410 stainless steel.

Thus, at 80 degrees, virtually all the energy is reflected; and
at 5 degrees, almost none is reflected. Almost any surface flaw could
be compared with an angle in this range.

Experiments run at 1, 2.25, and 5 megacycles prove that the edge
angle standard is not frequency dependent in this range. Therefore,
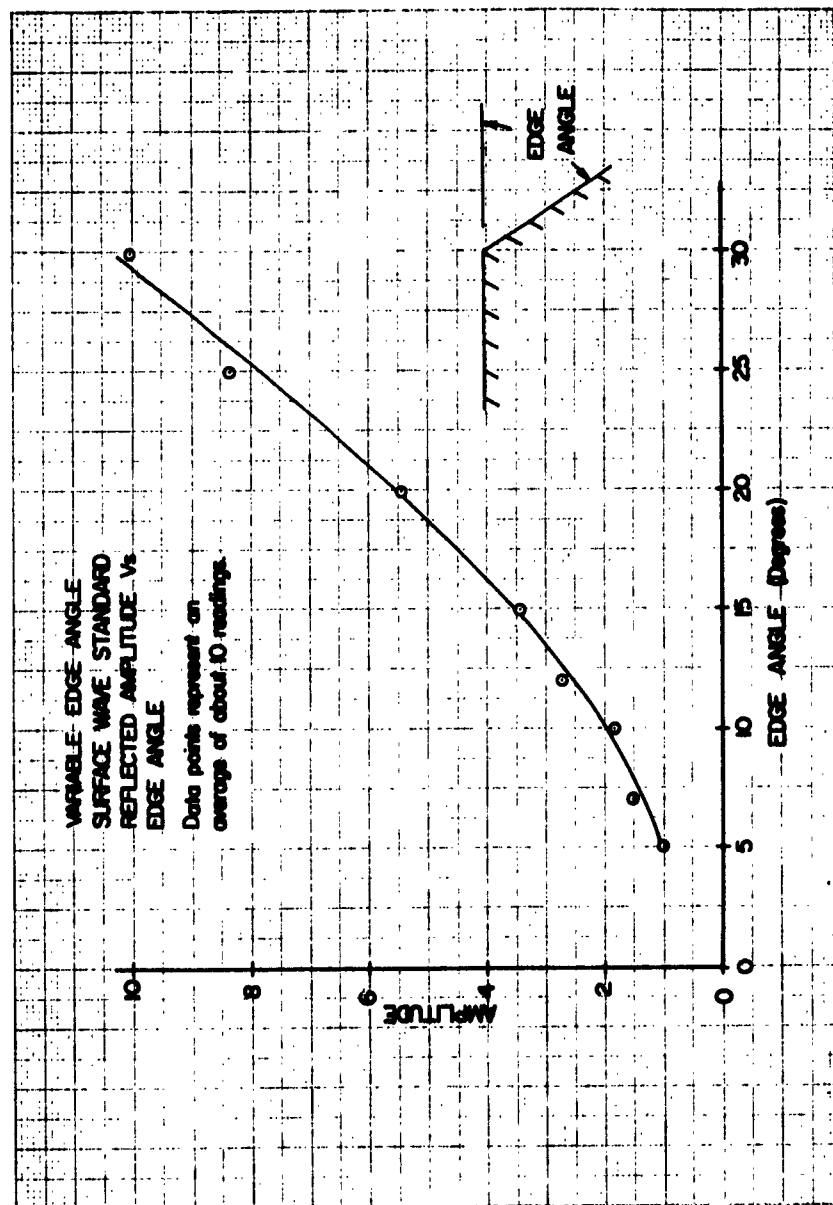this standard could be used for all common transducers.

48

VARIABLE EDGE ANGLE
SURFACE WAVE STANDARD
REFLECTED AMPLITUDE Vs
EDGE ANGLE

Data points represent an
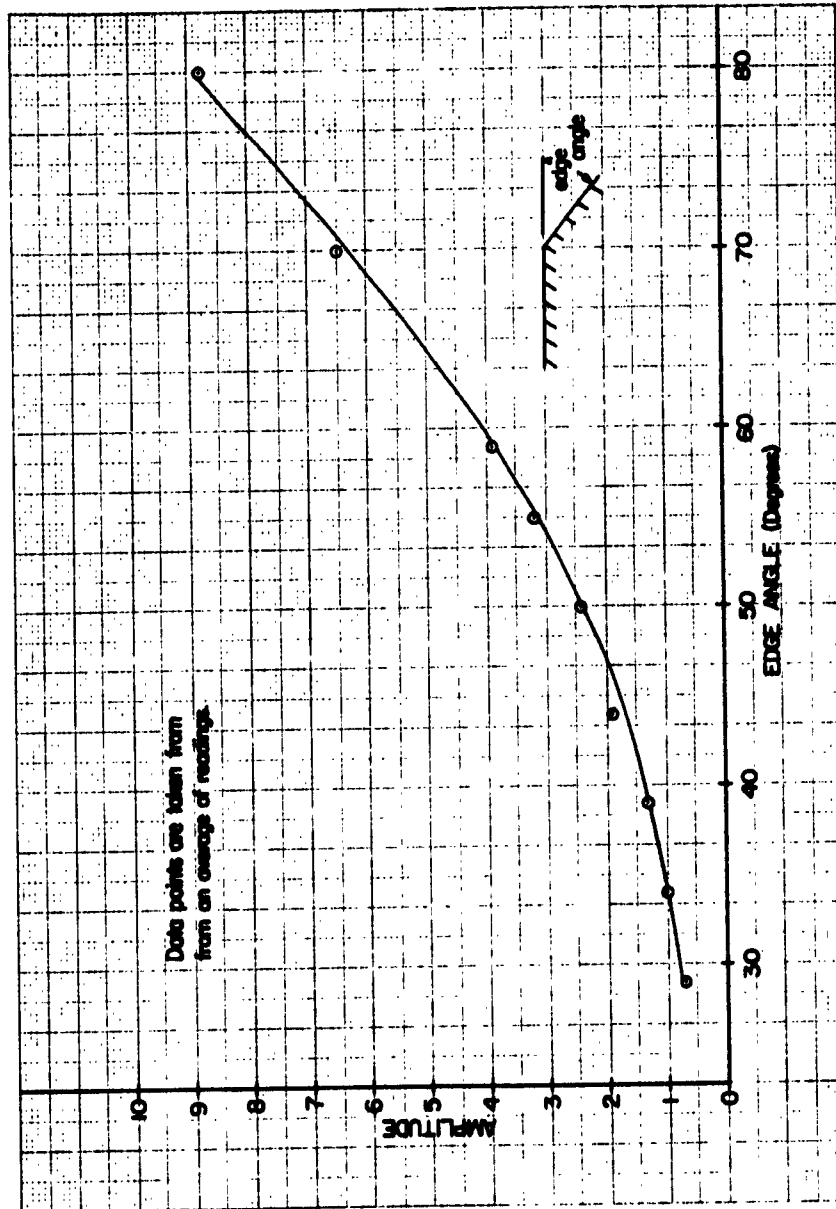average of about 10 readings.

Fig. 15.

49

Fig. 16.

50

VI. Secondary Standards for Compressor Blades

When use is made of specialized transducers, it is necessary to have a standard which is identical in physical configuration with the object to be tested. The need for this type of standard has been demonstrated in the development work with specialized transducers for testing of compressor blades. It is apparent that standards to be used with these transducers should be fashioned from compressor blades identical with those to be tested. In some of the work done to date, blades with small cracks have been used as guides for setting up the instrument. Since it would be very difficult to produce cracks which are similar enough to be used as a standard, small diameter round holes have again come forward as possible standards. The work which was done previously with round holes has made it possible to predict what size hole will produce echo signals of minimum strength. Also, the round hole can probably be correlated with other standards such as the variable edge angle and variable slot width.

A STUDY OF ULTRASONIC SURFACE WAVES

FOR COMPRESSOR BLADE TESTING

PROJECT PERSONNEL

Principal Investigator   Gerald Whitehouse

Project Associates   James D. Simpson

                                          James E. Gray

                                          Jesse McIlhaney

53

INTRODUCTION

The nondestructive inspection of compressor blades in jet engines during overhaul and periodic maintenance periods has narrowed mainly to two methods: fluorescent penetrants and ultrasonic inspection utilizing the pulse-echo technique.

The first attempts to introduce ultrasonic inspection of compressor rotor blades by means of surface waves were made in France in 1954. In Holland, Dr. J. Schijve (1)[1], of the National Aeronautical Research Institute in Amsterdam, had worked systematically to develop reliable and efficient probes and methods of inspection for field application. J. G. Rasmussen (2) of Massachusetts Institute of Technology, has done considerable work in this field, both here in the United States, and for the Royal Danish Air Force of Denmark.

The principle of pulse-echo ultrasonic inspection is analogous to that used in radar. However, acoustic wave pulses are used in ultrasonic inspection as opposed to electromagnetic pulses used in radar. At a certain frequency of repetition, the ultrasonic apparatus generates electric pulses to a piezoelectric crystal made from quartz, barium titanate, or an equivalent crystal substance which causes the element to vibrate at its natural frequency. These vibrations are transmitted directly to the material being tested. The transducers are coupled by

---

[1] Refers to Selected Bibliography for this section.

an oil or similar liquid placed between probe and specimen which allows
the sound waves to be transmitted to the specimen. The coupling block
or transducer adapter has to be constructed in such a manner, that
after the sound passes through it, the sound waves must enter the speci-
men as surface waves. These surface waves propagate in the material
until they reach a boundary condition, at which point, a portion of
the ultrasonic energy is reflected back to the transducer. The reflected
energy is detected, suitably amplified, and displayed on a cathode ray
tube.

Surface wave transducers are commercially produced in various
sizes and frequencies, ranging from 400 kilocycles to 10 megacycles.
This report concerns:

(1) The application of ultrasonic surface waves to detect flaws
in the blades of J-71, J-79, and J-35 compressors;

(2) The design and construction of suitable transducer adapters
to fit the first four stages of the compressors; and

(3) The results thus far obtained from their use.

SUMMARY

Many types of surface wave systems were designed, tested, and evaluated for the inspection of compressor blades of the J-35, J-71, and J-79 turbojet engines. At the present time, Table 1 presents the most suitable transducer system of all evaluated. It is probable these systems will be improved and further modified after a sufficient backlog of field testing experience has been gained. Table II is an evaluation of the main types of transducers with respect to demands on operator skill and ease of use.

TABLE I

Compressor Type	Transducers & Adapters Used in Ultrasonic Inspection	Adapter Best Suited for Inspection
J-35	1. Miniature surface wave transducer 2. Clamp-on Stationary-type adapter	Clamp-on Stationary type
J-71	1. Miniature surface wave transducer 2. Clamp-on movable-type transducer 3. Clamp-on pivot-type adapter	Clamp-on movable type
J-79	1. Miniature surface wave transducer 2. Clamp-on movable-type transducer 3. Clamp-on pivot-type adapter	Clamp-on movable type

Evaluation of Testing to Date

Type of Adapter Investigated	Advantages	Disadvantages
1. Miniature Surface Wave Transducer	1. Scanning Ability 2. One transducer can be used to inspect many stages. 3. Easily calibrated	1. Transducer pressure varies with operator 2. Back reflection is not stationary due to operator's inability to place transducer in same location each time. 3. More experience is required by the operator due to factors in (1) and (2) above.
2. Clamp-on Pivot-type Adapter	1. Scanning Ability 2. Easy to calibrate	1. Difficult to build 2. Back reflection changes as transducer scans.
3. Clamp-on Stationary Type Transducer	1. Fixed transducer eliminates variations in pressure and alignment.	1. Limited coverage depending upon size of transducer. 2. Critical angle for surface wave is only achieved at one point. 3. Requires secondary standardization.
4. Clamp-on Movable (Sliding) Transducer	1. Provides good scanning ability.	1. Some pressure variation 2. Oil coupling requires renewing between transducer and adapter. 3. Critical angle is only met at one point. 4. Requires secondary calibration.
5. Clamp-on Adapter with two fixed Transducers providing full coverage	1. Eliminates pressure and oil problems. 2. Ease of construction 3. Provides good coverage.	1. Critical angle is met at only one position on adapter. 2. Requires secondary calibration

57

DESIGN OF TRANSDUCER FIXTURES

After an extensive investigation of the feasibility of testing compressor blades with the standard miniature surface wave transducers, the following problems were encountered:

(1) It is difficult to place the surface wave transducer in an identical position on each succeeding compressor blade tested. Since the transducer is not always placed in an identical position on the blade, the amplitude of the reflected signal can change, thus making the interpretation of the signal on the flaw detector screen difficult. The conditions mentioned above require continuous adjustment of the sweep control.

(2) The force applied by the operator to the transducer in order to maintain coupling between the transducer and the blade can vary with operators and with blades. The variable coupling condition results in amplitude fluctuation of the signal on the flaw detector screen, and this condition also makes relative flaw size interpretation impossible. The conditions mentioned cause the operator to adjust the gain setting on the flaw detector continually.

(3) Duplication of results between different operators was poor due largely to factors mentioned in (1) and (2).

58

The laboratory inspection of compressor blades can easily be done by experienced investigators. However, the inspection of many engines on an assembly line basis would present difficulties if the test system used was of the specialized type used in the laboratory. Therefore, the studies covered in this report are intended to help provide a system of ultrasonic inspection suitable for use on the assembly line or in the field, by semi-skilled operators.

Some basic studies concerning the principle of pure surface waves had to be made before adapters could be designed for the inspection of the complex shaped compressor blades.

According to Snell's Law:

$$\frac{\sin\alpha_1}{c_1} = \frac{\sin\alpha_t}{c_t} \quad \text{(See Fig. 1)} \tag{1}$$
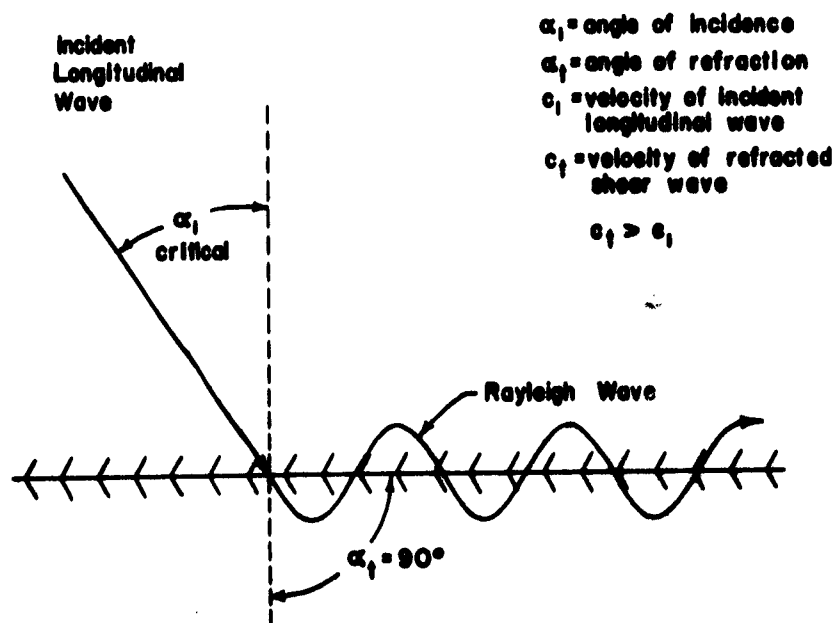
Figure I. Refraction of Wave at Interface

59

As indicated in Fig. 1, if the critical angle is achieved, pure surface waves will be generated in the second medium. If pure surface waves are required, α_t must be equal to 90° and Equation 1 will reduce to:

$$\sin\alpha_1 = \frac{c_1}{c_t} \qquad (1\text{-}a)$$

Since $\sin\alpha_1 \leq 1$, then from (1-a) it is obvious that

$$c_t \geq c_1 \qquad (1\text{-}b)$$

in order to generate pure surface waves in the second medium. This implies that the speed of propagation in the material being tested must be greater than the speed of wave propagation in the transducer block. To satisfy the requirement in 1-b, an acrylic plastic material, known as PLEXIGLASS, was chosen. The coupling block was formed from the acrylic plastic. All the compressor blades under test were of type 410 stainless steel which has a speed of wave propagation of about 3,200 meters per second. The speed of propagation for the acrylic plastic was 2,680 meters per second (3). The calculated theoretical angle (α_1) is found from Equation 1-a.

$$\alpha_1 = \sin^{-1} \frac{2860 \text{m/sec}}{3200 \text{m/sec}} = \sin^{-1} 0.835$$

$$\alpha_1 = 57°.$$

This angle (α_1), however, is not the actual angle used in the probe development. Due to certain diffusions of the ultrasonic wave beam, the size and shape of the crystal, and certain other factors (see reference 2), the angle of incidence sometimes must be increased to an angle greater than the calculated value of 57°. This value was

60

determined experimentally by using a variable-angle transducer.(Fig. 2)
which has the transducer block constructed of the same acrylic plastic
material as was being investigated (4).
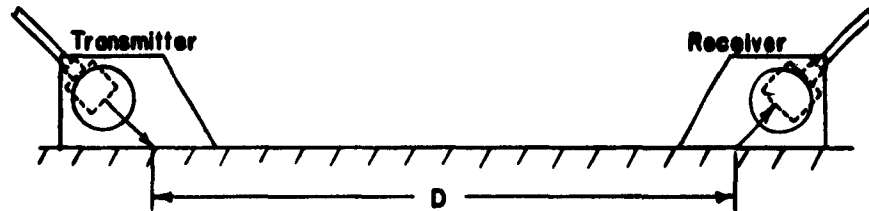
Variable Angle Transducer Holders

Figure 2. Transmitter-Receiver Setup

To determine the angle α_1 experimentally, a stainless steel plate
was selected; and the stainless steel chosen was an alloy similar to
the material from which the compressor blades were manufactured. Two
variable-angle transducers were used as is shown in Fig. 2. Both
transducers used have 2.25 megacycle crystals. One transducer was
used as a transmitter and the other was used as a receiver. The trans-
ducers were placed at a preset distance from one another on the plate.
This distance was chosen as either 6, 8, or 10 inches as these dis-
tances roughly correspond to the lengths of the compressor blades.
The transmitting angle was varied from 55° through 75° while readings

were taken from the receiver. The amplitude of the received signals was read from the scope of the flaw detector, and these amplitudes were then normalized on the maximum signal amplitude. The results were plotted in Fig. 3. From the curves on Fig. 3, the critical angle was determined to be 66°.
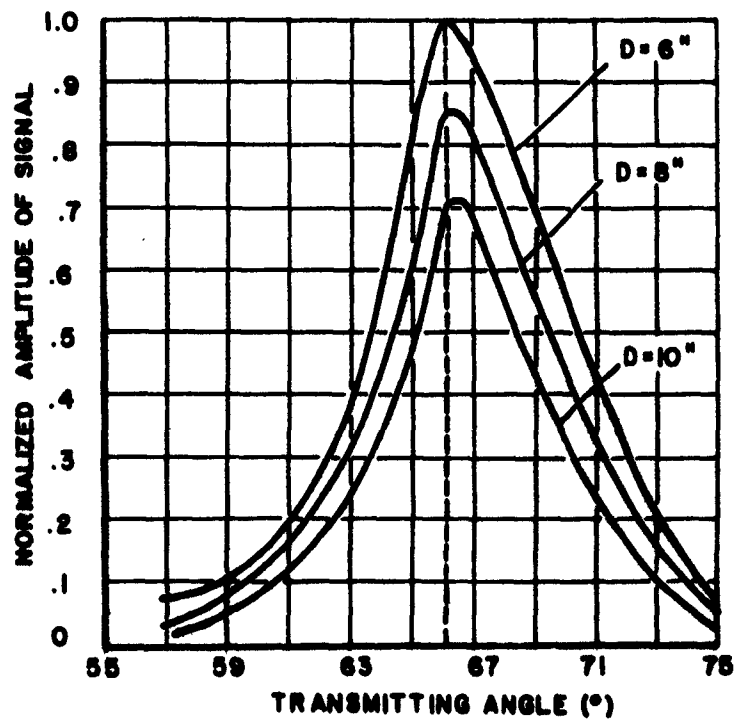
Figure 3. Effect of Angle on Signal Amplitude

After the angle α_2 had been determined experimentally for an adapter which is made from acrylic plastic, consideration had to be given to the geometry of the compressor blades. From previous work done in this field, experience has shown that flaws appearing in the compressor blades occurred predominately in the first four stages, and in the areas indicated by Fig. 4 (1, 2). Designing an adapter or probe to cover up a portion of the blade near the tip, therefore, would not hamper the crack detection efficiency since the flaws were not occurring at this location.
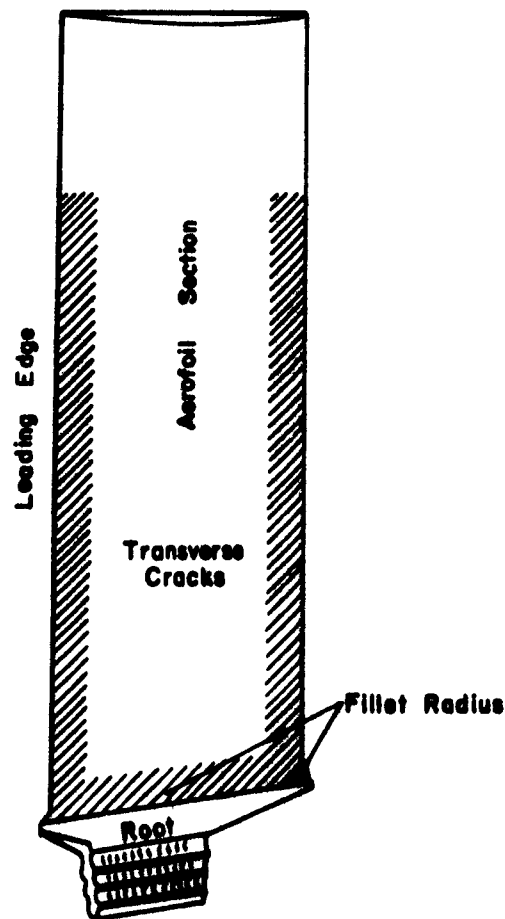
Figure 4. Normal zones of formation of cracks

Several factors had to be considered before arriving at one particular design:

(1) An adapter would have to be constructed to contact the blade surface uniformly so that the ultrasonic wave could be propagated into the blade and any reflections could thus be returned or received.

(2) Ease of removal from one blade and subsequent ease of attachment to the next blade had to be an essential condition of the adapter. This condition also led to elimination of all unnecessary tools, equipment, and associated equipment required.

(3) The time required for movement of the adapter from one blade to another should be accomplished with a minimum amount of delay.

Obviously, the adapter needed to be a clamp-on type device to standardize some phases of the testing and to eliminate problems discussed previously. The geometry of the blades was complicated in that the blade surface was curved in two directions. The double-curvature of the blade surface eliminated simple milling processes to form the adapter. Thus, the adapter had to be shaped to fit the blade by either a process of (heat and pressure) plastic forming, or a process of casting the plastic to shape.

Of the designs under consideration, Figs. 5 and 6 show the designs given the most consideration. The adapter shown in Fig. 5 is an adaptation of a design by J. G. Rasmussen (2), which has functioned very well in his applications to certain compressor sections of jet engines. The design of Fig. 6 was a "clothes-pin" type arrangement

64

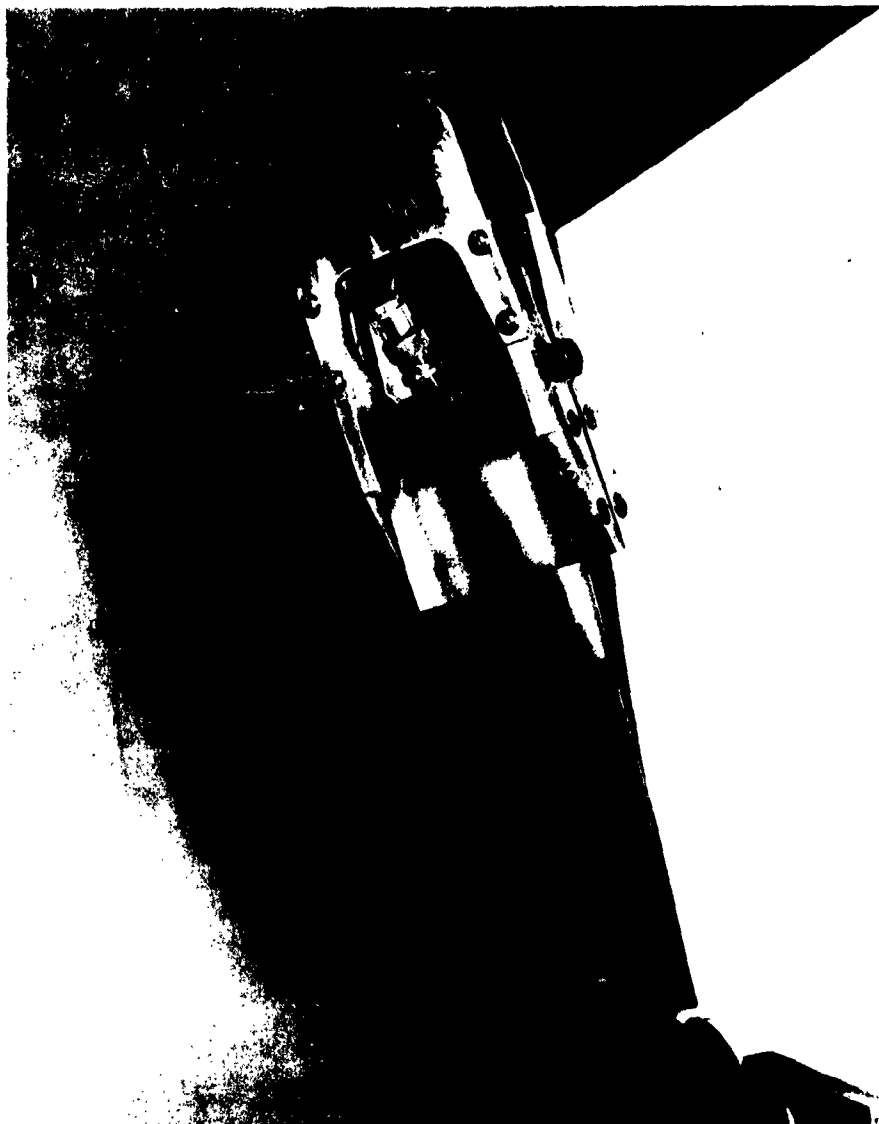Fig. 5. Clamp-on Pivot Adapter for J-79 Compressor.

Fig. 6. Clamp-on Stationary Adapter for J-79 Compressor.

and at this time is the type finally settled upon for our testing procedures. Note that in order to fulfill factor one in the above considerations, the adapters had to fit the complicated curvature of the blades.

CONSTRUCTION OF TRANSDUCER FIXTURES

The construction of the adapters for the first four stages of compressor blades involved a repeated forming process. The basic forming process consisted of:

(1) heating the acrylic plastic into its thermoplastic range,

(2) applying pressure to shape the plastic,

(3) allowing the plastic to cool so that the temperature is lower than the thermoplastic temperature, and

(4) handworking to ready the plastic for additional plastic deformation.

The actual formation of the adapters was specifically done as follows. Blocks of one-inch thick plastic were cut to the approximate dimensions required. The two blocks, one on each side of the blade tip, were then damped in a spring-loaded clamp, and the entire assembly placed in an oven. Experimentation showed that a temperature of 380°F for a period of 45 minutes gave the plastic the necessary plastic workability; shorter periods at higher temperatures proved detrimental to both the springs in the clamp and the plastic block. No advantage was gained by using lower temperatures. The blocks were formed in three stages. Fig. 7 shows the deformation of the plastic after each of the three forming stages.

After the assembly had been in the oven for 45 minutes, it was removed, placed in a vise, and force applied to deform the plastic
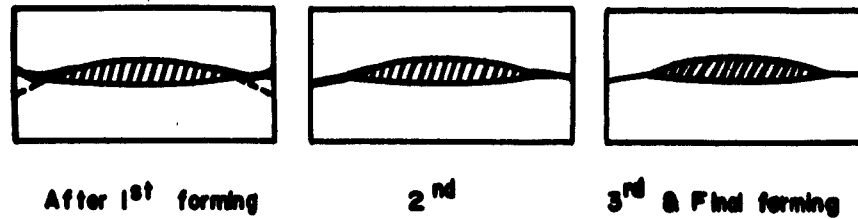
68

After 1st forming   2nd   3rd & Final forming

Figure 7. Forming of Plastic Adapters

such that it would conform to the shape of the blade. After a 30 minute cooling period, during which the plastic acquired a permanent set, the plastic blocks were filed in such a manner as to allow the blocks (when formed the second and third time in the ovens) to conform completely to the complex surface shape of the blade and to fit properly in the corners and along the edges of the blade.

After completion of the handwork, the procedure was repeated a second and third time. After the third run through the oven, no more handwork was necessary; and the blocks were then machined precisely to form the 66° angle and also to form the final dimensions. After forming, the external surface of the adapter block remained almost parallel with the direction of the centerline of the blade (see Fig. 8). Since the angle of incidence from the plane surface of the transducer to the complex blade surface varied, the average value determined approximately by the direction of the centerline of the blade was used as the reference for the angle α_1.

For this reason, the 66° angle required for the transducer was machined relative to the exterior surface. This assumption makes a
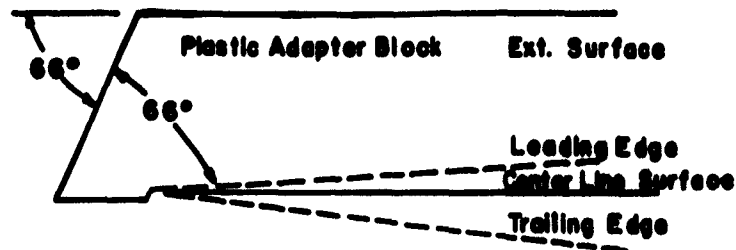
Figure 8. Machining of Critical Angle

good approximation to an average angle of incidence of 66° to the blade. Fig. 3 shows that the angle incident to the material being tested could deviate as much as ± 3 degrees and still maintain 70 per cent of maximum energy transfer to the blade.

After the plastic blocks were milled to the proper size, and the critical angle was milled to the proper value, aluminum parts were then assembled with a stiff spring to give the adapter a suitable amount of surface contact pressure. Previous adapters were built with serrations milled in the top and ends of the adapter to attenuate reflection signals within the plastic block. Other methods that have been tested on attenuating the signal in the blocks used an external damping mass (2). The addition of a mass with a low acoustical impedance will eliminate most of the signals reflecting from the plastic adapters. However, in this application of the ultrasonic technique, the elimination of these signals was unnecessary because the reflections were easily identified and did not interfere with the analysis of the blade.

EVALUATION OF TRANSDUCER SYSTEMS

A J-79 Transducer

The evaluation of the J-79 fixtures at this point has consisted entirely of laboratory testing. In the near future, these transducer adapters will be subjected to an actual environment of assembly line and overhaul operations. These evaluation results were compiled from difficulties and other factors that arose when different operators attempted to use the transducers for inspection of the J-79 compressor blades. Using the original design shown in Fig. 6, the adapter was placed on a blade with five small holes (.050" diameter) drilled as shown in Fig. 9.
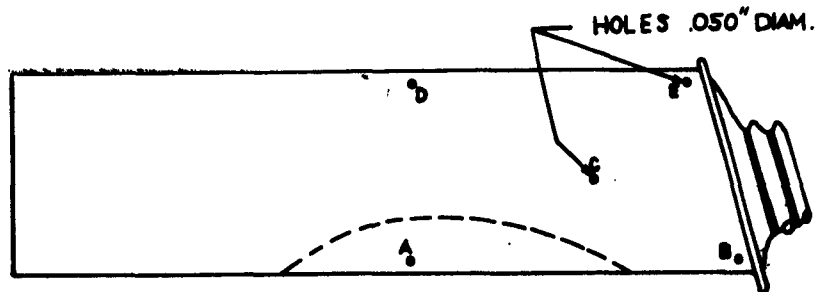
FIGURE 9.   TEST BLADE J-79

Scope picture gave an indication similar to Fig. 10 as shown below.
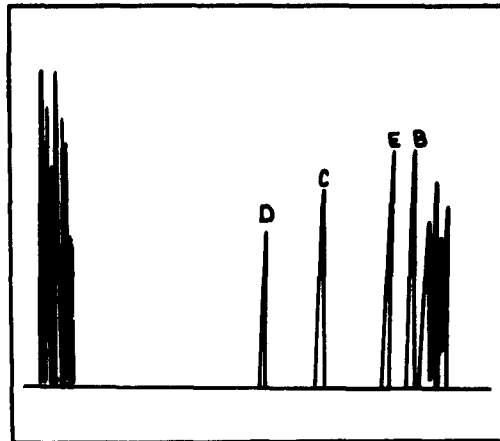
FIGURE 10. SCREEN PICTURE

It was learned from this trace (Fig. 10) that hole A as shown in Fig. 9 was not being detected. It was found that hole A was being detected, but the signal was so weak that it could be concluded that the zone shown in dotted lines (Fig. 9) was nearly a dead area. This caused concern due to the fact that a stationary transducer attached at the end had a directed beam and might not adequately sweep the entire surface of the J-79 compressor blade.

A modification was performed to the existing adapter and resulted in the apparatus shown in Fig. 11.

Using the same blade with the five holes drilled (Fig. 9), the modified adapter was used and the following were observed:

(1) The movable transducer located at the rear of adapter produced

72
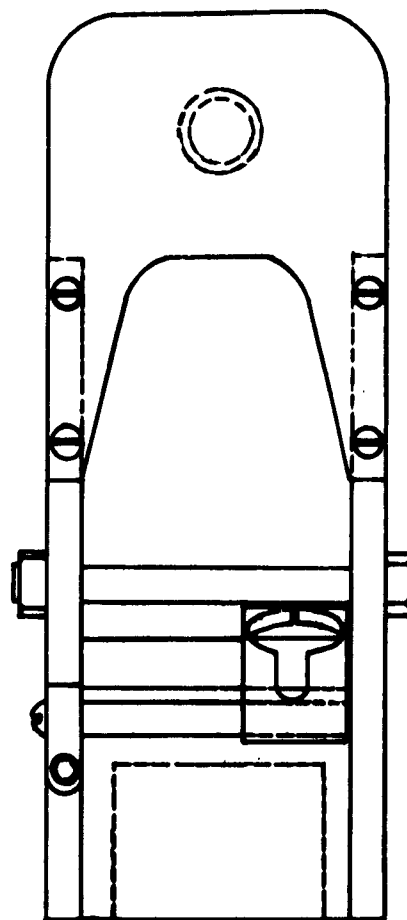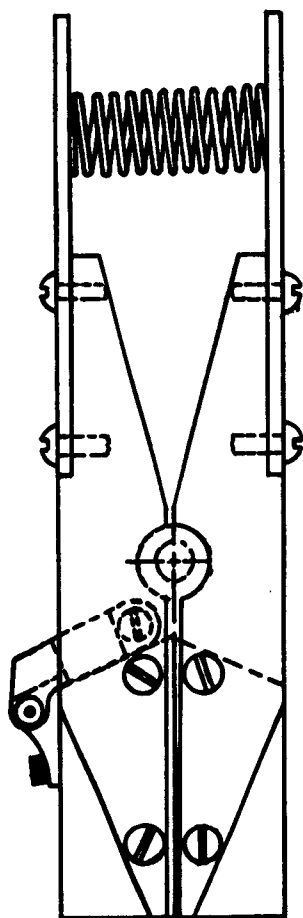
FIGURE 1L   TRANSDUCER-ADAPTER   J-79 4th STAGE   FULL SCALE

a directed beam as was expected.

(2) By moving the transducer, it was observed that the areas directly in front of transducer were having the strongest energy reflection.

(3) By slowly traversing from one side of the adapter to the other, with the straight beam transducer, the operator can detect any flaws appearing in the blade perpendicular to the path of the beam.

(4) By changing to a movable transducer, certain variables that were originally part of the problems encountered were again being introduced; these being

   (a) Back reflections on the screen will move while the transducer is being traversed on the adapter due to the sloping platform of the blade.

   (b) Pressure can vary somewhat on applying the sliding transducer to the adapter.

Notwithstanding the varibles introduced by the sliding transducer, this is the best adapter developed at present for the J-79 compressor.

B. J-35 Transducer

The J-35 transducer adapter as shown in Fig. 12 has had somewhat more extensive testing than the other two adapters (J-79, J-71). Only the first stage of the J-35 compressor was tested primarily because of the availability of the blades. However, since these blades were somewhat smaller than the other compressors that were tested, if the adapter worked satisfactorily for the first stage, there would be no problem on the succeeding stages, as the smaller blades were much easier to test.
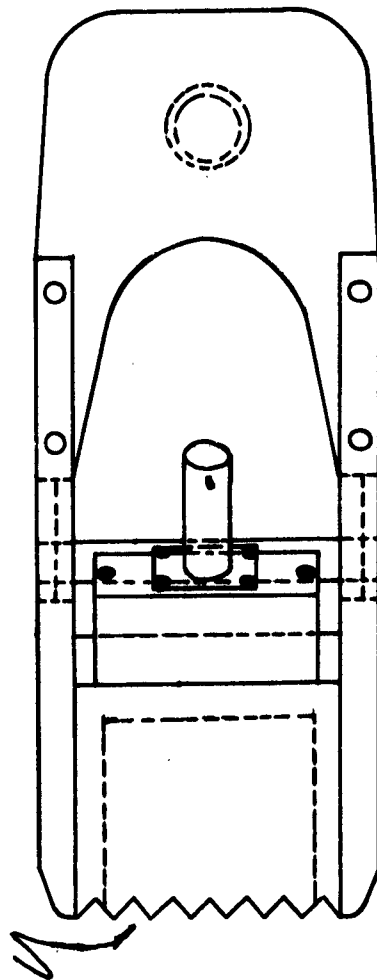
74
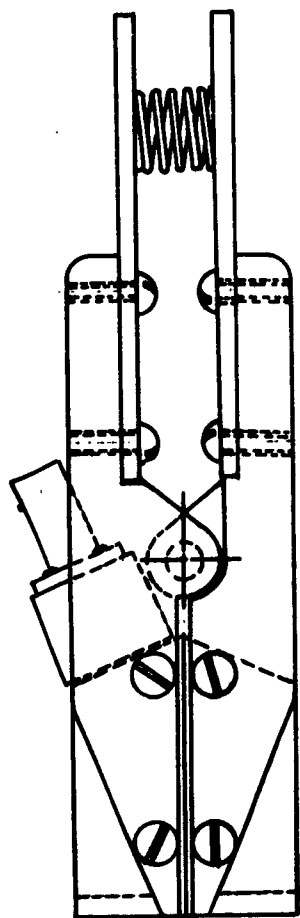
SERRATIONS

FIG. 12.- TRANSDUCER-ADAPTER J-35 1ST STAGE   FULL-SCALE

Sixty J-35 compressor blades with flaws were tested with the adapter and then were compared to the results from testing with the miniature surface wave transducer and with Zyglo dye penetrant.

The miniature surface wave transducer worked very well on the J-35 blades. The only objection, again, is:

(1) The operator must have a certain degree of competence and experience.

(2) The pressure and position of the transducer on the blade will be variable factors, depending upon the operator.

The adapters for the J-35 compressor have only been made for the first stage, due mainly to the availability of the blades.

It was learned from testing of the first stage blades that the clamp-on stationary type transducer would function properly provided the following are observed:

(1) Oil Coupling -- A good film of oil must be applied between adapter and blade.

(2) Transducer Size -- A transducer with sufficient width must be used to allow complete coverage of the blade from trailing edge to leading edge.

(3) Frequency of Transducer -- A 5.0 megacycle transducer functions better than a 2.25 megacycle for the J-35 compressor blades. The blades are shorter than those of the corresponding stages of the J-79, and less range is required of the transducer.

76

SELECTED BIBLIOGRAPHY

1. Schijve, J. "Ultrasonic Testing of Compressor and Turbine Blades for Fatigue Cracks," <u>Report MP157 of the National Lucht-vaartlelaboratorium</u>, Amsterdam, Holland, Feb. 1959.

2. Rasmussen, J. G. "Ultrasonic Inspection of Turbine and Compressor Rotor Blades for Cracks and Other Flaws," <u>Nondestructive Testing</u>, Vol. XVI, No. 3, 1958.

3. American Institute of Physics Handbook, Chapter 3, page 80.

4. Randles, P. W., "The Behavior of Elastic Waves Near a Free Boundary," Master's Thesis, Oklahoma State University, Stillwater, Okla., August 1963.

5. Redwood, M., <u>Mechanical Wave Guides</u>, The MacMillan Company, New York, 1960.

APPENDIX I

The following figures illustrate designs and application to blades that were investigated:

Fig. 13. Overhead View of Pivot Type Adapter

Fig. 14. J-35 Clamp-on Stationary Type Adapter

Fig. 15. Clamp-on Adapter, Utilizing Straight-beam Movable Transducer for Third State J-79 Compressor.

Fig. 16. Small Aluminum Adapter with Positioning Stop Utilizing Miniature Surface Wave Transducer

Fig. 17. J-35 Adapter with Serrations Milled in Plastic Block

Fig. 18. Adapter on J-79 Blade Utilizing Sending and Receiving Technique

Fig. 19. Adapter on J-79 Blade Utilizing Dual Sending Transducers

Fig. 20. Clamp-on Adapter for J-71 Utilizing Straight Beam Movable Transducer

Fig. 21. Testing of J-79 Compressor Utilizing Transducer Adapter.
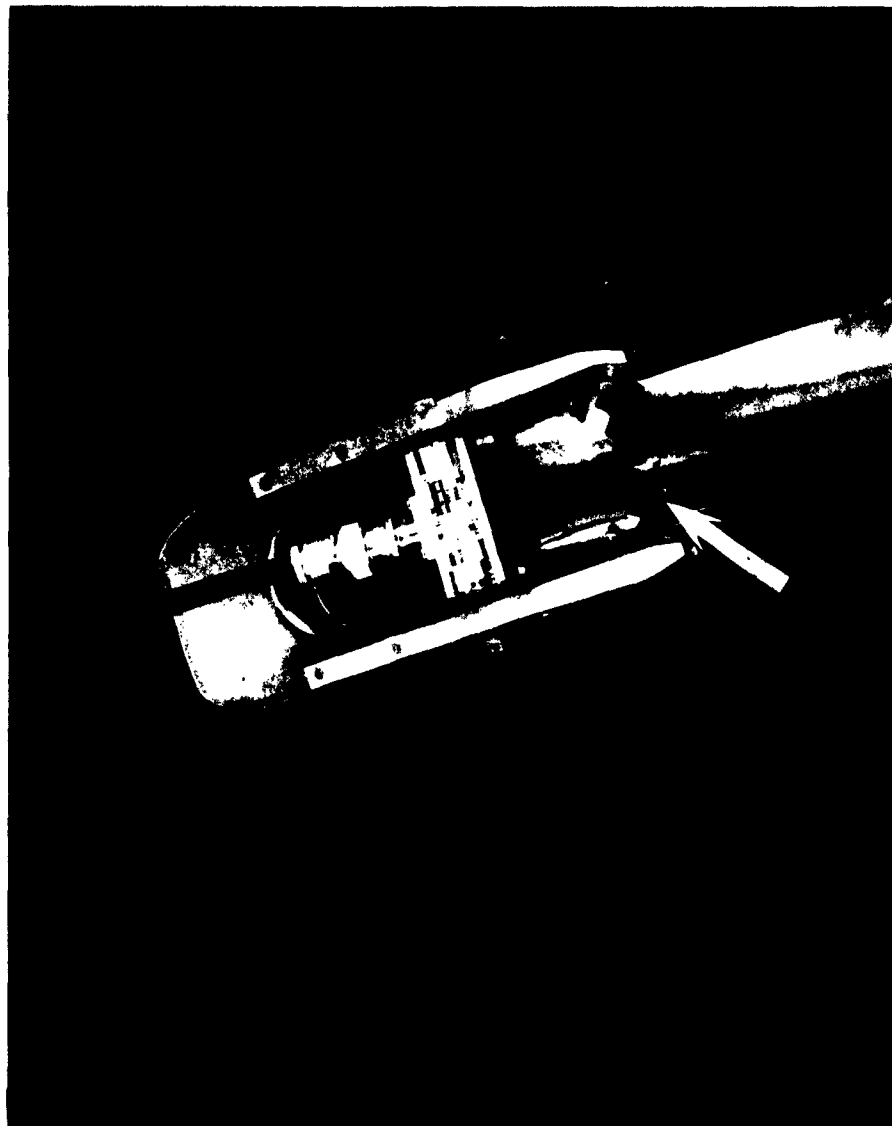
Fig. 13

Fig. 14.

Fig. 15.

Fig. 16.
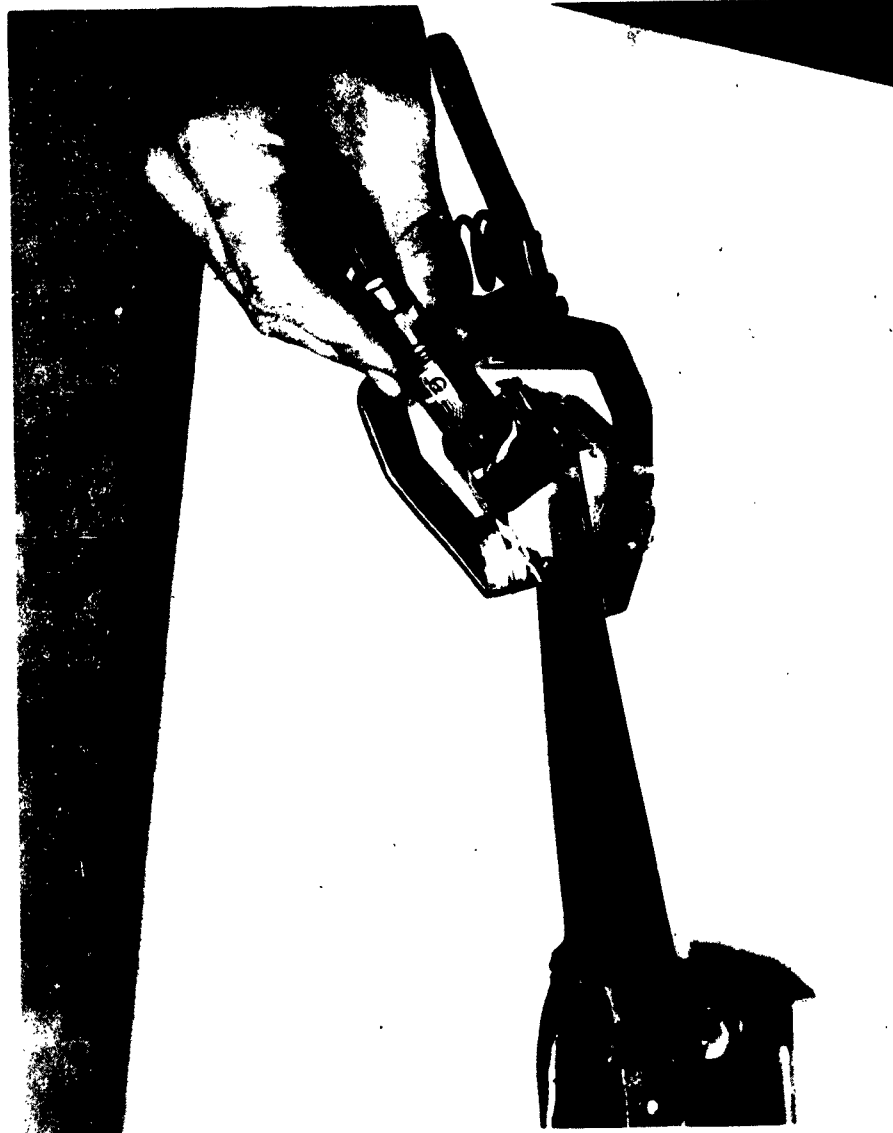
82

Fig. 17.

83

Fig. 18.

Fig. 19.

Fig. 20.

Fig. 21.

THE BEHAVIOR OF ELASTIC WAVES NEAR A FREE BOUNDARY

PROJECT PERSONNEL

Principal Investigator   Phillip Wayne Randles

89

INTRODUCTION

The question of how an elastic wave behaves near a free boundary originated from a proposed method of measuring surface fatigue flaw depth by using a shear wave beam aimed near the surface. The shear wave would be aimed so as to skim very close under the surface of the material and reflect when it struck a fatigue flaw as shown in Fig. 1.

This proposed method requires that a sizable portion of the energy could be concentrated into a narrow, straight beam shear wave. These requirements immediately present the question of whether or not a shear wave can continue to travel in a straight path when in a region near a free boundary. A free boundary will not support normal or shearing stress at the boundary surface.

A shear wave is conveniently produced in a steel bar by an incident longitudinal (compressive) wave passing through a plastic material in contact with the steel. The longitudinal wave is refracted at the interface, and a shear wave is produced in the steel. Snell's law of refraction, which related the velocity and angle of the incident wave to the velocity and angle of refracted wave, is given in Equation 1 on the following page (1)[1]. Refraction of the beam is shown in Fig. 2 for various different incident angles.

---

[1] Refers to Selected Bibliography for this section.

90

I = known distance
Θ = known angle
d = unknown flaw depth
d = I tan Θ

Fig. 1. Method of Measuring Flaw Depth.

Fig. 2. Refraction of Elastic Waves at a Solid-Solid Interface.

$$\frac{c_1}{\sin\alpha_1} = \frac{c_t}{\sin\alpha_t}$$ (1)

where c_1 = velocity of incident longitudinal wave

α_1 = angle of incident wave

c_t = velocity of refracted shear wave

α_t = angle of refracted wave.

A variation in the angle of incidence of the incoming longitudinal wave was easily obtained by mounting a straight beam piezoelectric transducer on a Lucite plastic block with a rotating cylindrical base as shown in Fig. 3. This design was taken after a similar transducer by Rasmussen (2).
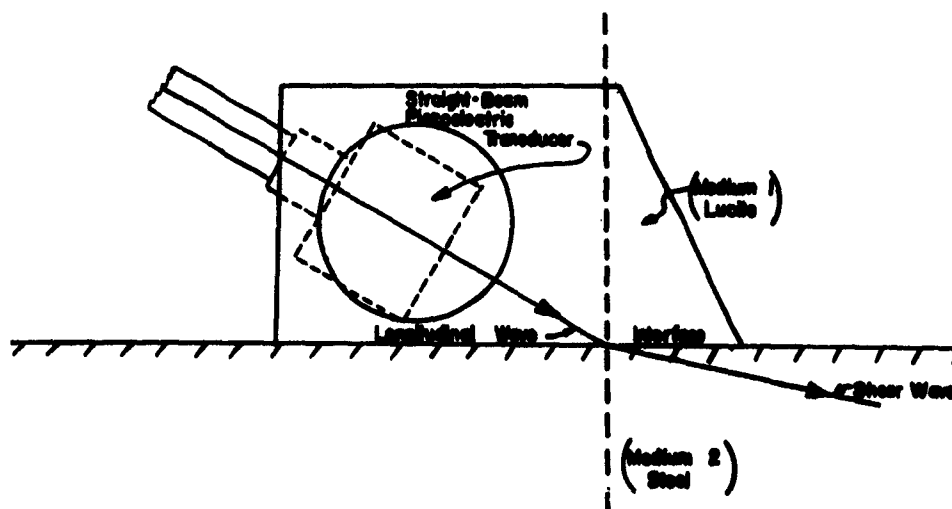
Fig. 3. Variable Angle Transducer Holder.

Since the longitudinal wave velocity is less than the shear wave velocity in steel, the shear wave is refracted further away from the normal than the incident longitudinal wave as shown in Fig. 2. This fact makes it possible to adjust the incident wave at a critical angle and produce a Rayleigh surface wave along the interface between the Lucite and steel. The high incidence shear wave should be produced when the angle of incidence is slightly smaller than the critical angle.

Ultrasonic elastic waves are interpreted from a signal, which is picked up by a receiving transducer, amplified, and displayed on a screen. The electronic network and schematic of the receiving instrument is explained by Daniel (3) and will not be repeated here.

The signals are interpreted by considering the base line of the signal as time and the ordinate as the amplitude, as shown in Fig. 4. The output of the transmitter is shown as the initial pulse on the left side of the screen representing zero time, and any signal appearing to the right is from a wave resulting from this output. The distance between the initial pulse and any subsequent signal is directly proportional to the time required for the initial pulse to be transmitted and received again.
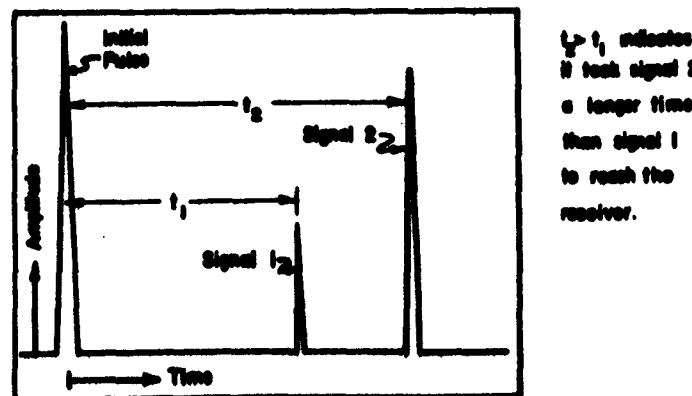
Fig. 4. Typical Screen Picture.

93

SUMMARY

The object of this investigation is to study the behavior of shear waves near a free boundary. Previous experimental analyses have led to the belief that a shallow shear wave may be instrumental in determining the depth of transverse fatigue cracks.

Experimental studies proved that a shear wave near a free boundary curves in a predictable manner, with a positive rate of change of slope. Although the curvature is slight, a shallow shear wave can be directed to re-emerge to the surface.. The curving path of the wave can be oriented in such a manner as to pass under a given flaw depth, within limits, without producing a reflection.

The success of the laboratory tests indicates that the principle may be feasible for discriminating flaw depths in some complex configurations of turbojet compressor blades and allied parts. The difficulties in this application lie in the setting of the critical angle of incidence of the transducer. The critical angle variation for the curving shear beam is quite narrow, and it may prove to be difficult to produce a uniform shallow shear wave over a broad surface of the blade. Further investigation should be carried out to determine whether this obstacle is serious.

EXPERIMENTAL OBSERVATIONS

The experimental work consisted of two parts. The first was finding and identifying a signal which was thought to be from a shear wave that was being influenced by the boundary. The second part was determining as much as possible about this wave including the manner and degree in which it was being influenced.

Transmitter-Receiver Setup

The most effective method to detect a signal from an elastic wave is to use a transducer for this purpose alone. Another transducer is used to produce the wave allowing it to travel directly from one transducer to the other without requiring energy losing reflections, which is the case when a single transducer is used both to transmit and receive the wave signal. The use of two separate transducers will be called a transmitter-receiver setup, and this is the arrangement which was used to produce and detect the elastic waves in this investigation.

The transmitter-receiver setup consisted of two straight beam piezoelectric transducer mounted on Lucite plastic blocks (as in Fig. 3) so as to give a variation of the angle of incidence for both the transmitter and receiver. The setup is shown in Fig. 5.

The frequency of both transducers was 2.25 mc (megacycles per second), and the material in which the waves were transmitted was a 4-inch square steel bar 18-inches long.
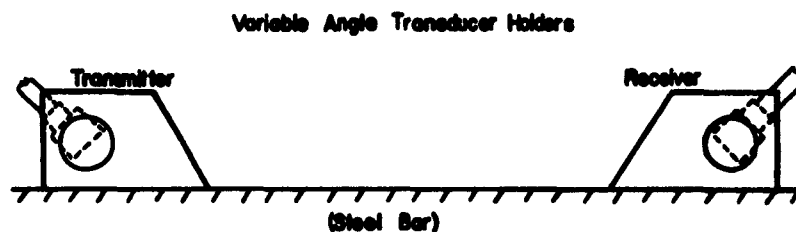
Variable Angle Transducer Holders

Transmitter   Receiver

(Steel Bar)

Figure 5. Transmitter - Receiver Setup

Dispersion of Beam

The piezoelectric transducers used to produce and receive an ultra-
sonic elastic wave emit a relatively narrow focused beam; however, it
could not be expected that the beam of waves would travel in a coherent
path and not disperse to a certain extent. Since this dispersion was
present, a beam of elastic waves produced by aiming a transducer in a
certain direction was found to be a field of waves with a maximum ampli-
tude occurring in the center of the beam, but with a decreasing ampli-
tude in all directions away from the center. There was never a well
defined boundary of the beam as would be expected if dispersion were
not present.

Rayleigh Surface Wave Signal

The critical angle at which the maximum Rayleigh surface wave is produced for refraction of a longitudinal wave from Lucite into steel was found to be approximately 66°. It can be seen from Fig. 2 that the energy transmitted in this surface wave is made up of that energy which would go into the refracted shear wave if the angle of incidence were decreased. In the transmitter-receiver setup with both angles set at 66°, a large signal was displayed on the screen of the receiver corresponding to the first wave front of Rayleigh surface waves to arrive at the receiver. The surface wave was the first to arrive at the receiver since there were no signals on the screen between the initial pulse and this signal. However, to the right of the first signal was a large number of signals corresponding to trailing surface waves and reflection paths through the plastic block. These trailing waves were of no interest since only the first direct Rayleigh surface wave signal gave any useful information for this arrangement. Since the transmitter-receiver setup was the optimum arrangement for receiving Rayleigh surface waves and the dispersion of the beam was present, a large signal remained on the screen for angles substantially different from 66°.

Identification of Waves

Any wave propagating in the steel bar was easily identified as a surface or internal wave by damping on the surface of the bar. A surface wave signal can be greatly decreased by damping since it is possible for a large portion of the energy to be absorbed. The damping was easily

done by placing a finger in contact with the surface of the bar between the transmitter and receiver. An internal wave, such as a longitudinal wave or shear wave is unaffected by damping on the surface except at points where the wave reflects from the surface, and damping at these points absorbs a small amount of energy as compared to a surface wave.

The S-wave Signal

When the angles of incidence were decreased, making a shear wave more probable, the surface wave signal was decreased by a large degree; but the signal still remained strong due to the dispersion of the beam described earlier. When the angles were decreased by about 7° from the critical angle of 66°, a small signal appeared on the screen just to the left of the Rayleigh surface wave signal. This signal reached a maximum when both the angle of the transmitter and receiver were adjusted to approximately 57°. This small signal was interpreted to be from a curved shear wave and will be called the S-wave. The reasons for this conclusion will be given in the remainder of this chapter.

The first observation was that the S-wave signal could not be damped at any point in the surface between the transmitter and the receiver and thus was traveling beneath the surface.

The S-wave signal remained a maximum for the angles of incidence adjusted at approximately 57° regardless of the distance between the transmitter and the receiver. This eliminated the possibility that the wave path length was a function of the angle at which it entered the bar.

The fact that the S-wave signal appeared to the left of the surface wave signal, indicated that the S-wave had made the trip between the transmitter and receiver in less time than the surface wave. The ratio of the time required for the S-wave to travel from the transmitter to the receiver to the time required for the Rayleigh surface wave to travel the same distance remained approximately constant at 0.92 regardless of the distance between the transmitter and receiver. These signals are shown in Fig. 6. This constant ratio indicated that the S-wave and the Rayleigh surface wave were taking approximately the same length path, but the S-wave was traveling at a slightly greater velocity. The paths being of approximately the same length rules out the possibility that a high velocity longitudinal wave was being reflected from the bottom of the bar. It is well known from Rayleigh (4) and Sokolnikoff (5) that a Rayleigh surface wave in steel travels with a velocity of slightly over nine tenths of the shear wave velocity, which is consistent with the ratio of the times required to travel approximately the same distance.

The S-wave was not present on the surface of the bar, but the path it had taken between the transmitter and receiver was approximately the same as the Rayleigh surface wave path directly along the surface. Therefore, it was concluded that the wave was traveling very near the surface in a curved path as shown in Fig. 7.

While damping in the region between the transmitter and receiver did not damp the S-wave signal, it did produce very interesting results. By expanding the range of the receiving instrument, the portion of the signal between the S-wave signal and Rayleigh surface wave signal could be displayed across the entire screen. Damping on the surface caused

99
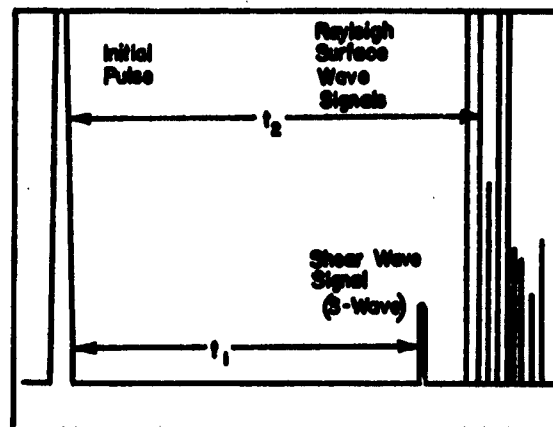
$t_1/t_2 \approx 0.92$
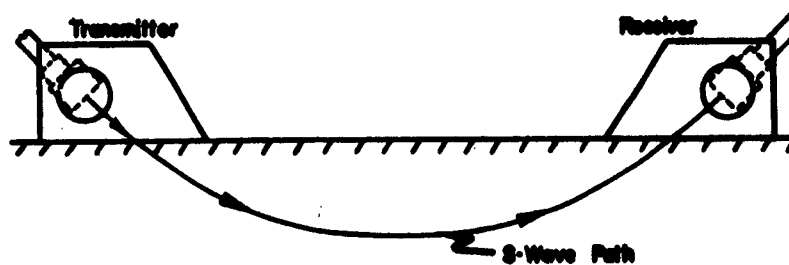
Figure 6. S-Wave Signal on Screen

Figure 7. Curved Shear Wave Path

a new signal to appear on the screen between the S-wave signal and the Rayleigh surface wave signal which looked similar to the S-wave signal. It required a longer time to reach the receiver than the S-wave signal and a shorter time than the Rayleigh surface wave signal. Further investigation indicated that the wave causing this new signal traveled to the point of damping beneath the surface and continued from that point to the receiver as a Rayleigh surface wave. The point of damping divided the distance the point of entering at the transmitter and the point of exiting at the receiver into the same ratio as the new signal divided the distance between the Rayleigh surface wave signal and the S-wave signal. This is shown in Fig. 8. When the damping was applied very near the receiver, the new signal almost coincided with the S-wave signal. Similarly, when the damping was applied very near the transmitter, the new signal almost coincided with the Rayleigh surface wave signal. The assumed path of the wave causing the new wave is also shown in Fig. 8.
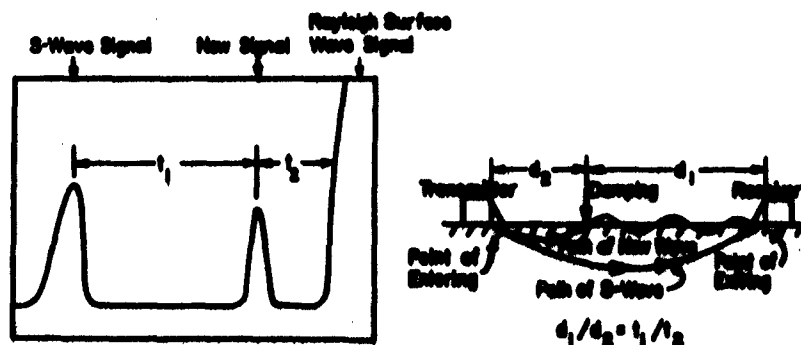

Figure 8. New Signal Caused by Damping

Depth and Shape of S-wave Paths

A true picture of the S-wave paths requires knowledge of the depth of the wave beneath the surface which would lead to a plot of the actual shape of the paths. A method was needed to measure the depth of the wave at various points along its path, then the path itself could be plotted.

On preliminary investigation, it was found that a certain thickness of metal was required to support the S-wave. For instance, a signal for the S-wave could not be produced in a $\frac{1}{2}$-inch plate. There were some signals present ahead of the Rayleigh wave signal, but the well defined S-wave signal was not present. The conclusion was that the wave was either being reflected and scattered by the bottom side of the plate or it was being affected equally by the bottom side, since it was also a stress-free surface. A $1\frac{1}{4}$-inch plate would transmit the S-wave signal just as well as the 4-inch bar.

The method used to measure the depth of the S-wave paths consisted of placing an obstruction in the path of the S-wave, thus determining how near the surface of the metal the obstruction could be before the S-wave struck it. The obstruction was a narrow saw cut made from the bottom side of the $1\frac{1}{4}$-inch steel plate. The cut was made with a band saw across the center of the 10 x 16-inch plate and it was made on a taper so that only 1/32-inch of metal was left above the cut on one side and 25/32-inch of metal was left above the cut on the other side as shown in Figure 9. This gave a variable depth of metal without imposing another stress-free boundary near the wave as would be done with just a tapered plate. The top of the plate was ground very smooth to avoid inconsistencies in the readings because of roughness of the surface.
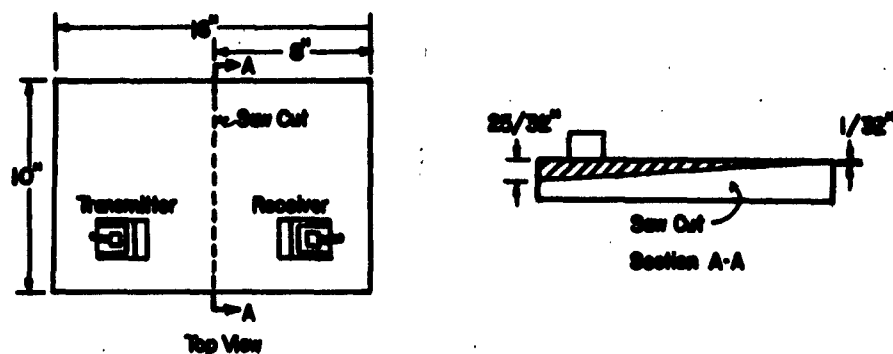
102

Figure 9. Plate With Tapering Saw Cut

The transmitter and receiver were placed on the top surface so that a line connecting the two and presumably the S-wave path would be perpendicular to the saw cut as shown in Figure 10. By moving the transmitter and receiver laterally across the plate parallel to the saw cut, when the metal above the cut became thinner than the depth of the S-wave path, the signal on the screen would begin to decrease and then disappear completely when it blocked all of the path of the wave (see Figure 10). A set distance between the transmitter and receiver fixed one S-wave path, where one path means the path taken by that portion of the wave which is received by the receiver transducer.
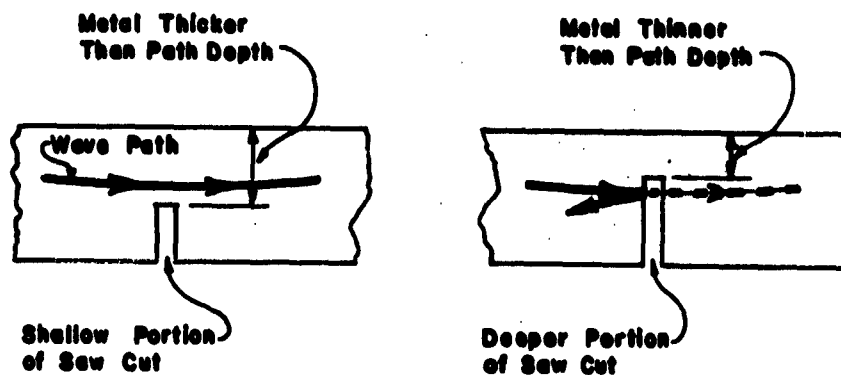
Figure 10. Curved Wave Hitting Saw Cut

A spacer was placed between the transmitter and receiver thus fixing
the distance between the point of entering and exiting the metal. For
each spacing, readings were taken for various points along the path. The
readings were taken by picking a point on the path where the depth was to
be determined and moving the transducers laterally so that this point
always remained over the saw cut. The amplitude of the signal corre-
sponding to a certain point on the path was recorded for points laterally
across the plate. Since the tapered cut was made linear, the lateral dis-
placement corresponded directly with a depth of metal above the cut. The
amplitude of the received signal was plotted versus the metal depth as
in Figure 11. These plots indicated that in the region of the plate
where the metal was very thin, no signal was able to get past the cut and
as the setup was moved in a direction to increase the depth, some portion

of the signal began to pass over the cut. Through this transition region, the amplitude increased approximately linearly with the increasing metal depth until at a certain depth, all of the wave passed over the cut; and no matter how much deeper the metal got, the signal would not increase.
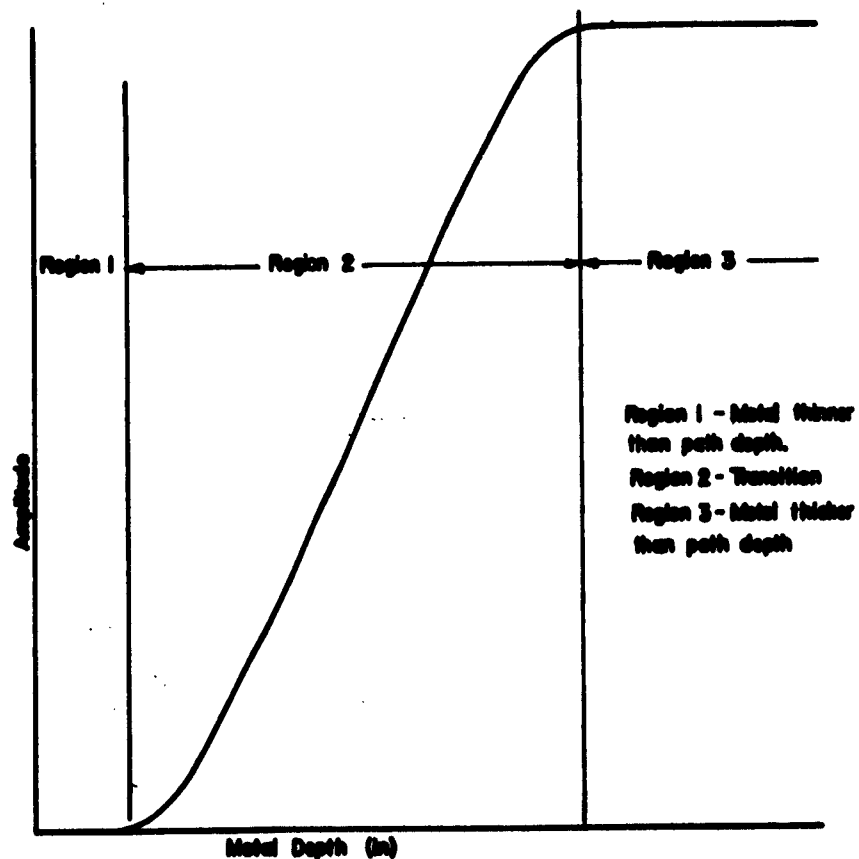

Figure II. Typical Plot of Amplitude vs. Metal Depth

Each plot of the type shown in Fig. 11 represents the amplitude of the signal versus metal depth for just one point along the path, and it gives information about the depth of the path at the point. The data were normalized so that the maximum signal had an amplitude of ten corresponding to no obstruction in the path of the S-wave. Since there was some question about the exact location of the top and bottom of the path, it was decided to call the depth of the location of the path a single point corresponding to an amplitude of five. This point gave the approximate depth of the center of that portion of the wave which reached the receiver. A family of amplitude versus metal depth plots is shown in Figs. 14, 15, 16, 17, and 18 in the Appendix for just one path length.

A smooth line drawn through each depth point and connecting with zero depth points at each end where the wave entered and exited gave a plot of the wave path for a given distance between the transmitter and receiver (see Fig. 12).

Similar curves were drawn for each of five different path lengths (see Figs. 18, 19, 20, 21, and 22 in the Appendix). Superimposing the path plots onto one plot produced a family of paths which represents the direction of travel of the entire beam (see Fig. 13).

Rather than thinking of each line in Fig. 13 as a distinct path, the entire plot should be thought of as a field of a shear wave beam with the lines indicating the direction of travel of each portion of the beam.

Discussion

All of the experimental observations can be explained by the beam shown in Fig. 13. The angle of entering and of exiting for the wave
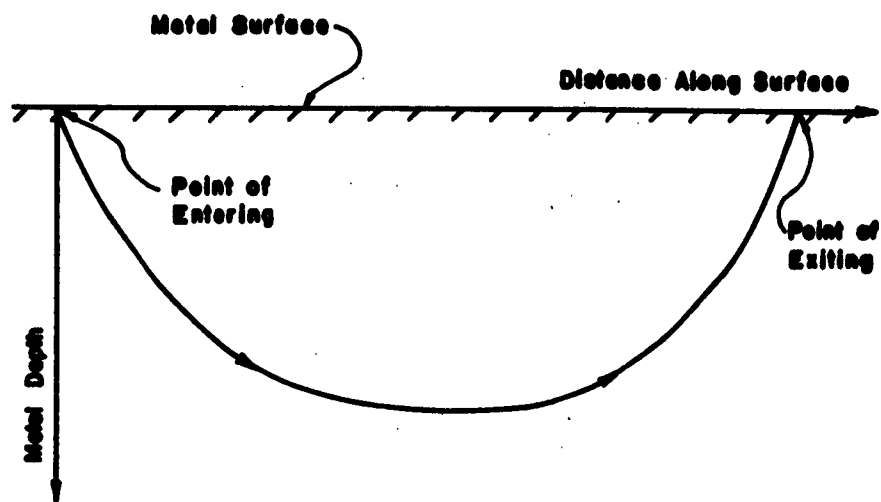
106
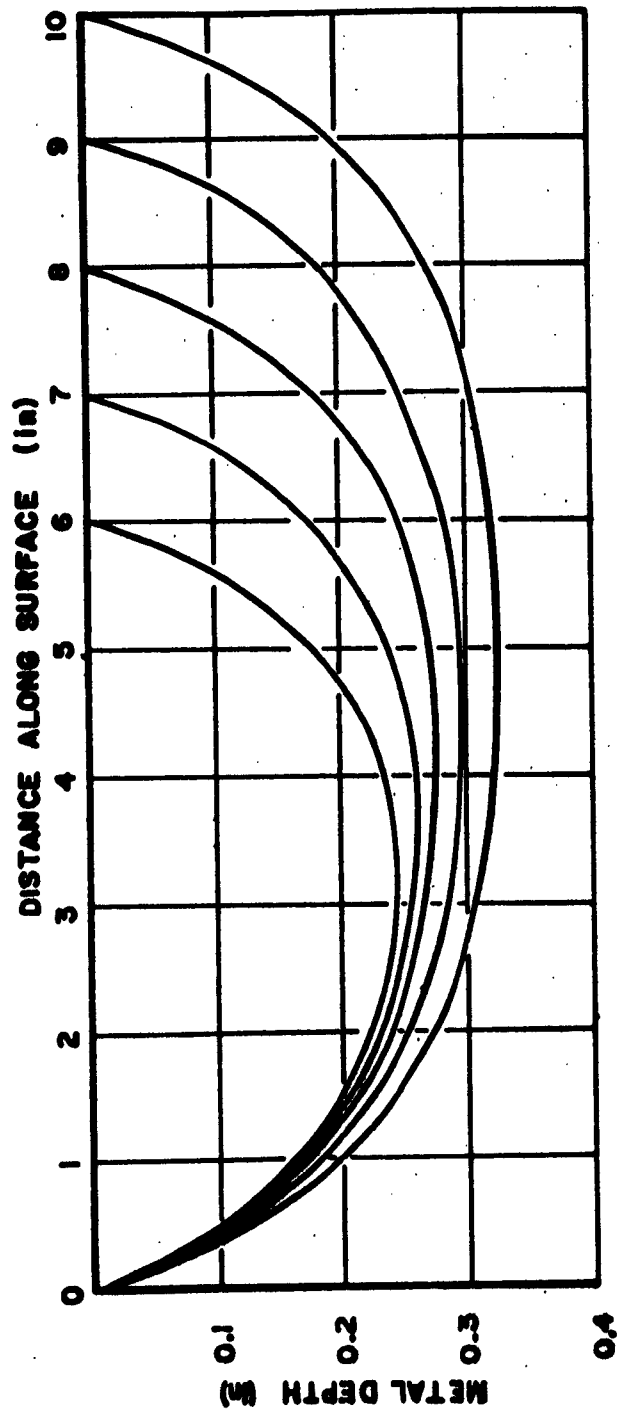
Figure 12. Typical S-Wave Path

FIGURE 13. CURVING SHEAR WAVE BEAM

can be measured from tangents to the curves at each end. The curves are symmetrical about the centers of the paths so that the angles at each end are the same, as was observed. The data were difficult to take near the ends of the paths because the transmitter and receiver were sitting almost directly over the saw cut, and this caused additional signals which interfered with the S-wave signal. There were not enough data available near each end of the path to give a very accurate value for the angles, so the curves were drawn tangent on an angle which was calculated from Snell's law, Equation 1, and the known angle of incidence of the longitudinal wave in the Lucite block.

At the critical angle

$$\alpha_1 = 66°$$

$$\alpha_t = 90°.$$

Giving

$$\frac{c_t}{c_1} = \frac{\sin\alpha_t}{\sin\alpha_1} = \frac{\sin 90°}{\sin 66°} = 1.095.$$

At maximum S-wave signal

$$\alpha_1 = 57$$

giving

$$\sin\alpha_t = \frac{c_t}{c_1} \sin\alpha_1 = 1.095 \sin 57° = 0.914$$

$$\alpha_t = 66°$$

It can be seen from the paths that they did not have to be distorted to cause them to come in on a tangent to 66° from the vertical normal. All of the lines for each path are seen to enter and exit the surface a at the same angle regardless of the path length.

The S-wave signal could not be damped on the surface between the transmitter and receiver simply because it was not present on the surface. In order to explain the new signals which were produced when damping was applied, it is necessary to say that the portion of the wave which strikes the surface between the transmitter and receiver is reflected and scattered so that practically none of it reaches the receiver. When damping is applied, some of this energy which strikes the boundary is converted into a Rayleigh surface wave and continues to the receiver in that form and produces a signal. It was found that when an ordinary straight shear wave is reflected from a boundary, some of the energy can be converted into a Rayleigh surface wave by applying damping at the point of reflection.

The constant ratio of the time required for the Rayleigh wave to the time required for the S-wave is explained by the fact that all of the path lines in Fig. 13 have approximately the same shape. Also, the length of the paths are almost the same as the ditance in a straight line between the two points. The large plots in Figs. 18, 19, 20, 21, and 22 in the Appendix are plotted with the depth scale expanded ten times the distance scale, but the actual path shapes are plotted below each figure. These paths are seen to be almost the same length as a line along the surface.

The resulting path plots are actually the only logical way to account for all of the experimental observations on the S-wave signal.

110

SELECTED BIBLIOGRAPHY

1. Redwood, M. _Mechanical Wave Guides_. The MacMillan Company, New York, 1960, p. 44.

2. Rasmussen, J. G. "Prediction of Fatigue Failure Using Ultrasonic Surface Waves," Nondestructive Testing, Vol. XX, No. 2, March-April, 1962, p. 106.

3. Daniel, J. A. "Development of an Ultrasonic Surface Wave Testing Standard," M. S. Thesis, Oklahoma State University, 1963, pp. 6-7.

4. Rayleigh, "On Waves Propagated along the Plane Surface of an Elastic Solid," _Proceedings of the London Mathematical Society_, Vol. 17, 1887.

5. Sokolnikoff, I. S., _Mathematical Theory of Elasticity_, McGraw-Hill Book Co., Inc., New York, 1956, pp. 71-73, 370-376.

6. Cagniard, L. _Reflection and Refraction of Progressive Seismic Waves_, McGraw-Hill Book Co., Inc., New York, 1962.

7. Fredicks, R. W. and L. Knopff. "The Reflection of Rayleigh Waves by a High Impedance Obstacle on a Half-Space," _Geophysics_, Vol. XXV, No. 6, Dec., 1960.

8. Jones, O. E. and A. T. Ellis. "Longitudinal Strain Pulse Propagation in Wide Rectangular Bars," _Journal of Applied Mechanics_, Vol. 30, Series E, No. 1, March 1963.

9. Kolsky, H. _Stress Waves in Solids_, Oxford University Press, London 1953.

10. Lindsay, R. B. _Mechanical Radiation_, McGraw-Hill Book Co., Inc., New York 1960.

11. Morse, P. M. and H. Feshbach, _Methods of Theoretical Physics Part I and II_, McGraw-Hill Book Co., Inc., New York 1953.

12. Sneddon, I. N. _Elements of Partial Differential Equations_, McGraw-Hill Book Co., Inc., New York 1957.

111

APPENDIX

112

APPENDIX

Several plots will be given in the following figures in order to illustrate how Fig. 13 was obtained. Figs. 14, 15, 16, and 17 give the Amplitude versus Metal Thickness plots for several positions along the nine-inch path. Figs. 18, 19, 20, 21, and 22 give the wave path shapes for each path length on which data were taken. In each of these figures, a small plot of the actual path shape is given at the bottom of the page. On these plots, both the ordinate and abscissa are on the same scale, enabling the actual shape of the wave travel to be visualized.

Two quantities will be defined which are used in the plots.

D = distance from point of entering to point of exiting

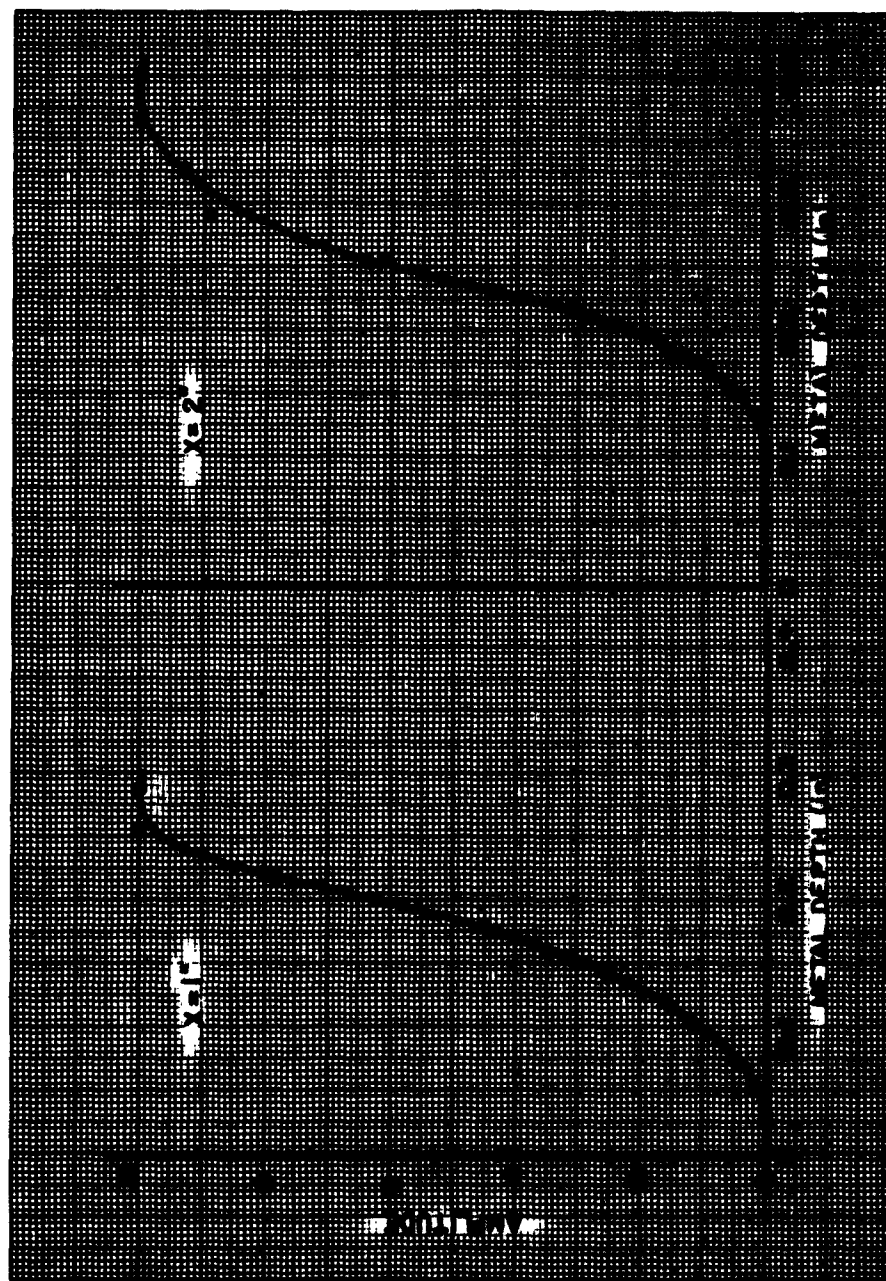x = distance from point of entering to some point along the path.
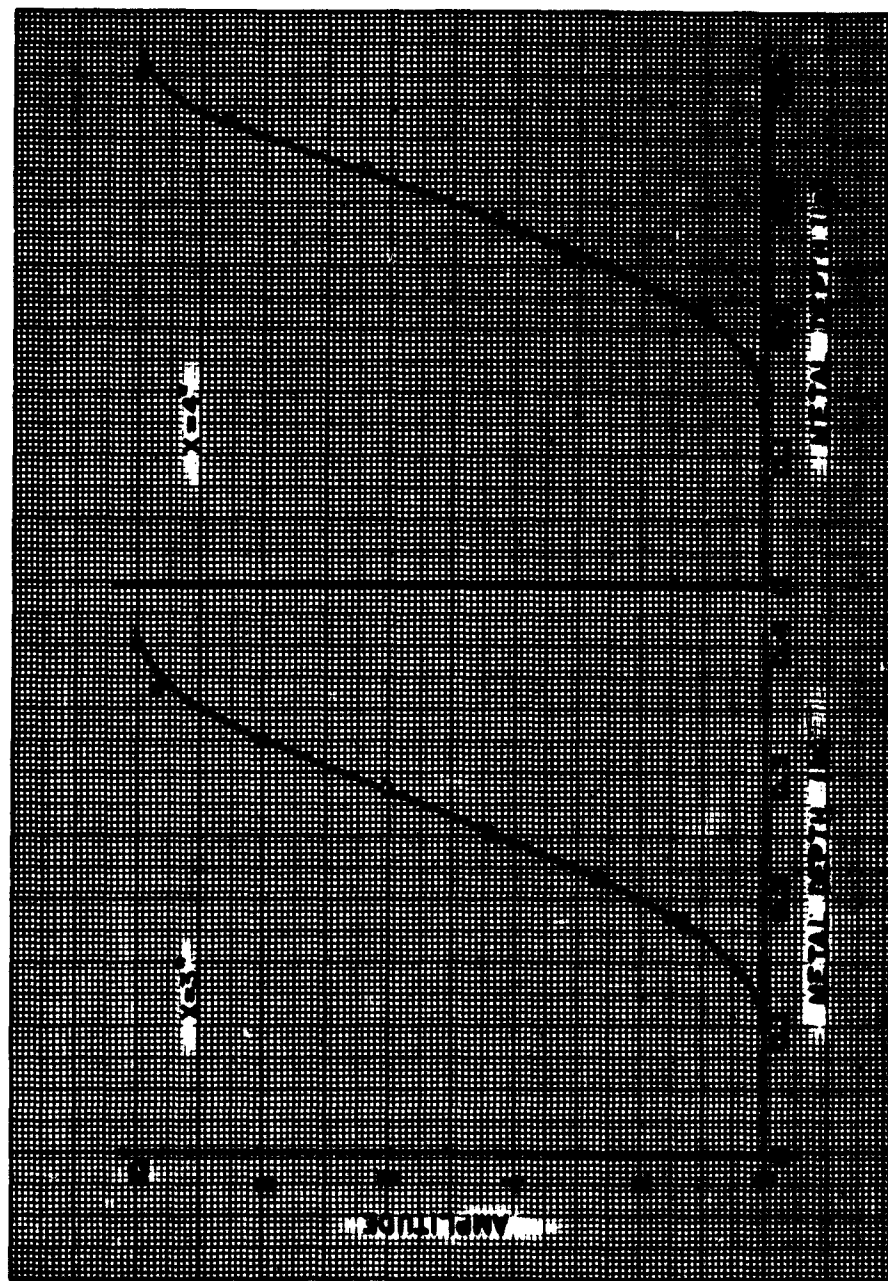
FIG. NO. 14 AMPLITUDE VS. METAL DEPTH D=9"
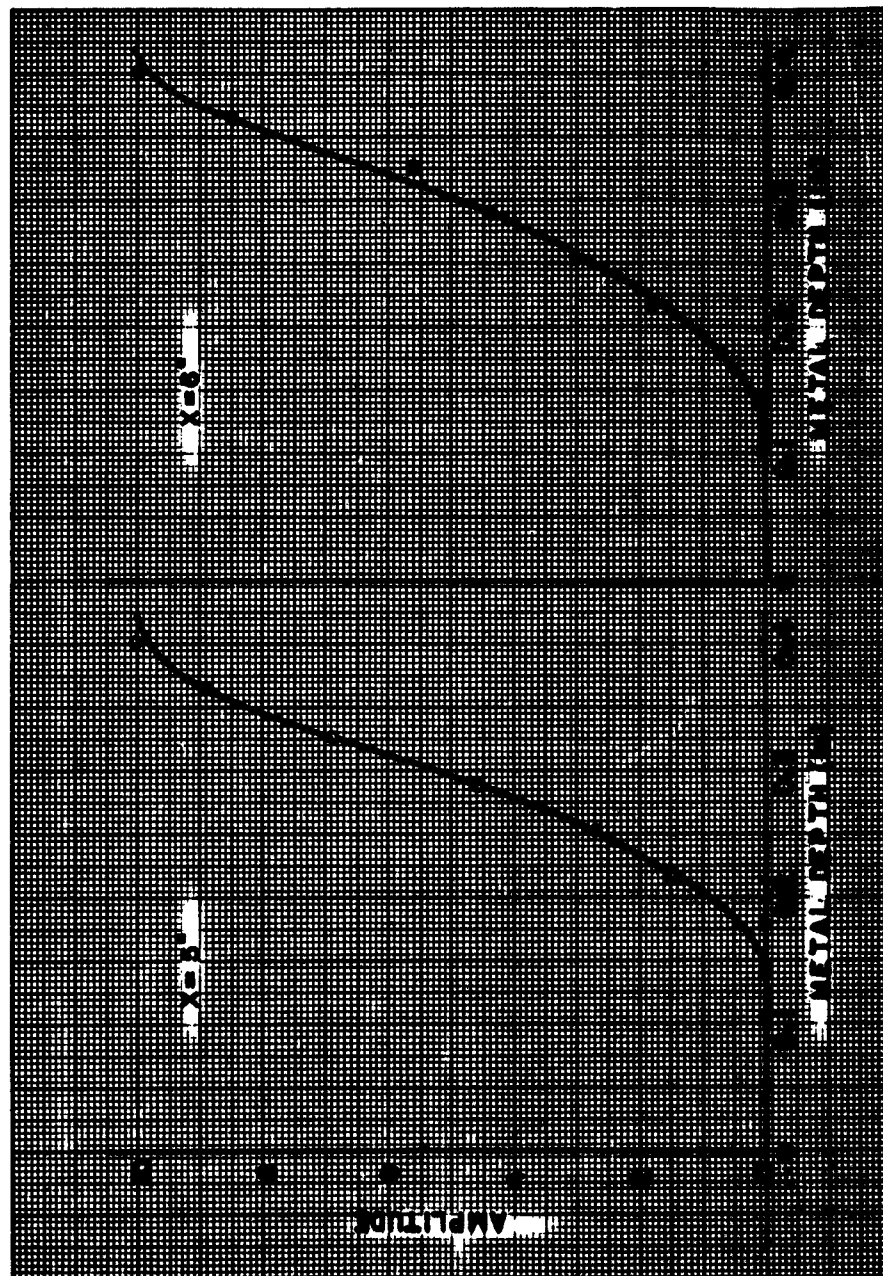
114

FIG. NO. 15 AMPLITUDE VS. METAL DEPTH D=8"

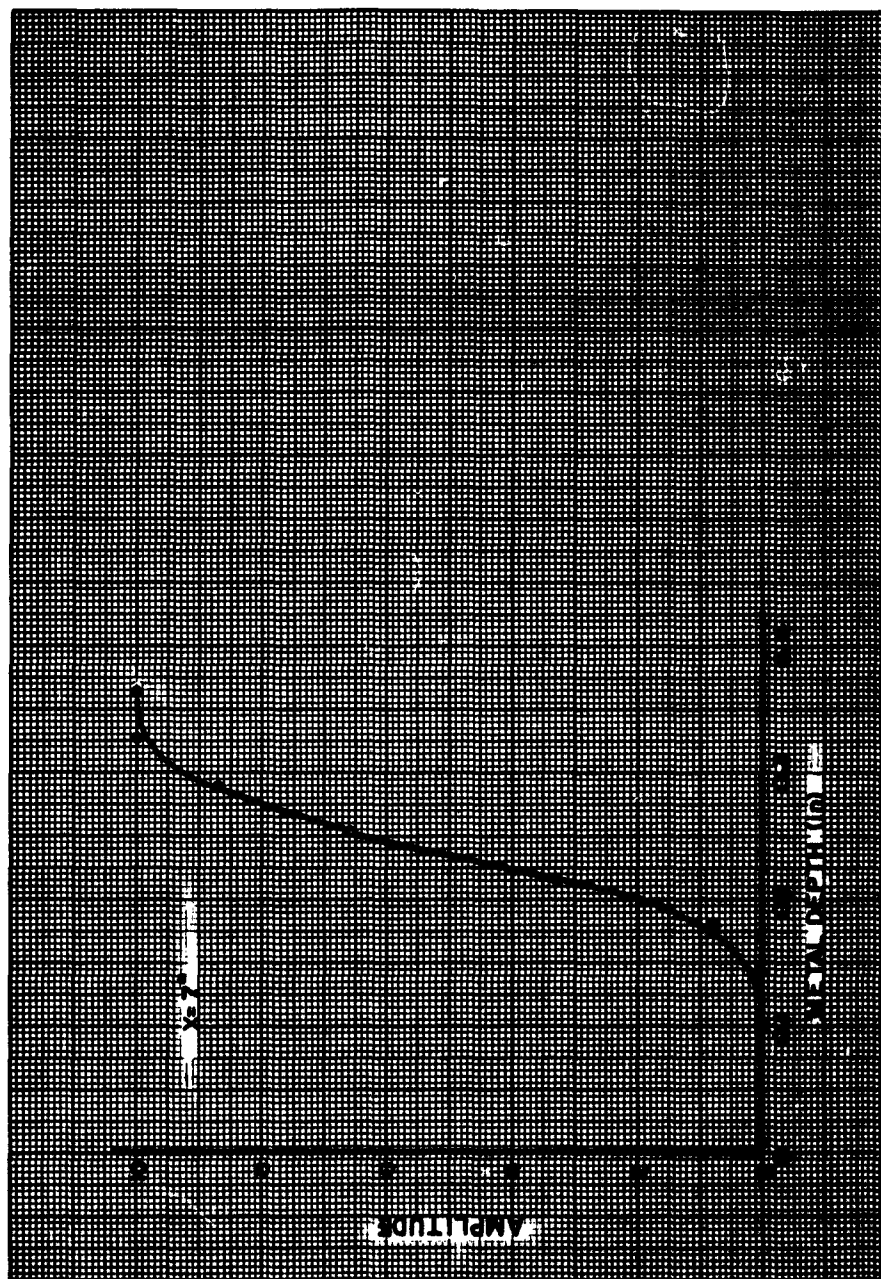FIG. NO. 16 AMPLITUDE VS. METAL DEPTH D = 9"

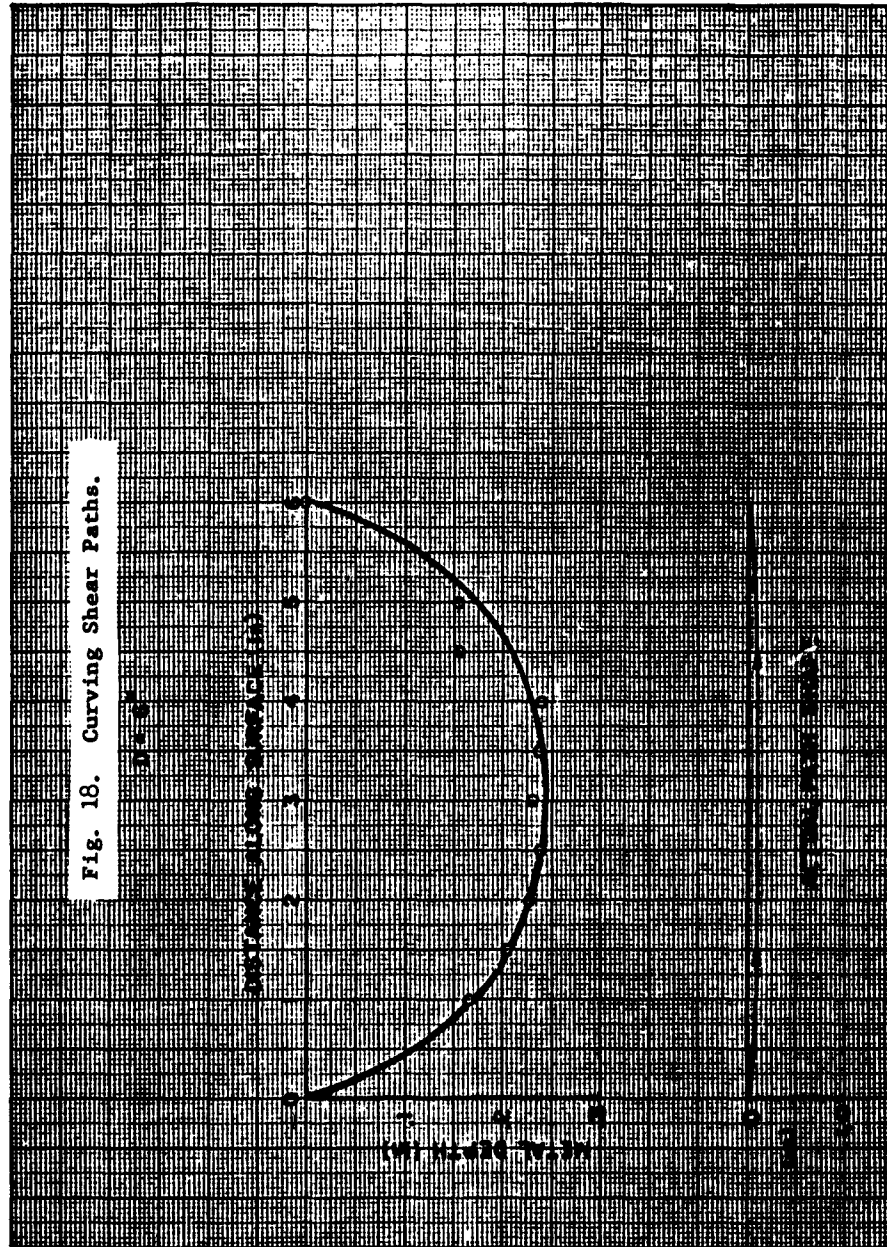FIG. NO. 17 AMPLITUDE VS. METAL DEPTH D=9"

117

Fig. 18. Curving Shear Paths.

Fig. 19. Curving Shear Paths.
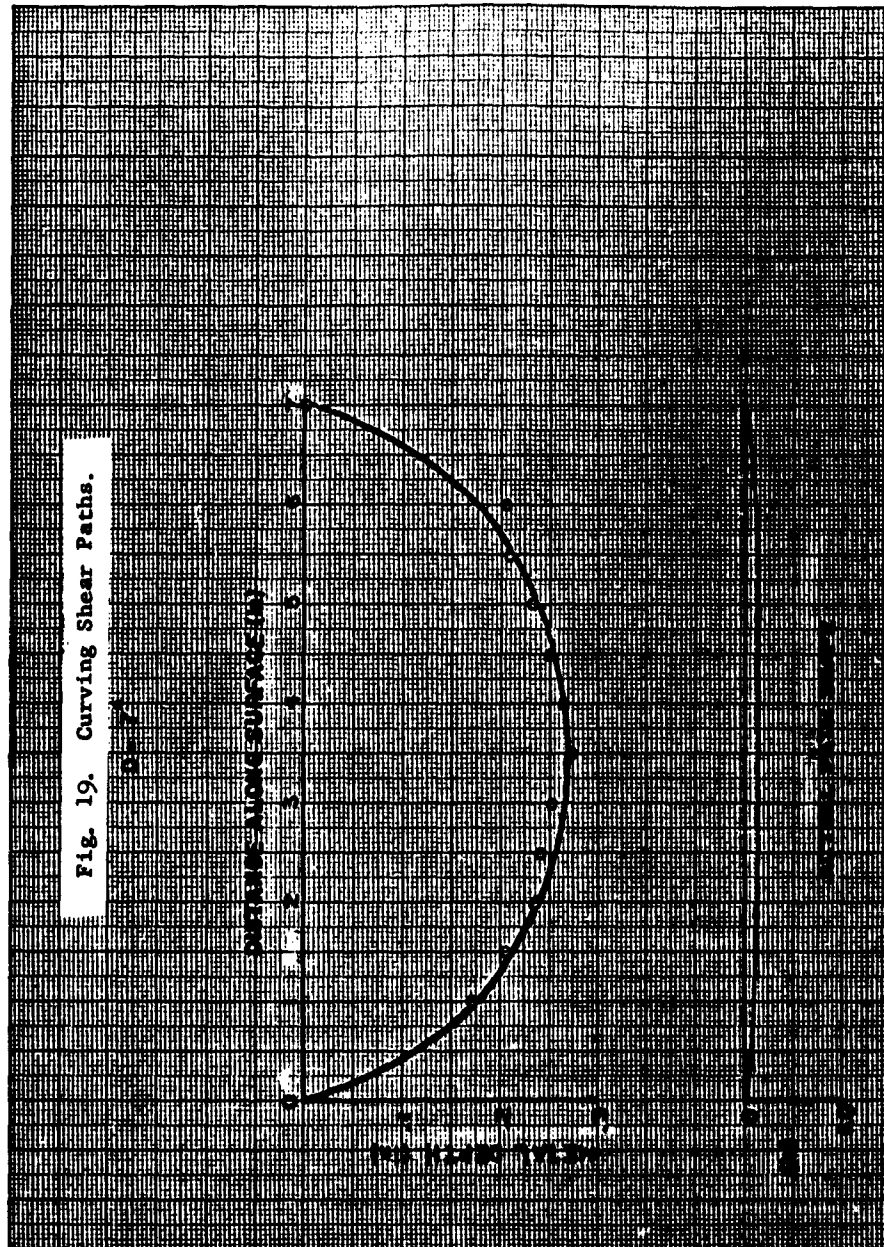
Fig. 20. Curving Shear Paths.

Fig. 21. Curving Shear Paths.
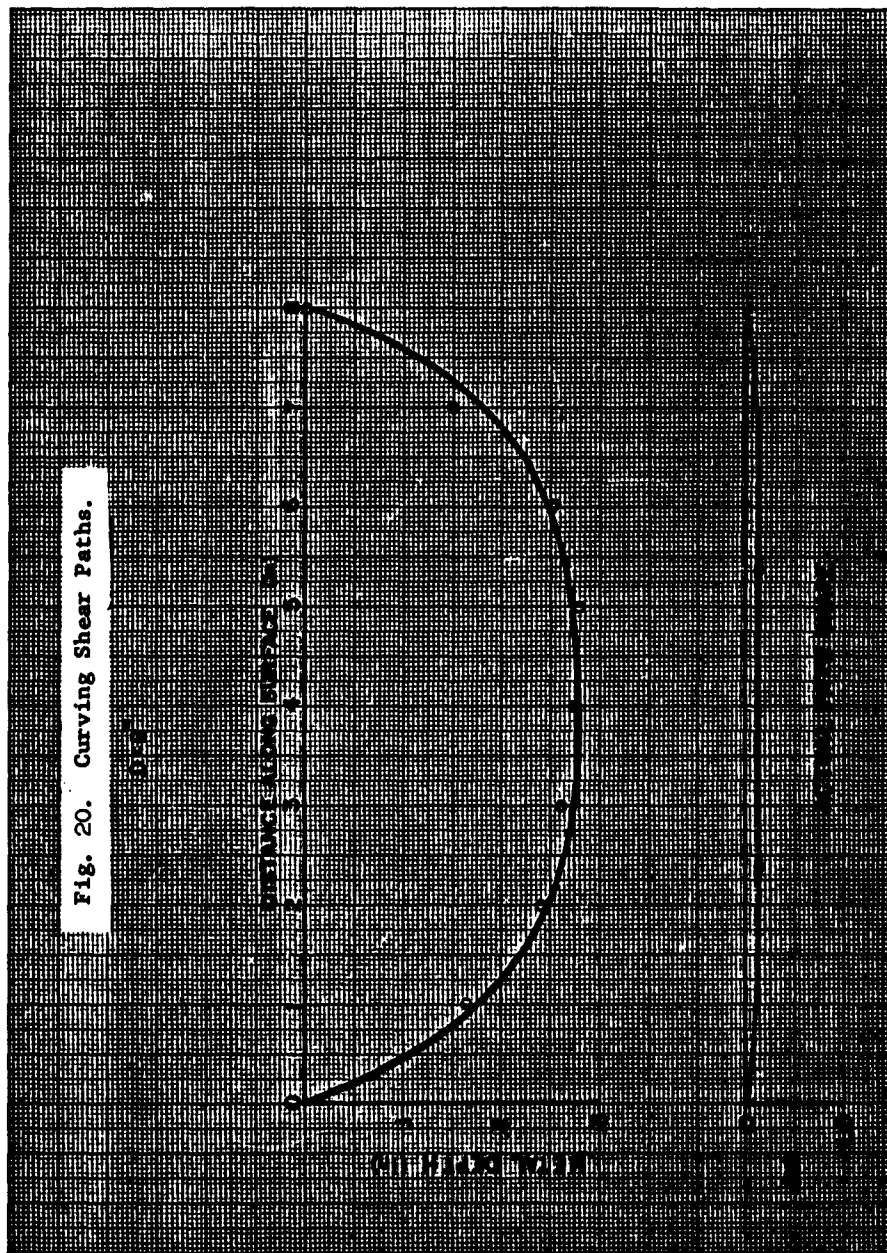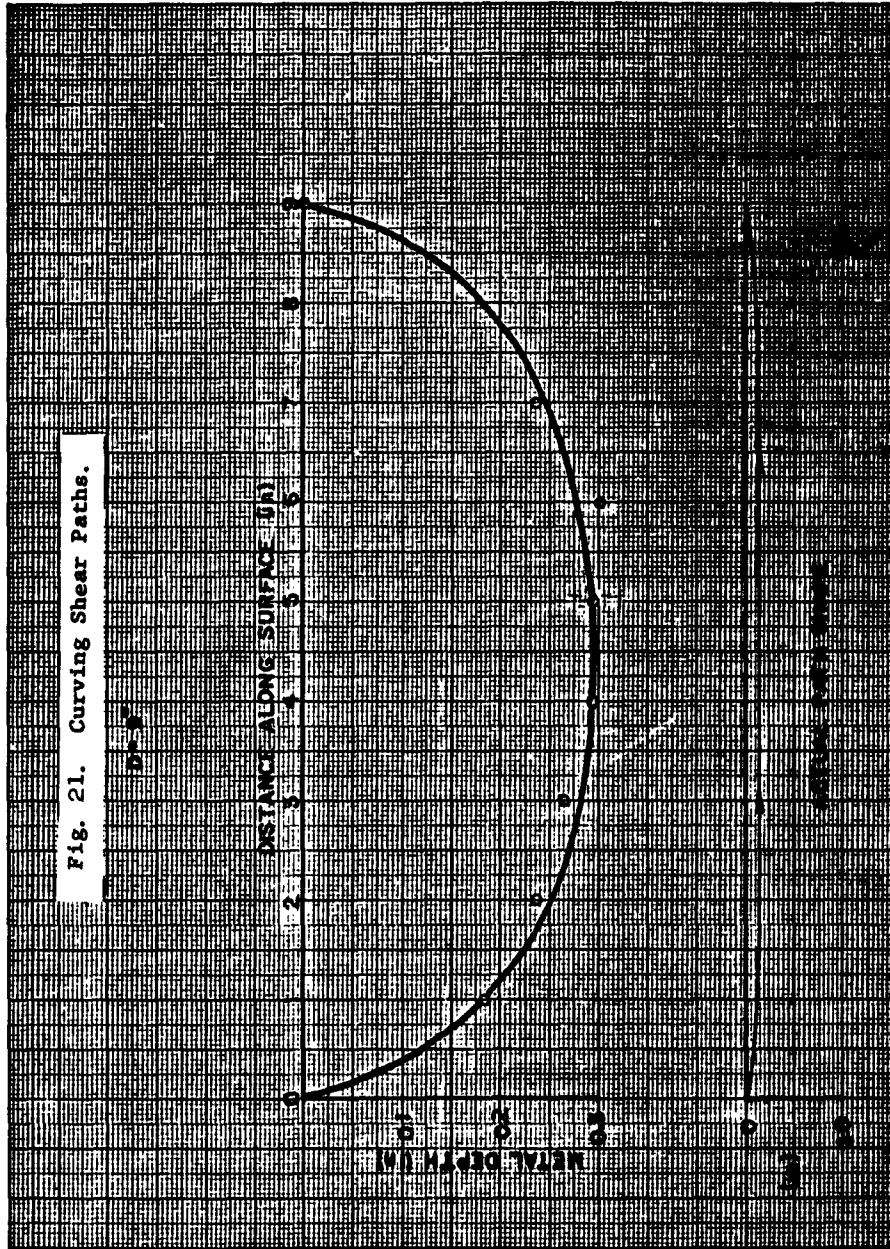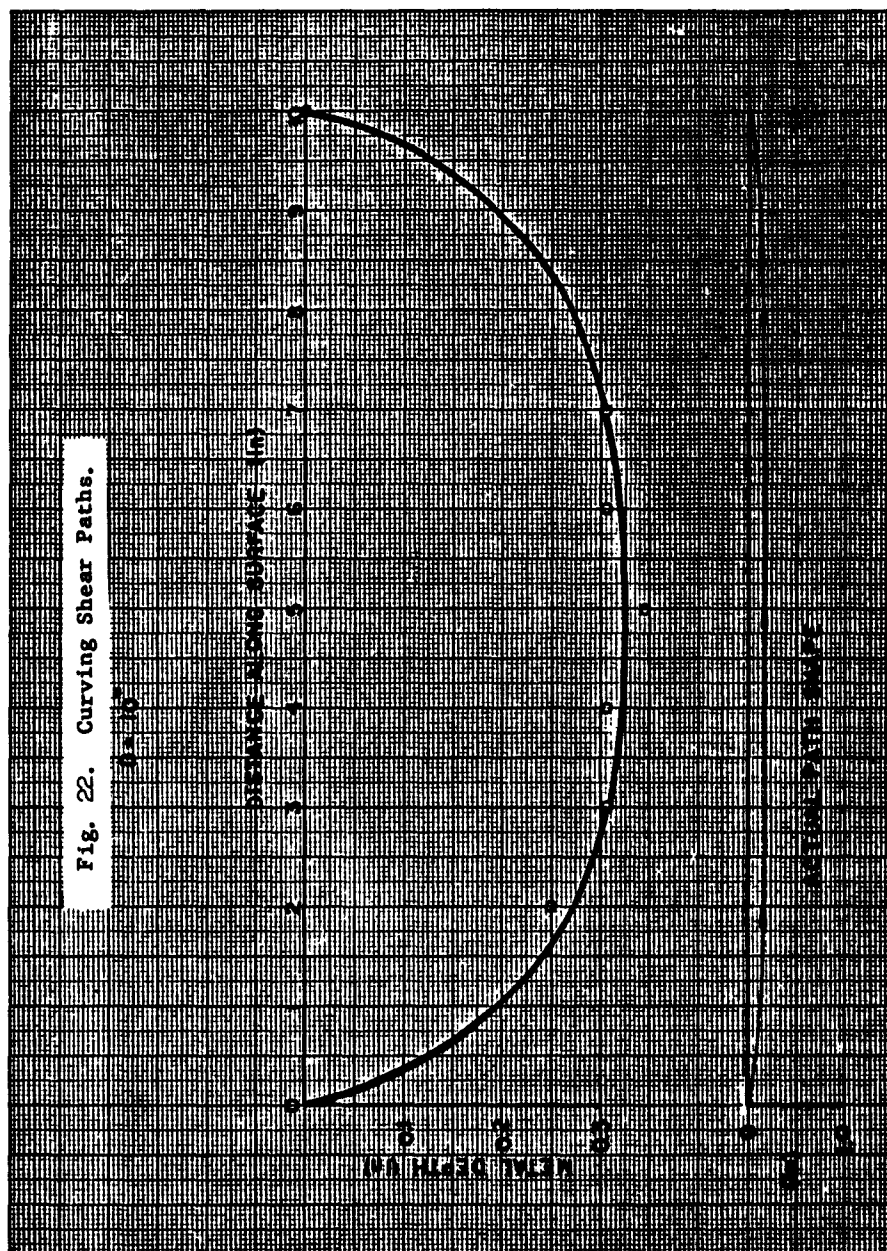
Fig. 22. Curving Shear Paths.

AN IMPROVED PROCESS FOR CLEANING COMPRESSOR BLADES

PROJECT PERSONNEL

Principal Investigator   James Townsend

124

INTRODUCTION

During the overhaul procedure of turbojet engines, the compressor blades must undergo a thorough inspection before reinstallation. The success of this inspection is dependent upon a high degree of cleanliness since any foreign deposits tend to obscure the cracks. Also, the fluorescent penetrant that is used for crack detection is absorbed to some degree by some types of contaminants and conversely, the presence of oil may impair the capillary action of the cracks.

At present, certain blades are being cleaned by a chemical solvent process followed by a mechanical abrasive process. Other blades are being cleaned by an agitated soak utilizing an alkaline cleaner. The mechanical abrasive process was necessary since the chemical solvent process often does not remove all the foreign deposits.

The abrasive action can result in a surface roughness which might reduce the operational efficiency of the jet engines. From the blade inspection standpoint, the mechanical abrasive process results in a burnishing action which has been shown to obscure cracks. It also complicates the cleaning at successive overhauls, due to the difficulty of cleaning the rough surface.

The purpose of this investigation was to develop a more effective method for cleaning compressor blades than is presently used which would eliminate the need for mechanical abrasion.

Alkaline cleaning literature commonly refers to the following three methods as conventional methods:

125

1. Soak Cleaning

2. Spray Cleaning

3. Electrolytic Cleaning

Since electrolytic methods have previously been thoroughly investigated by the project, the first two methods were selected for this investigation.

SUMMARY AND RECOMMENDATIONS

As a result of experimental testing, it was determined that compressor blades could be completely cleaned in a short period of time by utilizing conventional methods. The cleaning system selected consisted of one large soak tank and a spray washing machine. The spray washing machine consisted of two rinse stages. If this machine were used as a preliminary step to painting the blades, a third rinse stage should be included to completely remove all traces of the cleaning medium. A typical rinse stage is shown in Figure 3. Each stage should have its own temperature control, pump, water overflow weir, steam-heating coil, and regulator. Fresh water should be piped to each rinse stage. An adequate flow of fresh water is imperative to acceptable cleaning.

A conveyor is necessary for the operation of a system of this nature. For experimental work, a manual conveyor system was used. For a commercial unit, the conveyor should be mechanized.with a speed of approximately four feet per minute. This feed as used in the experimental work yielded excellent results.

Preceding the rinse stages, there should be a presoak. This could easily be accomplished by using any of the numerous large chemical tanks already in use at Tinker. A fifteen minute presoak was found to be adequate with the chemicals tested. Extending the presoak appeared to have no beneficial effect. However, longer presoaks required by loading delays would have no damaging action providing the presoak temperature

127

does not exceed 180°F. Caustic attack of the blades is possible at elevated temperatures providing the presoak is extended into the range of hours. No evidence of caustic attack was noticed at temperatures below 180°F. Due to the large decrease in generation of fumes and for safety in general, it is recommended that all chemical solutions be used within the range of 160° to 180°F.

During experimental testing, a single bay rack was designed which could be transferred directly from the soak rack onto the conveyor line. At a flow rate of four feet per minute, this single bay conveyor system could handle approximately 25 blades per minute or 1500 per hour. Since an engine may contain approximately 1000 blades, this amounts to a rate of 1 1/2 engines per hour. Twelve engines could be cleaned in an eight hour day of continuous running, which is adequate to handle the cleaning requirement at OCAMA.

Two men would be required to operate the cleaning system for maximum output. One man would be required to load the blades and place the racks carrying them into the presoak tanks. Another man would be required to transfer the racks onto the conveyor line and to return the racks to the first man after they have run through the cycle. However, during slack periods, one man could operate the system at a slower rate without difficulty. And, if higher outputs were desired a double bay system, using a double rack, and a center nozzle bank could easily be constructed.

EXPERIMENTAL PROCEDURE

Regardless of the cleaning method selected, the results will be unsatisfactory if the cleaning agent utilized will not remove the contaminant from the blades. All methods of cleaning that have been considered consist only of different means of agitation which, when coupled with a satisfactory cleaning agent, will completely clean turbojet compressor blades.

As an initial step toward preliminary selection of a cleaner, correspondence was initiated with several of the major chemical suppliers. Representative samples of the cleaning problem were also submitted to three chemical research laboratories for their recommendations. All recommended cleaners were then tested on a comparative basis to determine which were best suited for the cleaning problem.

The laboratory equipment for these preliminary tests consisted of a stainless steel beaker of approximately one gallon capacity, a heating device, and a mechanical agitating device. Due to the limitations of the testing equipment, some latitude was allowed in interpreting the resulting data. Table I shows the results of the preliminary testing.

As shown in Table I, only four of the cleaners yielded complete cleaning. These four cleaners were then obtained in sufficient quantities for exhaustive testing and evaluation. Before this evaluation could be carried out, an expanded experimental system had to be designed and constructed.

TABLE I

RESULTS OF PRELIMINARY TESTING

Cleaner	Cleaning Effectiveness	
	Carbon	Scale
Oakite OEM 163-C-195	Rapid Cleaning	Slow Cleaning
Bendix Dirl strip	Slow Cleaning	Rapid Cleaning
Wyandotte Ferlon	Slow Cleaning	Rapid Cleaning
Turco 4781	Slow Cleaning	Slow Cleaning
Oakite 33	Slow Cleaning	Incomplete Cleaning
Oakite Stripper	Slow Cleaning	Incomplete Cleaning
Oakite 77	Slow Cleaning	Incomplete Cleaning
Oakite Rustripper	Incomplete Cleaning	Slow Cleaning
Turco 4181	Slow Cleaning	Rapid Cleaning

EQUIPMENT DESIGN

The experimental system had to satisfy two requirements. First, the system must be sufficiently versatile to allow various means and degrees of agitation to be applied. Secondly, the system must be large enough to yield results applicable to an assembly line operation, yet small enough to allow testing to proceed utilizing the limited number of contaminated blades available.

The experimental system is shown in Figures 1 and 2. The soak tanks, shown in the right hand portion of the figures, were constructed of stainless steel with fittings located near the bottom to allow for agitating and heating of the solutions.

Since steam was available within the laboratory, an attempt was made to utilize this power source for both heating and agitation. Two steam nozzles were purchased and installed. These nozzles had the advantages of having no moving parts, and of combining both heating and agitation simultaneously. However, they also had the disadvantages of

dilution of the cleaning solution and cessation of agitation when the solution reached its operating temperature. Although these nozzles were of value during the start-up operation, due to their large heating capacity, it was found that other means were required during actual operation.

Recirculating centrifugal pumps were used as the principal agitating device for the soak tanks. By varying the size of the pump, the degree of agitation could be controlled.

It became apparent early in the investigation that complete separation of the blades was necessary during cleaning. To satisfy this requirement, racks were designed which would separate the blades during preliminary cleaning and brace the blades during spray action. In order to approximate assembly line conditions, a conveyer was built into the spray tanks. The conveyor tracks can be seen in Figure 3.

The spray tanks, shown in the left hand portion of Figure 2 were equipped with thermostatically controlled steam coils for heating. As shown in Figure 3, opposing banks of nozzles were arranged so that all surfaces of the blades would be completely covered by the spray action. V-jet nozzles were chosen for the spray banks due to their wide angle of spray and uniform coverage.

Centrifugal pumps were used to drive the spray tanks. It was found that any pump capable of delivering at least 20 psi at the rated flow of the nozzles was satisfactory for this application.

To satisfy the ventilation requirement, a hood was placed over the spray tanks. This hood may be seen at the top of Figure 3. An exhaust fan attached to the hood completely removed all fumes generated by the spray tanks.

TESTING PROCEDURES AND RESULTS

In order to obtain reliable data, a procedure was devised which would allow repeatable data to be obtained. Due to the fact that the degree and type of contamination found on the soiled blades varied considerably, a choice had to be made as to which stages were representative. The first few stages were characterized by a greasy deposit resembling carbon, with Stages 2 and 3 being selected as being representative. The latter stages were contaminated with deposits ranging from high temperature heat scale to a tenacious baked-on carbon. Stages 13 and 14 were selected as representative of the latter stages. Any cleaning sequence which would clean these three representative sections could be expected to clean the complete compressor section.

The experimental system was capable of three distinct cleaning operations. These were:

1. Soak Cleaning
2. Spray Cleaning
3. Spray Rinsing

These terms may be defined as:

Soak Cleaning: The article to be cleaned is immersed in a cleaning bath which is generally agitated by mechanical impellers or centrifugal pumps. When used in conjunction with other methods, this operation is commonly called "presoak."

132

Spray Cleaning: The article to be cleaned is sprayed with a cleaning solution in such a manner that all surfaces are covered by the spray.

Spray Rinsing: Same as spray cleaning except that water is used instead of a cleaning solution.

Three combinations of the above operations were chosen for experimental evaluation. These were:

1. Presoak, Spray-Clean, Spray Rinse

2. Presoak, Spray-Rinse

3. Spray-Clean, Spray-Rinse

Figure 4 shows the results of this evaluation. As the figure shows, all three combinations were capable of cleaning the three selected representative stages. To insure a valid evaluation of the test equipment, the same chemical was utilized in all tests described in Figure 4. Combination Number 2 was chosen as the most feasible method of solving the cleaning problem. This method did not yield the maximum speed in cleaning, but the large decrease in complexity of equipment required warranted this selection. By requiring that only water be pumped in the spray system, a considerable simplification is obtained in the mechanical equipment required. The chemicals under consideration have the ability to dissolve most packings found in standard centrifugal pumps. Also, extreme difficulty was experienced in sealing the spray tanks against the cleaners being used. Therefore, by limiting the cleaning solution to the soak tanks, many disturbing problems may be eliminated.

After the optimum cleaning cycle was determined, the next logical step was to determine which cleaning solution would deliver the best results utilizing this cycle. Figures 5, 6, 7 show the results of testing three of the previously selected cleaners. Tables II, III, and IV

show the data obtained from these tests.

It will be noted from the figures that all three cleaners were capable of cleaning the representative stages of the compressor section. The fourth cleaner, Turco 4181, is presently being used at Tinker. Insufficient numbers of soiled blades were available during the testing phase to allow a thorough evaluation of this cleaner by the procedure used in evaluating the other three cleaners. Therefore, it was decided to evaluate the Turco chemical on a comparative basis using the stages not cleaned during the initial testing. Stages 5 and 6 were used for this test sequence. The Oakite 195 cleaned the blades in a minimum time of 5 minutes, while the Turco 4181 took approximately 15 minutes. The Oakite chemical was received in liquid form and used full strength. The Turco material was used at 3 pounds per gallon.
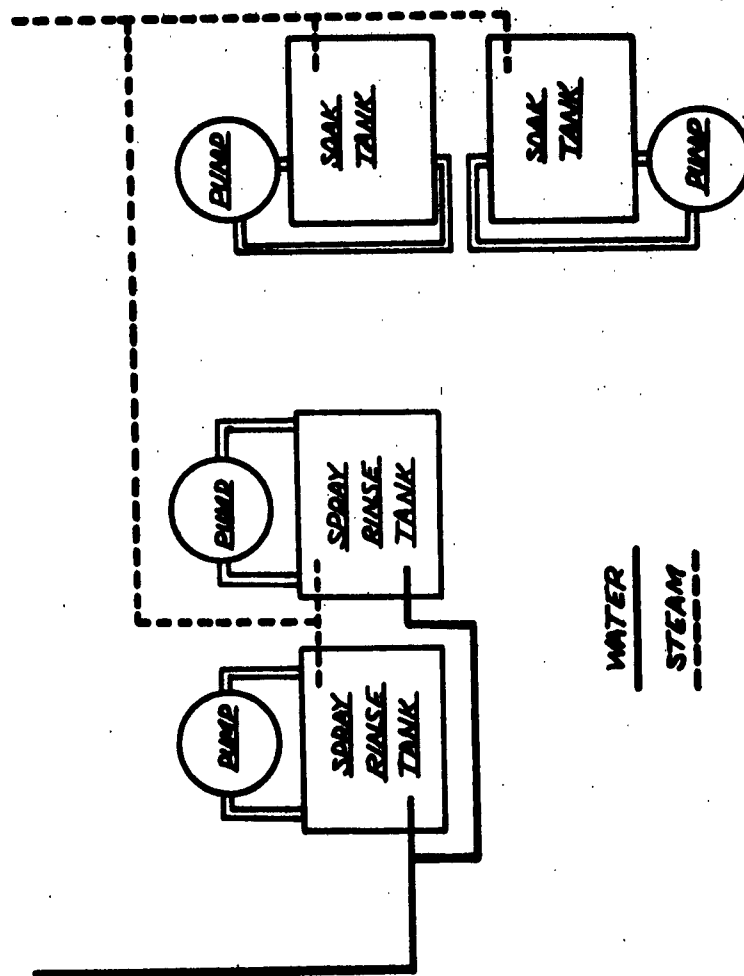
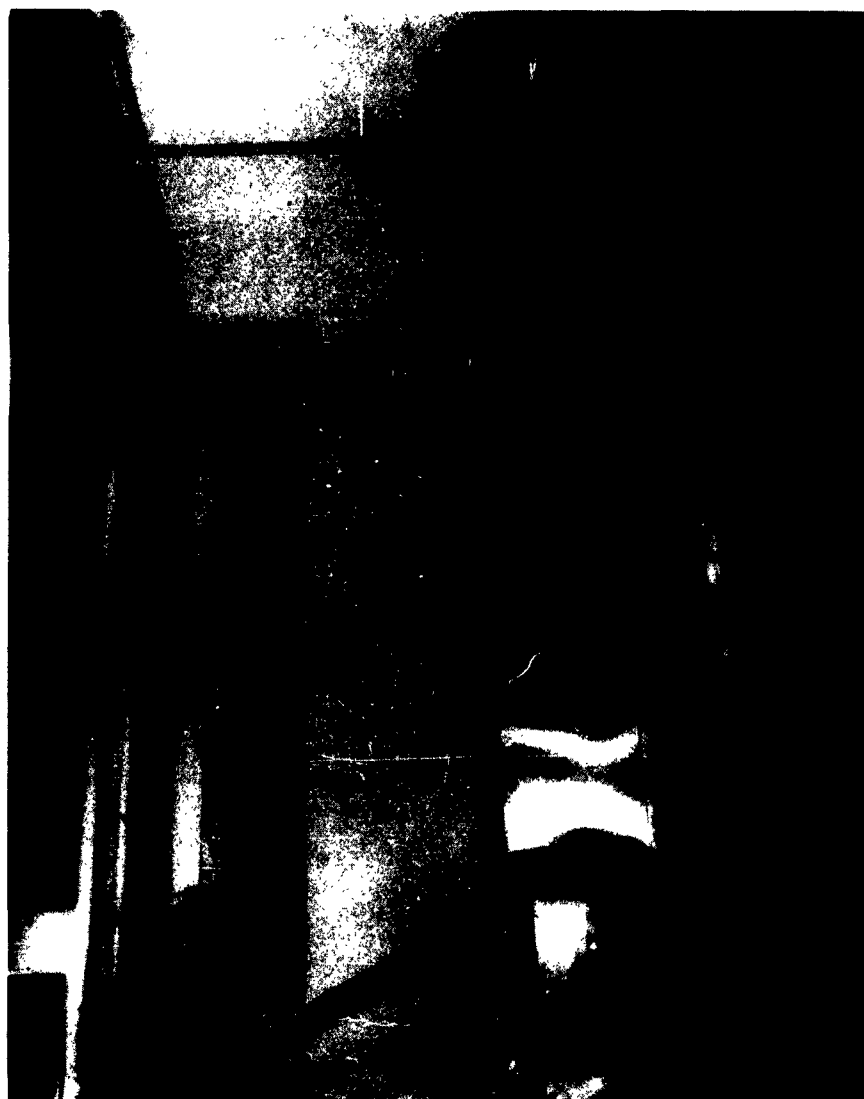Figure 1. Schematic of Experimental Testing System.

135

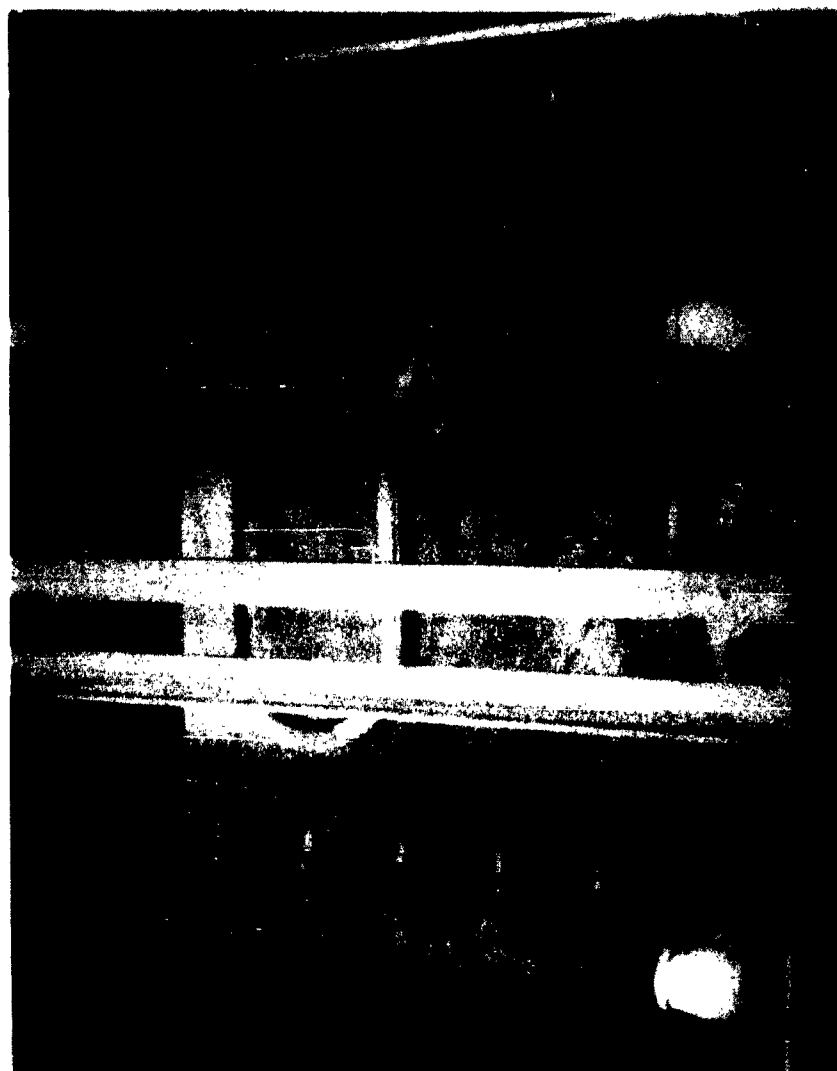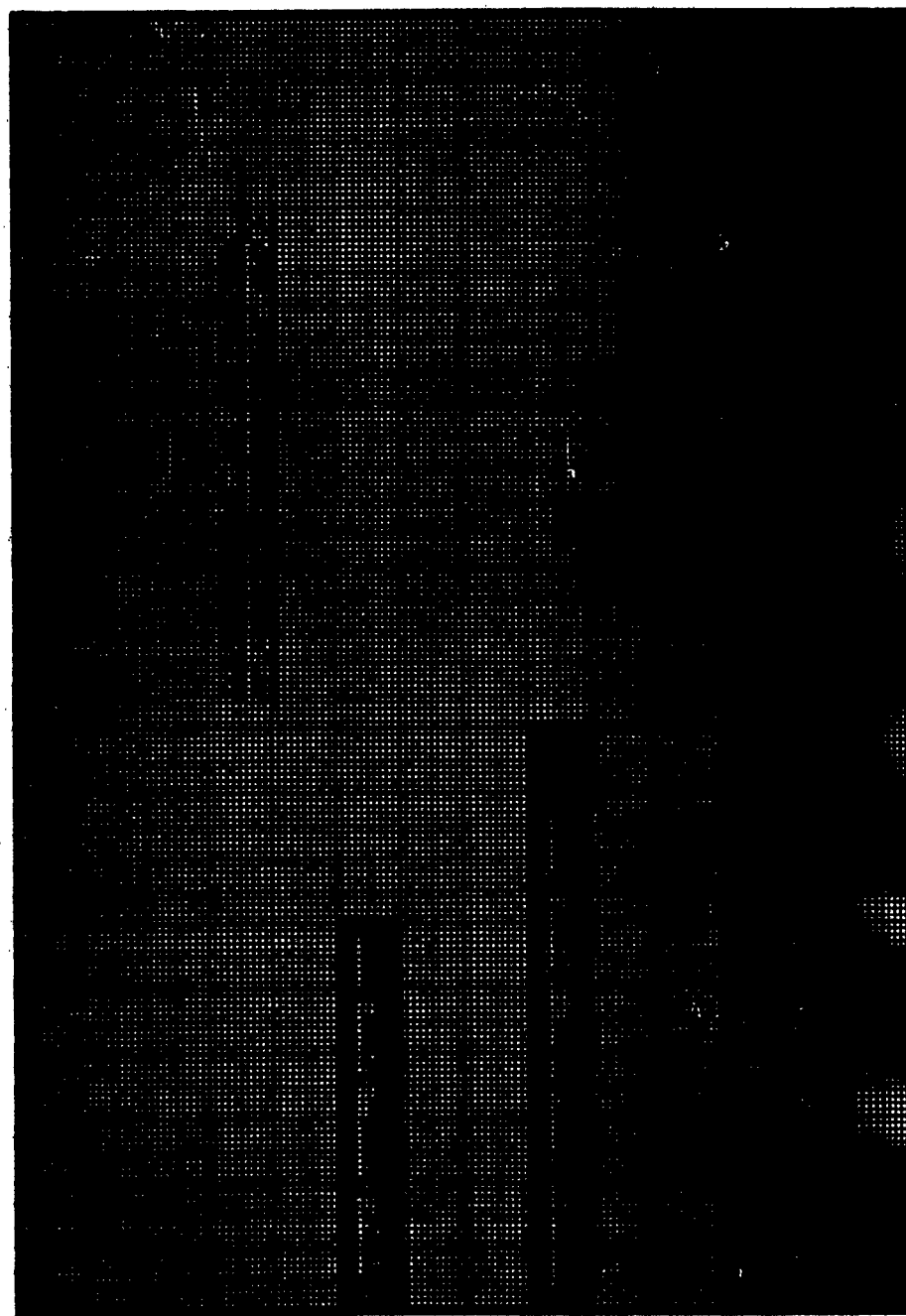Figure 2. Full View of the Experimental System.

Figure 3. Nozzle Arrangement of Spray Tanks.

137

CLEANING TIME - MIN.
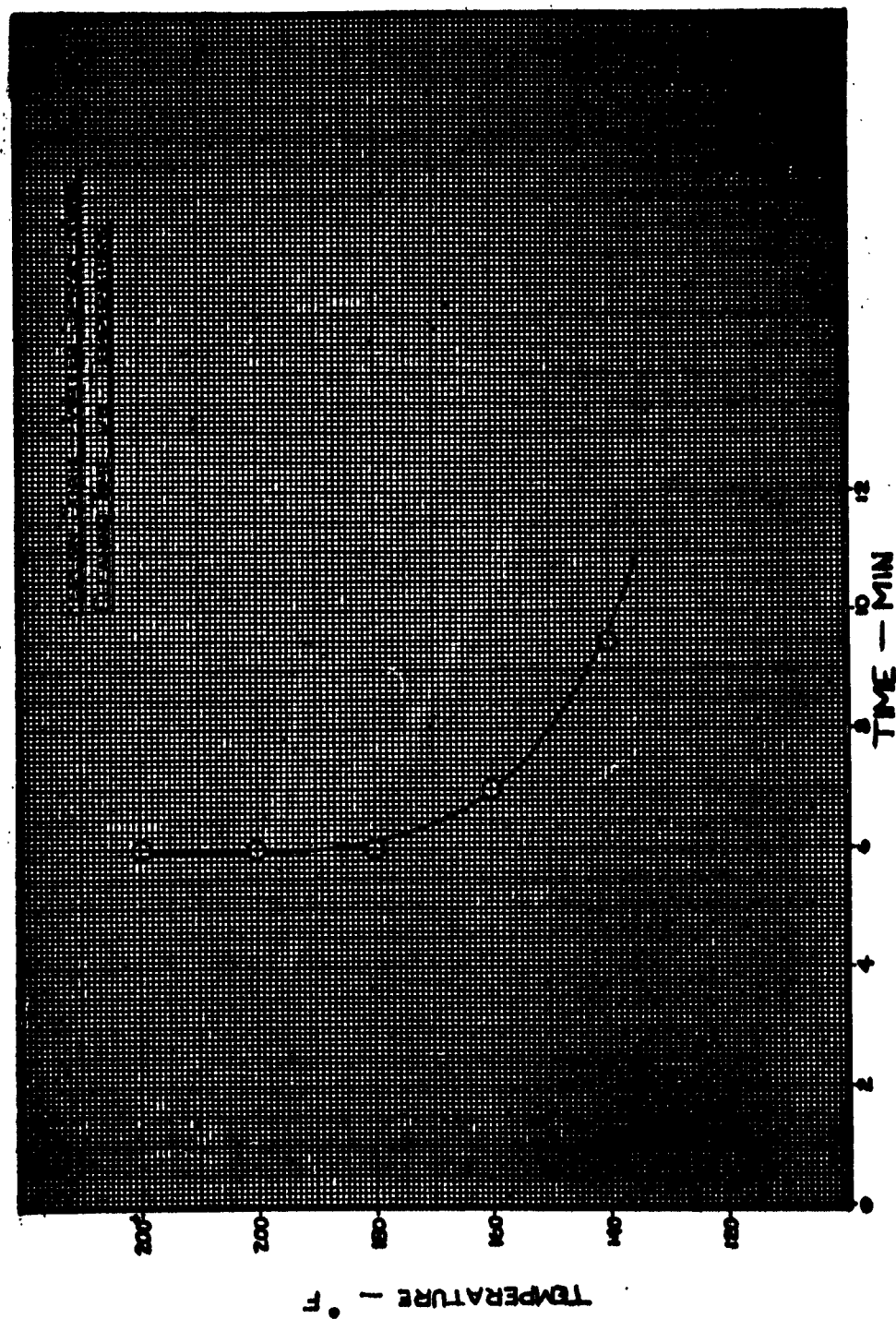
AGITATION

Figure 4. Cycle Selection.

138

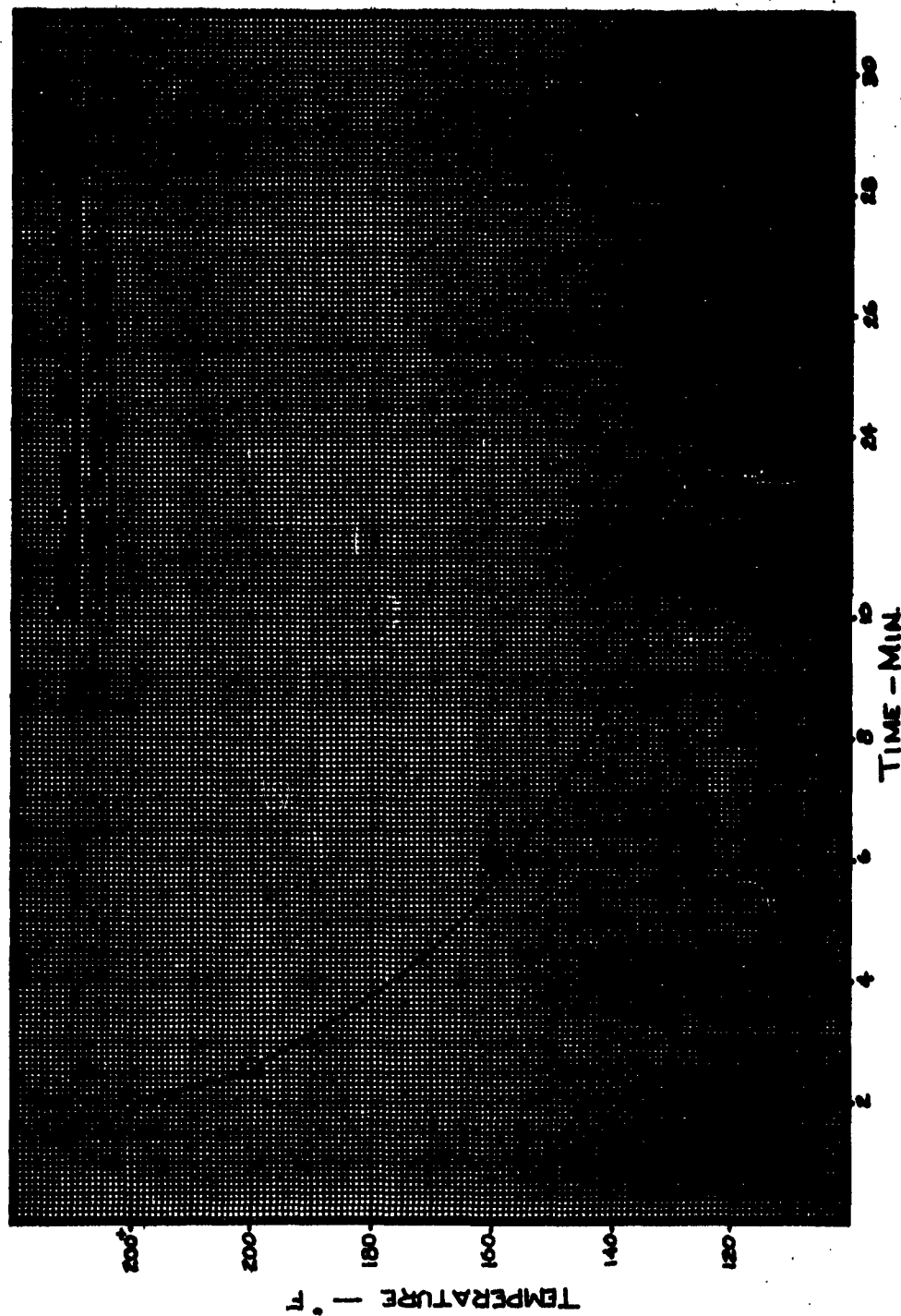Figure 5. Wyandotte Cleaning Rate.

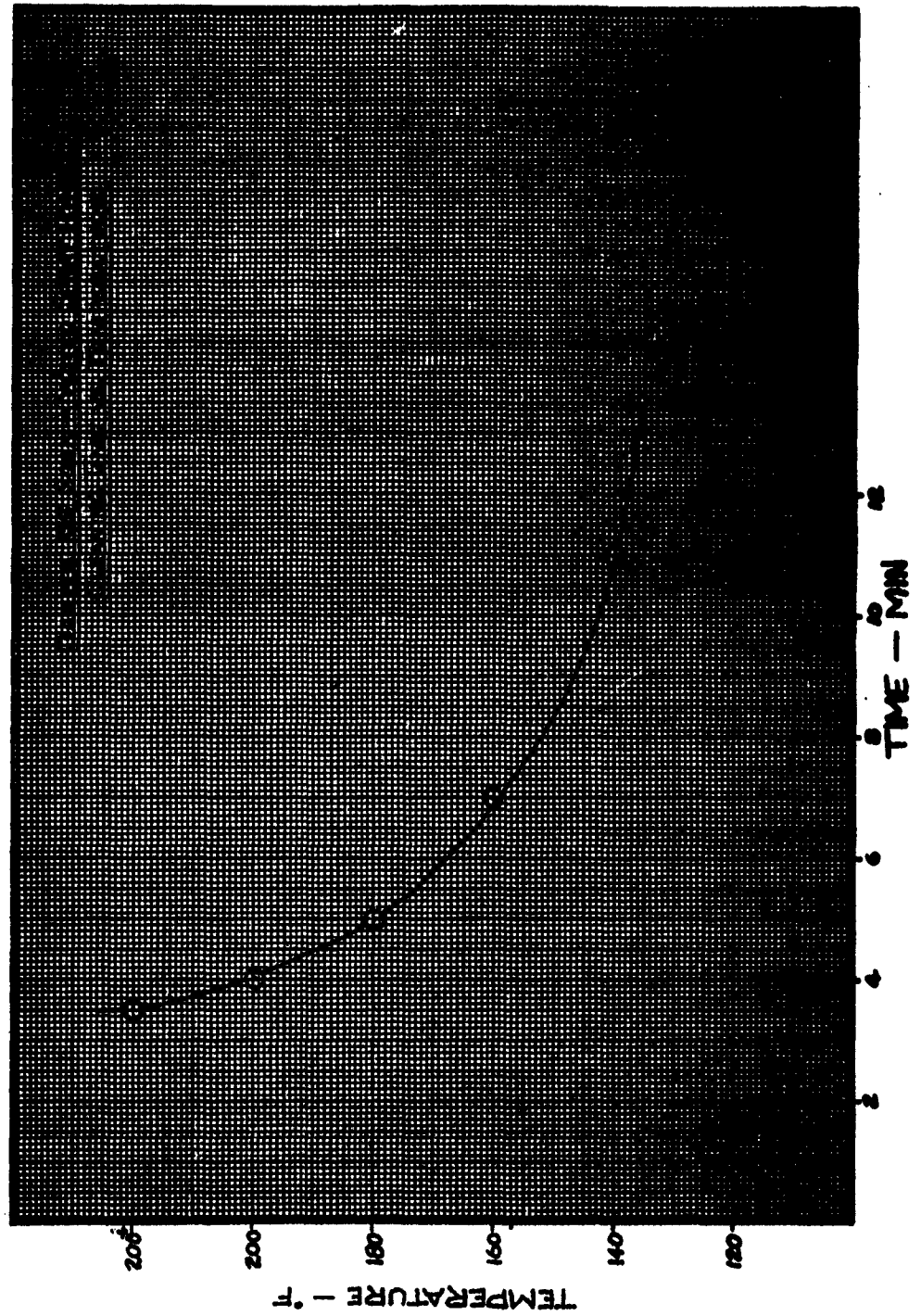Figure 6. Bendix Cleaning Rate.

140

Figure 7. Oakite Cleaning Rate.

TABLE II

CLEANING EVALUATION NUMBER 1
FERLON SOAK — WATER SPRAY RINSE
MAY 31, 1963
CONCENTRATION: 2.5 LB FERLON PER GAL. H_2O

TEMP	SOAK TIME	REMARKS
140°	6 MIN	SOME CONTAMINATE REMAINS
140°	10 MIN	COMPLETELY CLEAN
MINIMUM TIME 10 MIN		
160°	5 MIN.	SOME CONTAMINATE REMAINS ON LARGE BLADES
160°	8 MIN	COMPLETELY CLEAN
MINIMUM TIME 7 MIN		
180°	5 MIN.	SOME CONTAMINATE REMAINS ON MEDIUM BLADES
180°	7 MIN	COMPLETELY CLEAN
MINIMUM TIME 6 MIN		
200°	5 MIN	SOME CONTAMINATE REMAINS ON SMALL BLADES
200°	7 MIN	COMPLETELY CLEAN
MINIMUM TIME 6 MIN		
200+°	6 MIN	COMPLETELY CLEAN

TABLE III

CLEANING EVALUATION NUMBER 2
BENDIX SOAK— WATER SPRAY RINSE
MAY 30, 1963
CONCENTRATION: 1.5 LB. BENDIX PER GAL H_2O

TEMP	SOAK TIME		REMARKS
120°	15 MIN		SOME CONTAMINATE REMAINS
120°	30 MIN		COMPLETELY CLEAN
MINIMUM TIME		30 MIN	
140°	5 MIN		SOME CONTAMINATE REMAINS ON LARGE AND SMALL BLADES
140°	10 MIN		COMPLETELY CLEAN
MINIMUM TIME		8 MIN	
160°	2 MIN		SOME CONTAMINATE REMAINS
160°	10 MIN		COMPLETELY CLEAN
MINIMUM TIME		6 MIN	
180°	1 MIN		SOME CONTAMINATE REMAINS
180°	3 MIN		COMPLETELY CLEAN
MINIMUM TIME		3 MIN	
200°	1 MIN		SOME CONTAMINATE REMAINS
200°	2 MIN		COMPLETELY CLEAN
MINIMUM TIME		2 MIN	
212°	2 MIN		COMPLETELY CLEAN

TABLE IV

CLEANING EVALUATION NUMBER 3
OAKITE 195 SOAK   WATER SPRAY RINSE
MAY 31, 1963

TEMP	SOAK TIME	REMARKS
140°	10 MIN	SOME CONTAMINATE REMAINS ON LARGE BLADES
140°	12 MIN	COMPLETELY CLEAN
MINIMUM TIME	11 MIN	
160°	5 MIN	SOME CONTAMINATE REMAINS ON LARGE BLADES
160°	8 MIN	COMPLETELY CLEAN
MINIMUM TIME	7 MIN	
180°	3 MIN	SOME CONTAMINATE REMAINS
180°	6 MIN	COMPLETELY CLEAN
MINIMUM TIME	5 MIN	
200°	3 MIN	SOME CONTAMINATE REMAINS
200°	6 MIN	COMPLETELY CLEAN
MINIMUM TIME	4 MIN	
212°	3 MIN	COMPLETELY CLEAN

TABLE V

SOAK AGITATION EVALUATION NUMBER 1
OAKITE 195 SOAK   WATER SPRAY RINSE
June 7, 1963

TEMP	MINIMUM CLEANING TIME	AGITATION
160°	5 min	STRONG
160°	5 min	MILD
180°	4 min	STRONG
180°	4 min	MILD
200°	3 min	STRONG
200°	3 min	MILD

ULTRASONIC CLEANING OF TURBOJET COMPRESSOR BLADES

PROJECT PERSONNEL

Principal Investigator

Project Associates

O'Neill Burchett

Donald Lumadue

Robert Rumbaugh

William Womack

INTRODUCTION

During the overhaul procedure of turbojet engines, the compressor blades must undergo a thorough inspection before reinstallation. The inspection should detect all defective blades so that the defective blades can thus be removed. The success of this inspection is dependent upon a high degree of cleanliness of the blades, especially when fluorescent penetrants are used to detect cracked blades. Any foreign deposits on the surfaces of the compressor blades tend to obscure cracks. Also, the fluorescent penetrant that is used for crack detection is absorbed to some degree by some types of contaminants and conversely, the presence of oil on the blade surface may impair the capillary action by which small surface cracks may be filled with fluorescent penetrant.

At present, certain blades are being cleaned by a chemical solvent process followed by a mechanical abrasive process to insure complete cleaning. Other blades are being cleaned by an agitated soak utilizing an alkaline cleaner.

From the blade inspection standpoint, the mechanical abrasive process can result in a burnishing action which has been shown to obscure cracks. It also complicates the cleaning at successive overhauls, due to the difficulty of cleaning the rough surface.

The purpose of this investigation was to determine the effects of ultrasonic cavitation on the cleaning processes used in Interim Report Number I where applicable.

148

Since electrolytic cleaning had been investigated previously, only the following processes were used:

1. Chemical soak -- ultrasonic hot water rinse.

2. Ultrasonic chemical soak -- hot water rinse.

The chemicals used in this investigation were limited to those found best in Interim Report Number I.

SUMMARY AND RECOMMENDATIONS

Under the conditions of this experimental testing, no beneficial cleaning results were found from ultrasonics over the system tested in Interim Report Number 1. It should be noted that this recommendation is made for articles with geometric shapes containing no intricate small passages.

It was found that the rinse stage of the cleaning process was more critical than the chemical soak process so far as ultrasonic energy is concerned.

It was found that ultrasonic cavitation caused by transducer diaphragms was more effective in cleaning or rinsing the blades when all three diaphragms were used (bottom and two opposing sides). It was also determined that loading the tank with more blades required a higher driving power level in order to clean or rinse the blades under similar conditions. The best power level used to drive the transducers was found to erode the diaphragm surfaces, especially when the cleaning solution was used in the ultrasonic tank. Also, the blades had a tendency to shade the effects of the ultrasonic cleaning on areas away from the face of a single transducer diaphragm.

The cleaning system tested in Interim Report Number 1 is recommended over the system evaluated in this report, for the cleaning of cold section parts.

150

EXPERIMENTAL PROCEDURE

Ultrasonic cavitation can be described, for the purposes here used, as a form of scrubbing action, or perhaps, mechanical agitation. Since the cavitation phenomena requires a continuous fluid (liquid) media, the spray portion of any of the cleaning processes of Interim Report Number I was deleted. The mechanical scrubbing action of the ultra-sonic cavitation was substituted for the spray action used previously. Also, since ultrasonic cavitation is not as effectively obtained in a flowing liquid, no agitation of this type (pump circulation) was used.

The ultrasonic rinse conditions were determined by:

1. The selection of a rinse water temperature range of 140-150°F.

2. The use of a chemical solution proven effective in Interim Report Number I.

3. The use of a soak (chemical) tank temperature proven effective previously.

4. The use of a soak (chemical) time duration proven effective previously.

5. Substitution of ultrasonic rinse for the usual spray rinse for a time duration necessary to clean the blades.

EQUIPMENT DESIGN

The equipment for the experimental system had to satisfy several requirements. The cleaning solution must be contained in such a manner that it could be heated and then maintained at a temperature for any duration of time necessary. Also, the container for the cleaning solution must have a means of applying ultrasonic energy so that cavitation would ensue.

A stainless steel tank (Figure 6) with transducerized diaphragms on the bottom and two opposing sides was constructed. A 1500 watt heater (electrical immersion type) was installed in a lower corner of the tank. A drain mechanism was also placed in another lower corner of the tank to facilitate removal of liquids.

A stainless steel rack was constructed (Figure 7) so that it would hold the blades in a given orientation. The rack could be adjusted as to depth of blade immersion in the liquid. The rack would accommodate approximately 100 blades of mixed stage numbers. The rack was built so that it could be easily transferred from the ultrasonic tank to a soak-rinse tank.

A soak-rinse tank of similar size to the ultrasonic tank was constructed from stainless steel (Figure 8). A 5000 watt immersion heater was installed, and an outlet and inlet provision was included so that rinse water could be circulated if later deemed necessary. This tank could hold the chemical cleaning solution and maintain a designated temperature level while the blades soaked, or it could hold the hot

rinse water for the blades.

Commercial Equipment:

1. Ultrasonic power generator -- 5000 watt variable power and
   frequency, manufactured by International Ultrasonics, Inc.

2. Ultrasonic power generator -- 1500 watt, manufactured by
   the Bendix Corporation.

3. Three transducerized diaphragms, manufactured by the Bendix
   Corporation.

TESTING PROCEDURES AND RESULTS

The procedure of testing was devised in such a manner as to promote the collection of accurate, reliable data. The availability of compressor blades of all stages which had consistent soil conditions was questionable. The available blades were sorted into groups, each of which contained at least three stages. Then three representative groups of blades were selected for testing. The three groups were from the low stage numbers, medium stage numbers, and high stage numbers (14-17). It should be noted that the high stage numbers included here were above the representative stage number selected in Interim Report Number I and were thus much nearer the hot section of the engine and considerably more difficult to clean. The blades did not have as consistent types of surface soil as the blades used previously. This hampered the accuracy of comparison of the effectiveness of cleaning processes. The large numbers of blades cleaned each test run soon depleted the stock of soiled blades and required the use of clean blades with soiled blades distributed among them. This was necessary as the cleaning processes were intended to approximate full scale cleaning operation conditions, and the cleaner must be completely loaded each time.

The first group of blades (low stages) was characterized by a surface soil consisting of a greasy carbon deposit. The second group of blades (middle stages) contained a surface soil of heavy, greasy carbon deposits. The final group of blades (high stages) were contaminated

154

THIS
PAGE
IS
MISSING
IN
ORIGINAL
DOCUMENT

The effects of ultrasonic cavitation on the cleaning processes were determined by using two chemical cleaners. The chemicals were Oakite OEM 163-C-195 and Bendix Dirl Strip, because these two chemicals were more thoroughly tested in the testing reported in Interim Report Number 1.

In ultrasonic rinse cleaning, the Oakite 163-C-195 cleaner was definitely the faster cleaner of the two. It should be noted that the Oakite cleaner was slower on the higher stage number blades. This would confuse the comparison results when later compared to the ultrasonic soak cleaning where a blade shortage forced the use of higher stage blades. Also, the blade shortage in the last tests also forced cull blades to be used,-- the term "cull" being applied to blades having a foreign-appearing surface soil or perhaps blades that were partly rusted.

The ultrasonic rinse cleaning was a faster cleaning process than the ultrasonic soak cleaning. This leads to the conclusion that the cleaning of the blades is principally a chemical action and that the rinse action is more critical than thought. The same chemicals were used for all the tests, and the chemicals could have been partly spent. The ph factor of the solutions never fell below 14, which was the highest ph value for which test paper was available.

The ultrasonics showed no improvement effects on the cleaning processes reported in Interim Report Number I.

The results of all testing revealed that blades of all stages of the compressor section of the J-57 could be cleaned by the processes used. The Oakite OEM-163-C-195 cleaner was on an average the fastest cleaner. The Bendix Dirl Strip was the most easily used due to its

low foaming qualities. The Turco 4181 seemed to be the best cleaner for the higher stage number blades. Any of these three chemicals would be satisfactory.

It was found that additional rinse processes would be needed to completely remove all traces of chemical cleaners from the blades.
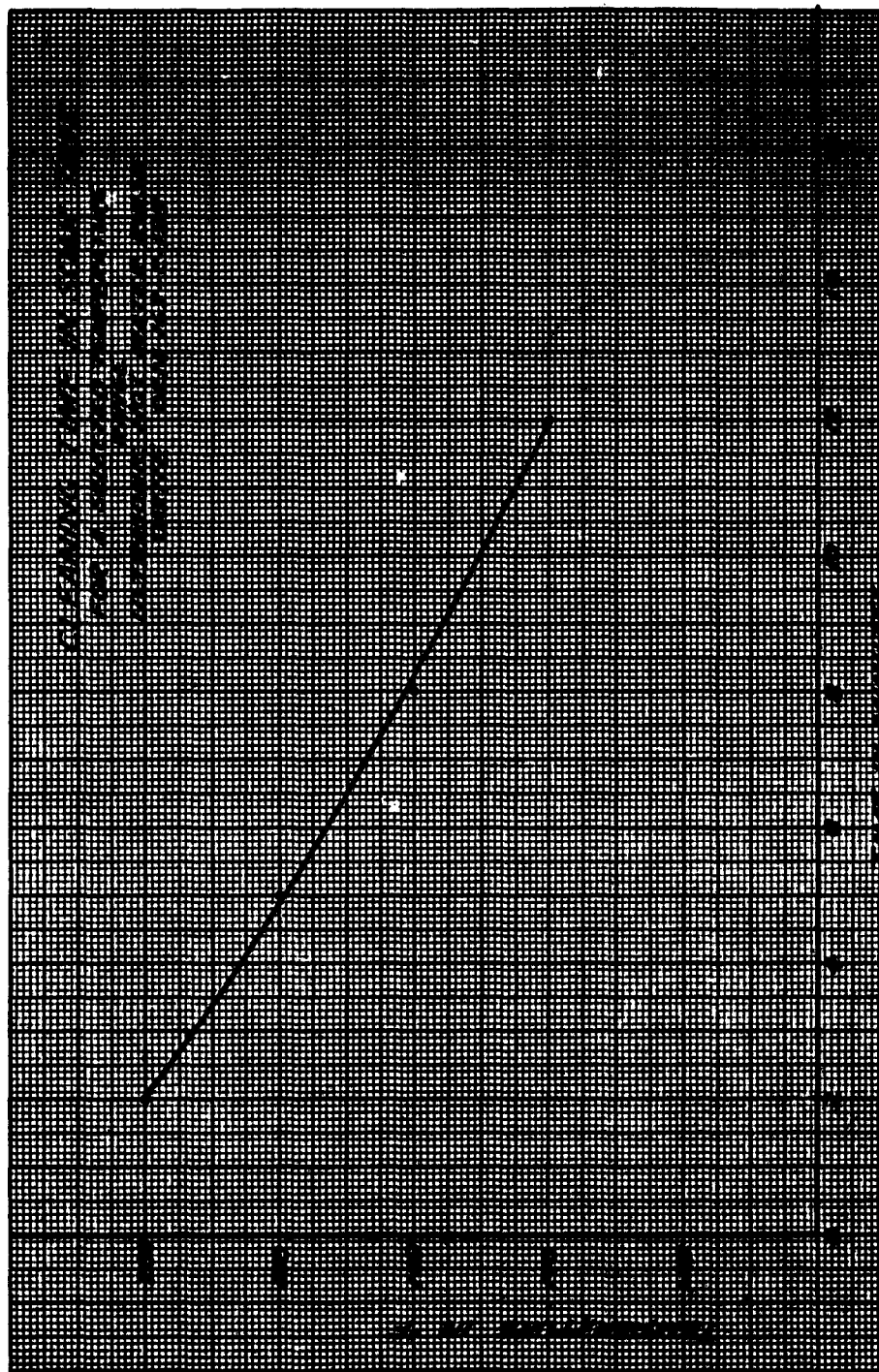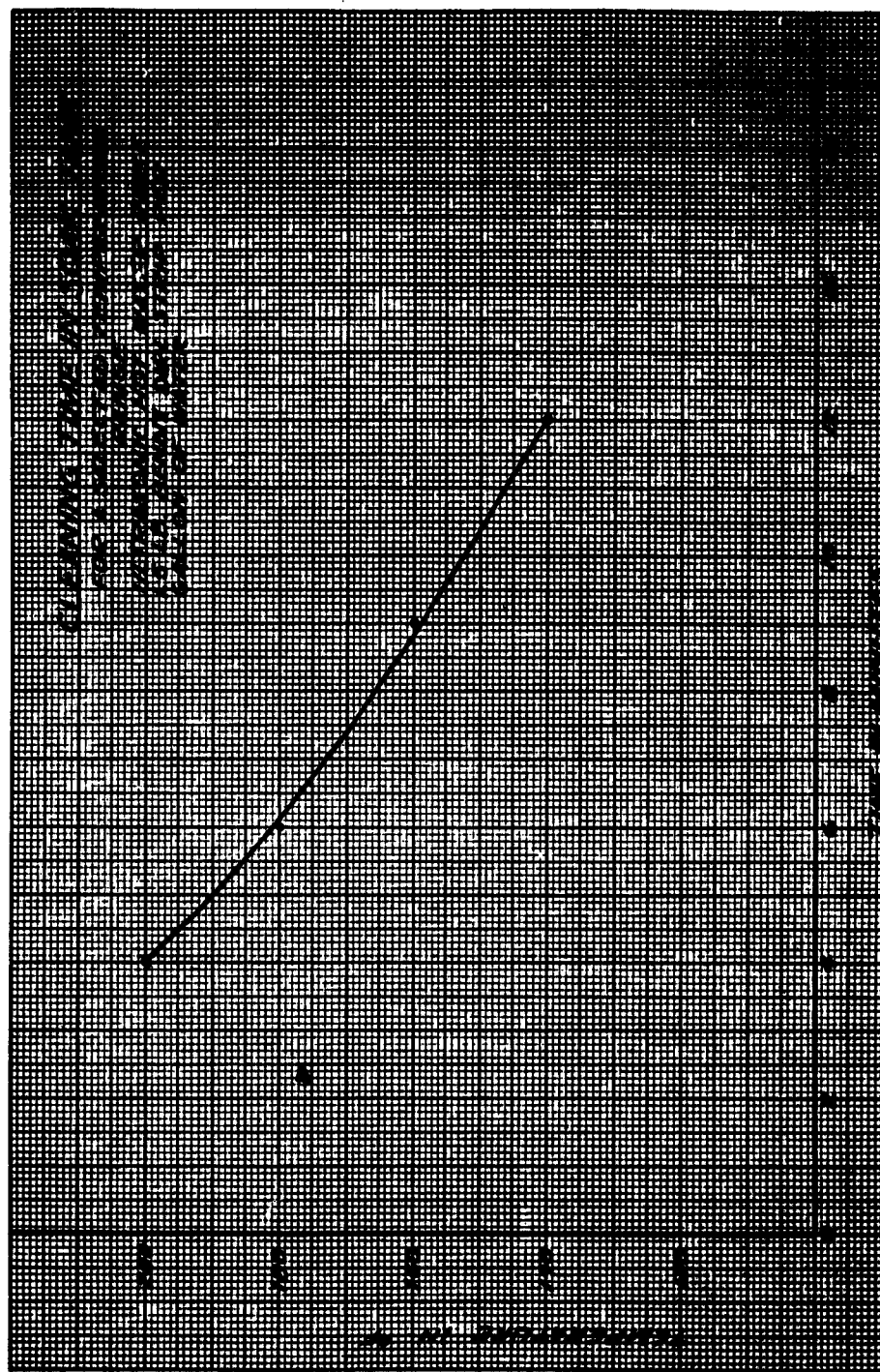
Figure 1. Soak Time - Oakite Cleaner.
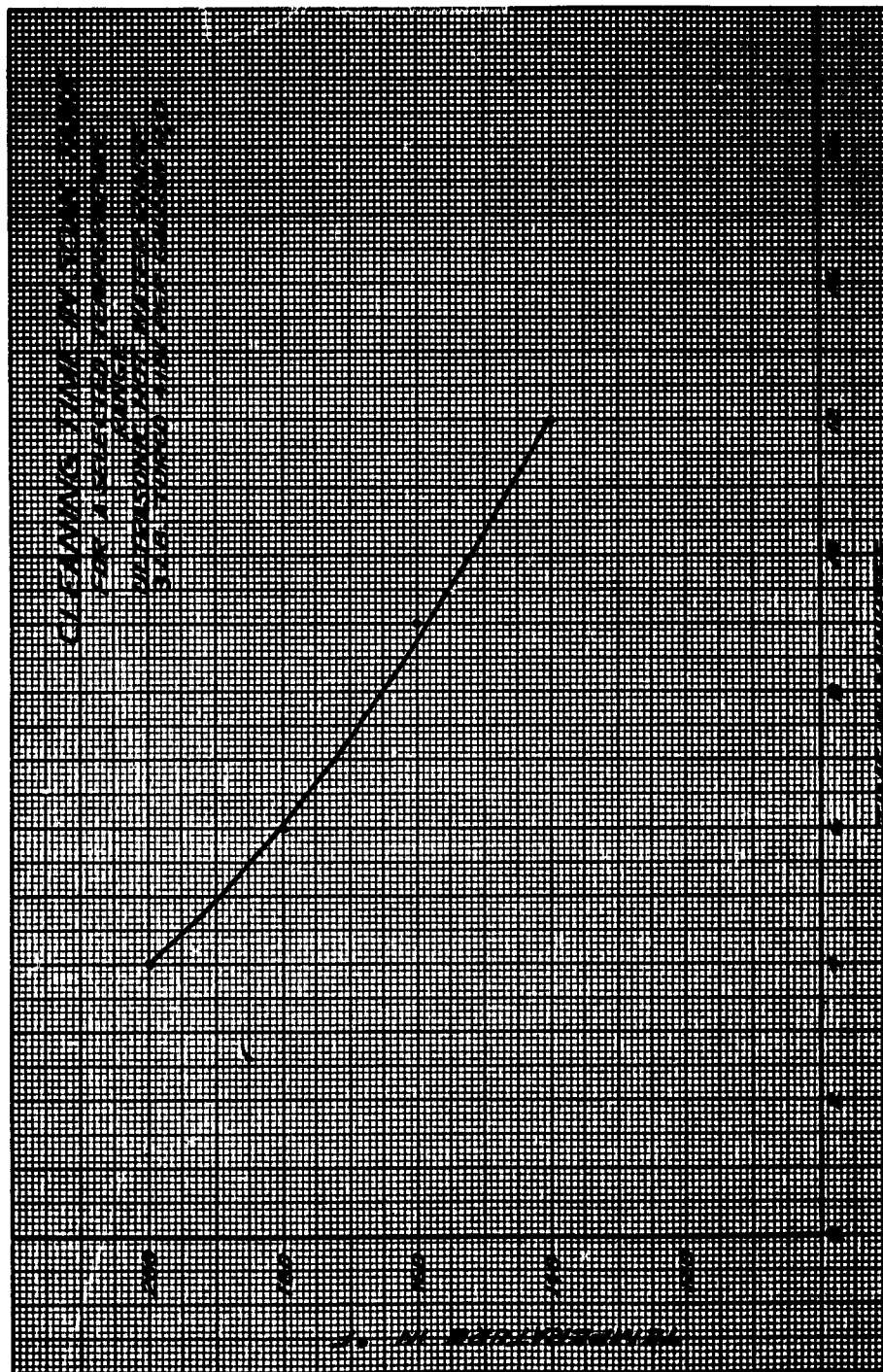
Figure 2. Soak Time - Bendix Cleaner

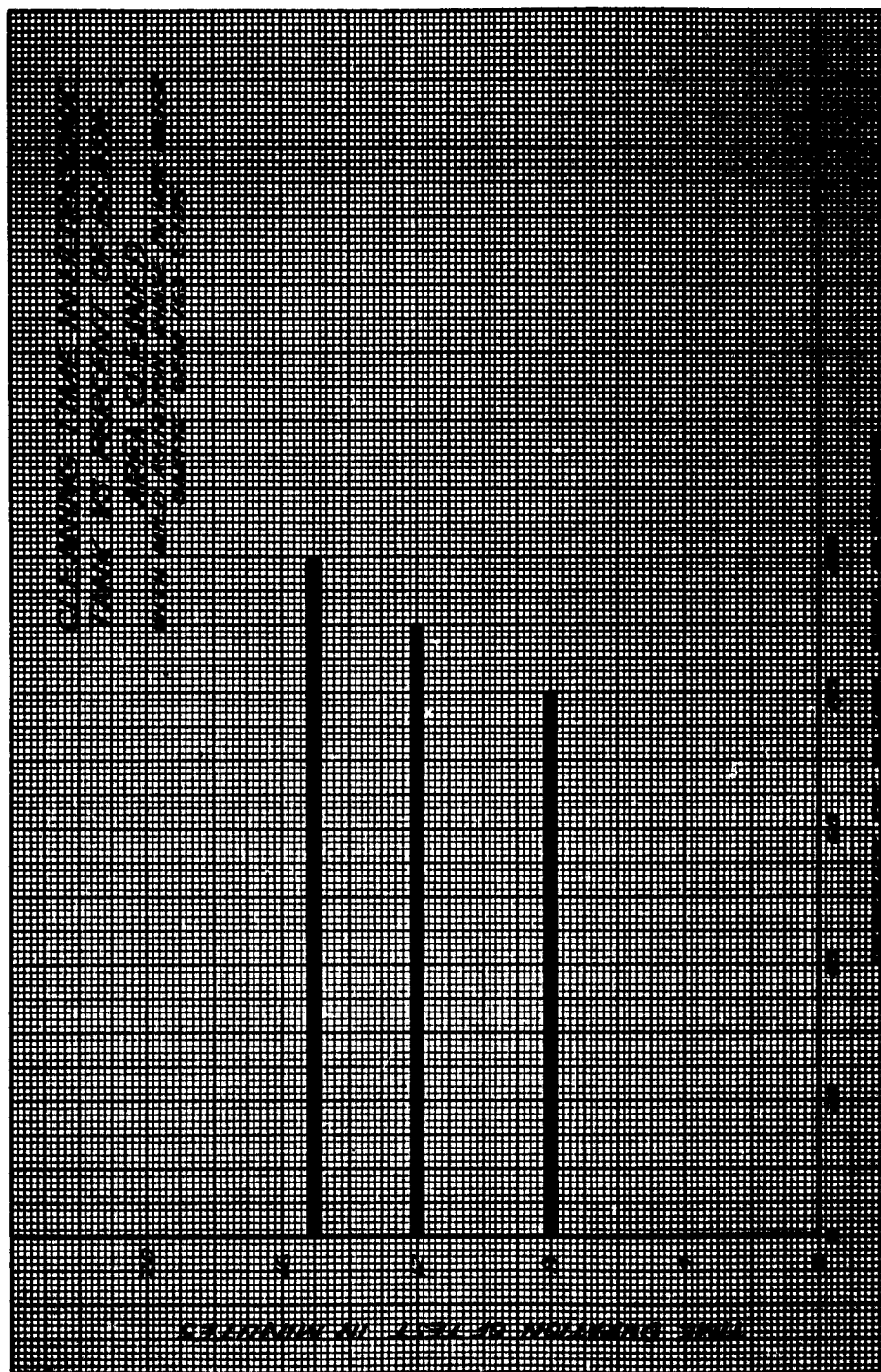Figure 3. Soak Time - Turco Cleaner.

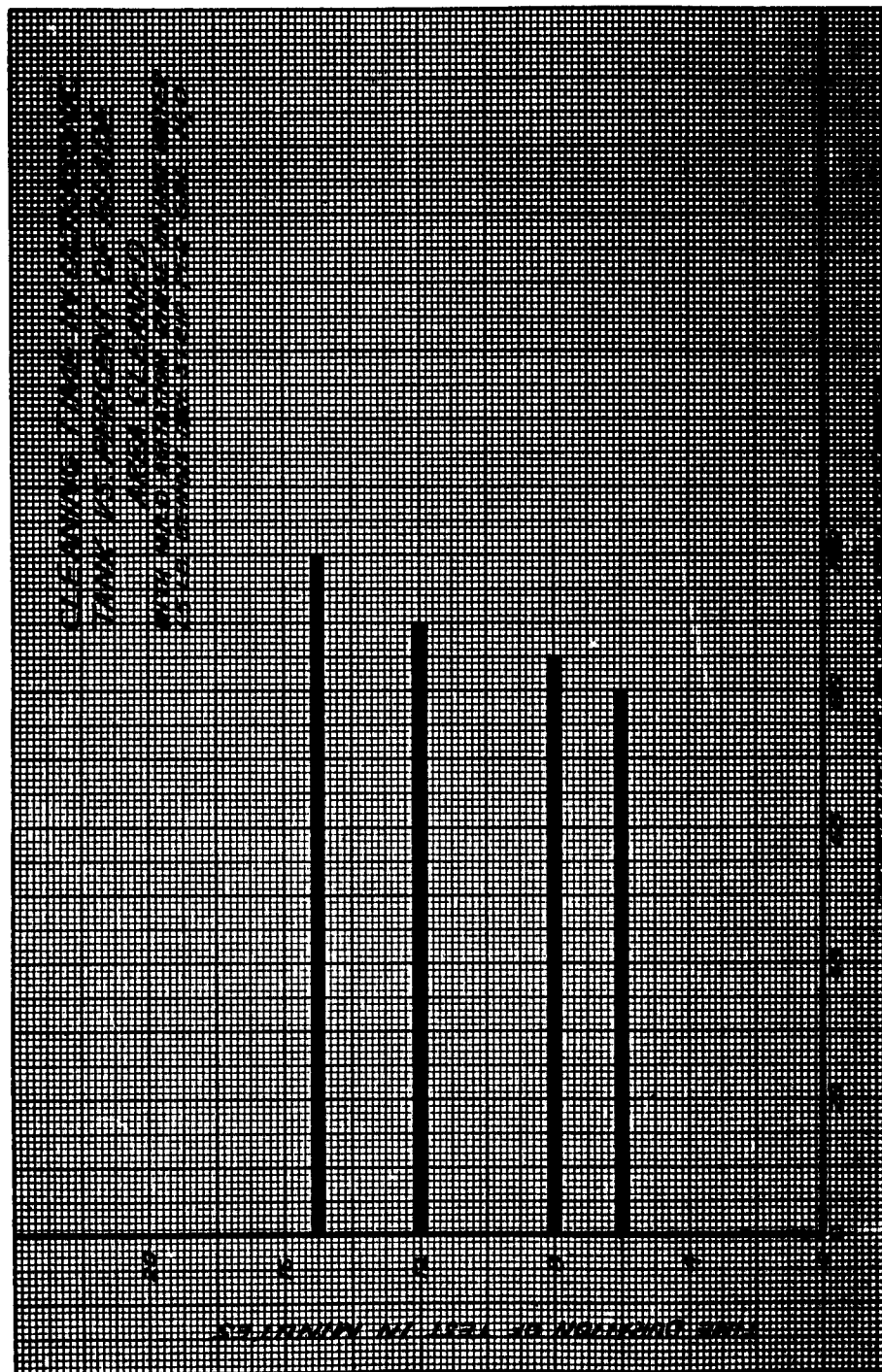Figure 4. Ultrasonic Soak Time - Oakite Cleaner.

161

Figure 5. Ultrasonic Soak Time - Bendix Cleaner.

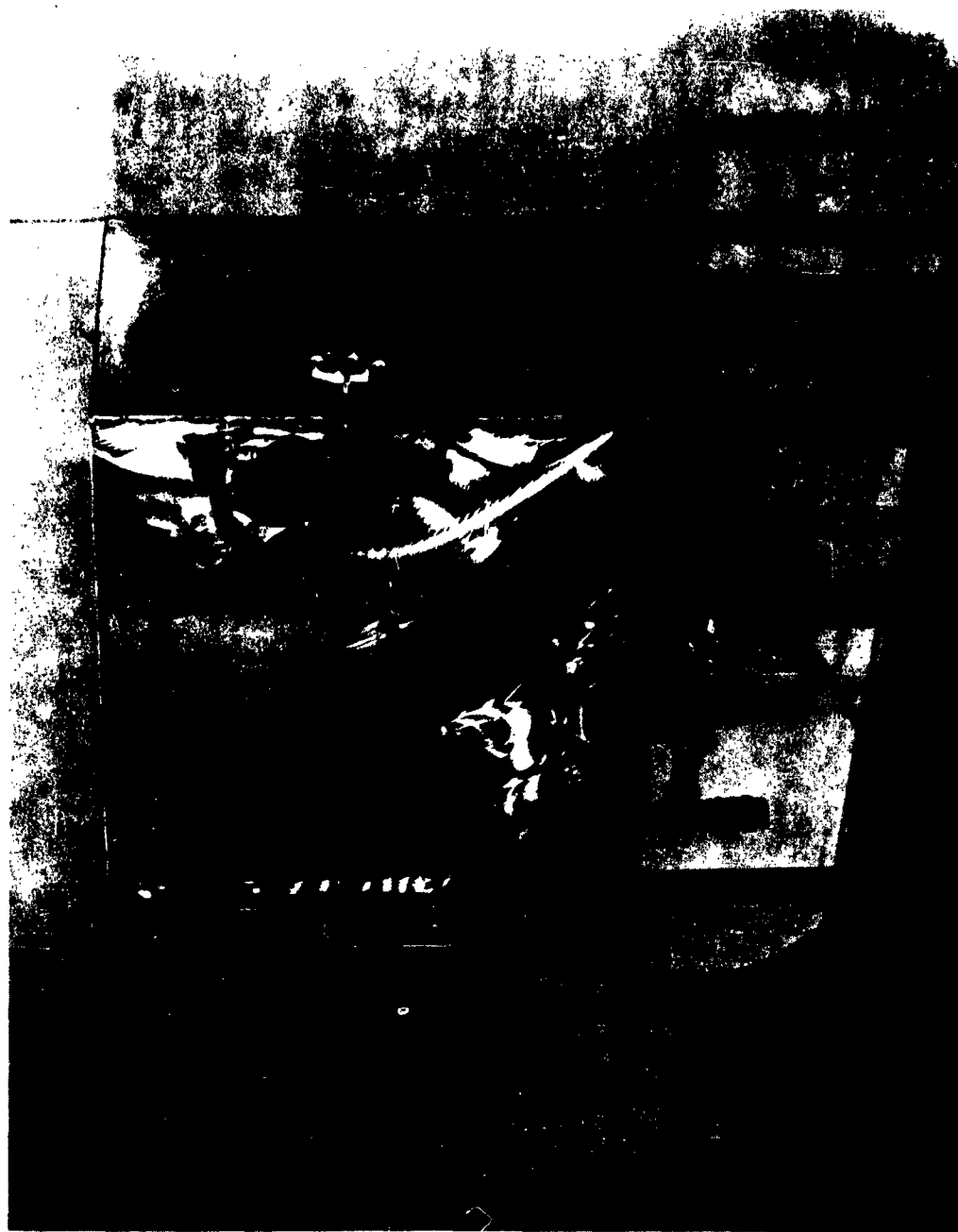Fig. 6. Ultrasonic Cleaning Tank.

Figure 7. Blade Rack.

164

Figure 8. Soak-Rinse Tank.

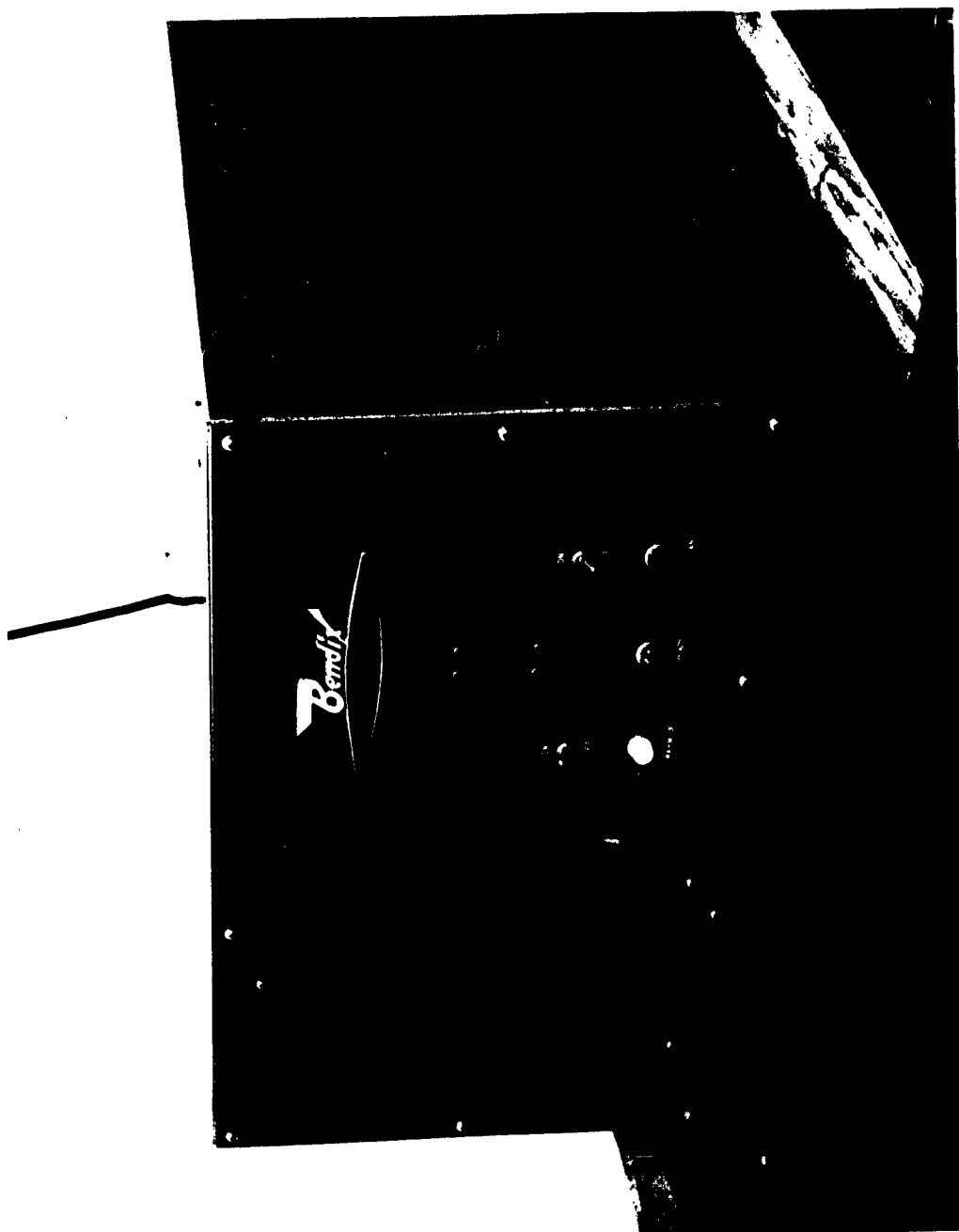Figure 9. International Ultrasonics, Inc. Power Generator.

166

Figure 10. Bendix Ultrasonic Power Generator.

TABLE 1

CLEANING EVALUATION
OAKITE OEM 163-C-195 SOAK -- ULTRASONIC WATER RINSE

Temperature	Soak	Rinse	Remarks
140°F	10 min.	2 min.	Loose carbon deposits on all blades
140°F	12 min.	2 min.	All blades clean
	Minimum Time - 12 Min.		
160°F	6 min.	2 min.	Loose carbon deposits on all blades
160°F	8 min.	2 min.	All blades clean
	Minimum Time - 8 Min.		
180°F	3 min.	2 min.	Loose carbon deposits on large and medium sized blades
180°F	5 min.	2 min.	All blades clean
	Minimum Time - 5 Min.		
200°F	2 min.	2 min.	All blades clean
	Minimum Time - 2 Min.		

TABLE 2

CLEANING EVALUATION
BENDIX DIRL STRIP SOAK -- ULTRASONIC WATER RINSE
CONCENTRATION: 1.5 LB. BENDIX PER GAL. H_2O

Temperature	Soak	Rinse	Remarks
140°F	10 min.	2 min.	Loose carbon deposits on medium sized blades
140°F	12 min.	2 min.	All blades clean
	Minimum Time - 12 Min.		
160°F	9 min.	2 min.	All blades clean
160°F	7 min.	2 min.	Loose carbon deposits on medium sized blades
	Minimum Time - 9 Min.		
180°F	6 min.	2 min.	All blades clean
180°F	4 min.	2 min.	Loose carbon deposits on large size blades
	Minimum Time - 6 Min.		
200°F	2 min.	2 min.	Loose carbon on all blades
200°F	4 min.	2 min.	All blades clean
	Minimum Time - 4 Min.		

168

TABLE 3

CLEANING EVALUATION
TURCO 4181 SOAK -- ULTRASONIC WATER RINSE
CONCENTRATION: 3 LB. TURCO PER GAL. H_2O

Temperature	Soak	Rinse	Remarks
140°F	10 min.	2 min.	Loose carbon on large blades
140°F	12 min.	2 min.	All blades clean
	Minimum Time - 12 Min.		
160°F	9 min.	2 min.	All blades clean
160°F	7 min.	2 min.	Loose carbon on medium and large size blades
	Minimum Time - 9 Min.		
180°F	4 min.	2 min.	Loose carbon on all blades
180°F	6 min.	2 min.	All blades clean
	Minimum Time - 6 Min.		
200°F	4 min.	2 min.	Loose carbon on medium sized blades
200°F	2 min.	2 min.	All blades clean
	Minimum Time - 4 Min.		

TABLE 4

CLEANING EVALUATION
OAKITE OEM 163-C-195 ULTRASONIC SOAK -- WATER RINSE
CONCENTRATION: PREMIXED
TEMPERATURE: 170°F ± 7°

Time	Remarks
8 min.	First and medium stage representatives were clean. Loose carbon deposit left on latter stage representatives.
12 min.	Small amount of loose carbon left on latter stage representatives.
15 min.	All blades clean
	Minimum Time - 15 Min.

TABLE 5

CLEANING EVALUATION
BENDIX DIRL STRIP ULTRASONIC SOAK -- WATER RINSE
CONCENTRATION: 1.5 LB. BENDIX PER GAL. H_2O
TEMPERATURE: 150°F ± 4°

Time	Remarks
6 min.	First and medium stage representatives were clean. Loose carbon deposit left on latter stage representatives.
8 min.	Small amount of loose carbon left on latter stage representatives.
12 min.	Same as 8 minute test.
15 min.	All blades clean.
	Minimum Time - 15 Min.

170

AN EXPERIMENTAL STUDY OF THE CAVITATION PATTERN

OF AN ULTRASONIC TANK HAVING A CLAMPED-CORE

TRANSDUCERIZED DIAPHRAGM

171

PROJECT PERSONNEL

Principal Investigator   Phillip R. Wilcox

INTRODUCTION

After cleaning numerous turbojet compressor blades in an ultrasonic tank, it was noted that the location and orientation of the blade in the tank had a decisive effect upon the effectiveness of cleaning. Obviously there existed an optimum manner of locating and holding the blades in an ultrasonic tank for cleaning. Therefore, a study of the cavitation "field" throughout the volume of cleaning fluid was undertaken to gain information which would aid in the design of holding racks for turbojet engine components.

The transducerized ultrasonic tank being used in these studies has transducers on two sides and the bottom. Since most typical ultrasonic cleaning baths have the transducers on one side only (the bottom), it was decided to study the cavitation field in the tank with only the bottom transducers operative. Also, to eliminate any effects of a vapor barrier at the transducer face, the driving power to the transducers was adjusted to a level such that cavitation could easily be detected throughout the tank. Aluminum foil was immersed in the tank and then searched for cavitation effects to verify the presence of cavitation. Then, under these conditions, pressure maps were made of the entire tank volume to determine the relative cavitation intensity. Such maps can be used to determine the optimum rack construction.

SUMMARY AND CONCLUSIONS

An experimental study was made to determine the relative cavita-
tion intensity pattern in a typical clamped-core magnetostrictive
system. Pressure maps were made of the tank by a piezoelectric trans-
ducer.

The conclusions drawn from this study are:

1. The cavitation intensity is non-uniform at all depths of the
   tank. The highest intensity occurs directly over each indi-
   vidual transducer.

2. Pressure and cavitation maxima occur at multiples of the
   half-wave length.

3. The cavitation intensity is lower over transducers adjacent
   to the walls of the tank.

4. For applications requiring high intensity, the rack should be
   sufficiently small to permit its location in the center of
   the high intensity area. The absolute size would depend upon
   the location of the transducers in a given system and upon
   the pressure maps of the individual system.

ULTRASONIC METAL CLEANING -- QUALITATIVE ASPECTS

"Ultrasonic" is referred to as vibrational waves of a frequency above the hearing range of the normal ear (1).[1] Although the hearing range varies among individuals, the threshold of the ultrasonic range may be taken as about 20,000 cycles per second. The basic mechanism of ultrasonic cleaning is achieved when the liquid cleaning agent is caused to cavitate.

The British engineer and author, Alan E. Crawford (2), shows that nuclei are necessary for intense vapor cavitation. A static surface such as a metal covered with an oil film or some other soil, is obviously a ready source of suitable cavitation centers. With sufficient sound intensity, there will be repeated cavitation bursts immediately adjacent to the surface of the solid material. Therefore, the actual cleaning may result from the very high instantaneous hydrostatic pressures produced by these bursts and subsequent minute high fluid flow velocities. The bursts are thought to "explode" the adhering particles from the solid surface; and when assisted by the alternating and steady liquid flow, the particles are quickly removed from the vicinity of the surface. If the surface tension at the interface between contaminant and work is lowered, this increases the wetting action of the liquid and thus assists in the removal of the foreign particles.

An example of the pressures generated and the time for the cavitation cavity to collapse can be found in Appendix A of this section.

---

[1] Refers to Selected Bibliography for this section.

THEORETICAL CONSIDERATIONS

Two types of sound waves may be transmitted by the transducers --
plane and spherical. In describing sound waves, Mr. B. Carlin (1)
states that "Ultrasonic waves may usually be considered as essentially
plane." A plane wave is one in which the amplitude of motion over a
plane perpendicular to the direction of wave travel is uniform. The
size of the vibrating area and the distance that the waves have
traveled both affect the shape of the wave front. Generally, as the
distance of propagation increases, the wave becomes more nearly plane.

A purely spherical wave is one produced by a point source, from
which the wave spreads out evenly in all directions. The difference
between a plane wave and a spherical wave is illustrated in Fig. 1 (1).

The load placed on the transducer face is determined by the imped-
ance of the water, as seen by the transducer, composed of real and
reactive components. It is the real component, or radiation resistance,
which determines the intensity of sound generated at the transducer face
and propagated into the liquid. (3).

For the case of plane wave transmission, the radiation resistance
for a given medium is a function of time and a single space coordinate.
The result is the well known characteristic impedance, ρ_c, the product
of the density and the velocity of sound in the medium. Hence, as long
as plane wave transmission exists, there will be no reactive component.
A representative value of the characteristic impedance of water is

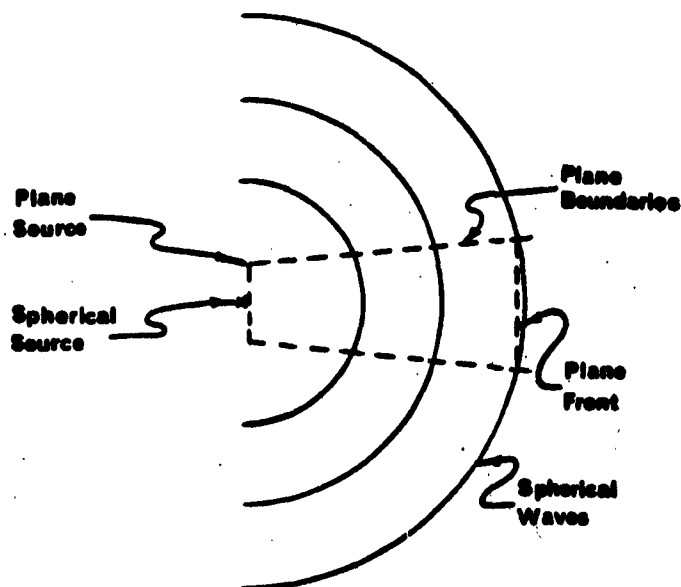$1.43 \times 10^5 \frac{dyne\text{-}sec}{cm^3}$ (2).

Fig. 1.   Path of Plane and Spherical Waves.

Transmission into an Enclosed Medium

The preceding theory has been based on transmission into a semi-infinite medium, commonly called a free field in which the wave form is not complicated by reflection or refraction.

In the case of the wave being transmitted into a closed medium, both of these phenomena are present to such an extent that the impedance cannot be determined analytically.

Consider a tank with a transducer in the bottom, as shown in Fig. 2, with plane waves transmitted into the liquid. It will be impossible to have pure plane wave transmission. Therefore, as the waves strike the vertical walls there will be a combination of reflection, refraction, and transmission due to the mismatch at the interface of the liquid and wall, and the angle of incidence of the wave. The impedance mismatch

177

is determined by the ratio of complex impedances of the medium forming the interface. The Russian author, O. I. Babikov (5), gives the energy loss at the interface due to reflection in the form

$$\Delta I = 1 - \frac{4 R_1 R_2}{(R_1 + R_2)^2}$$

where $R_1 = \rho_1 C_1 =$ impedance of the first medium

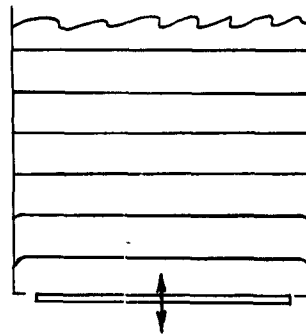 $R_2 = \rho_2 C_2 =$ impedance of the second medium.

Fig. 2. Plane Wave Propagation.

From this, it can be concluded that the reflectivity does not depend upon the way in which oscillations are propagated from the first medium to the second. For water-steel interface, about 12% of the energy is transferred through the interface into the steel. The energy which enters the walls encounters an even greater mismatch at the steel-air interface. The value of this energy transfer as given by Babikov (5) is approximately 0.04%. Since the walls cannot be

178

entirely rigid and have little sound absorption capacity, their internal impedance is almost purely reactive; and they act as secondary sound sources. (6). Still another complication is the fact that the walls, as solids, are capable of supporting shear waves whereas the liquid is not.

As the incident sound waves strike the liquid-air interface, they will be almost completely reflected. The results of this reflection from the surfaces is a complete scattering of sound energy throughout the liquid. The reflected wave will be 180° out of phase with the incident wave. The results of this may be addition of the incident and reflected waves at a particular point and time, or it may be complete cancellation at another point. This results in a totally unpredictable sound field and experimental means must be employed to determine the radiation pattern of the driving transducer into a given enclosed medium (4).

EXPERIMENTAL EQUIPMENT AND PROCEDURES

Schematics of the system with associated instrumentation and the
tank are shown in Figs. 3 and 4. Figs. 5, 6, and 7 are photographs of
the power generator, the bottom transducerized diaphragm of the tank,
and the instrumentation used to monitor the power input to the trans-
ducers.

System Design

The tank, made of 12 gage stainless steel, was designed so that
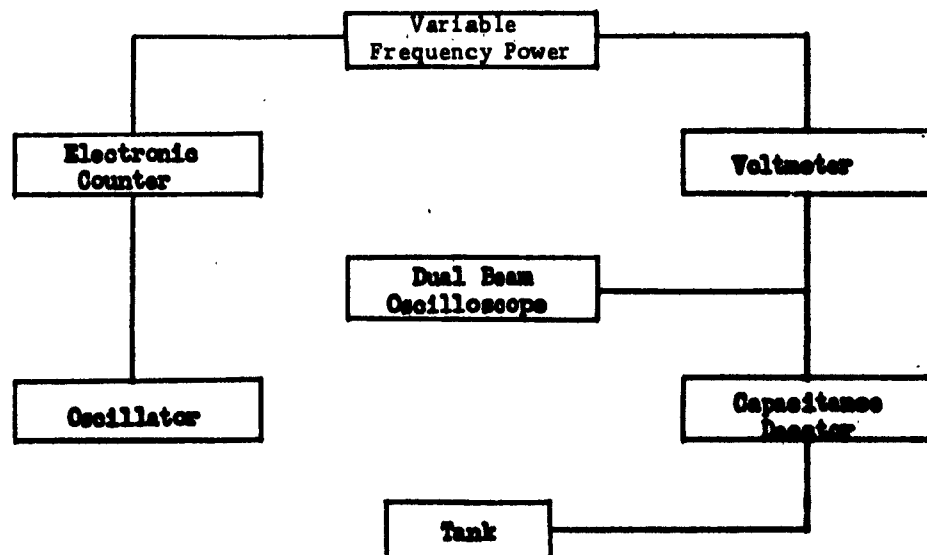transducer plates could be mounted on two sides as well as the bottom.

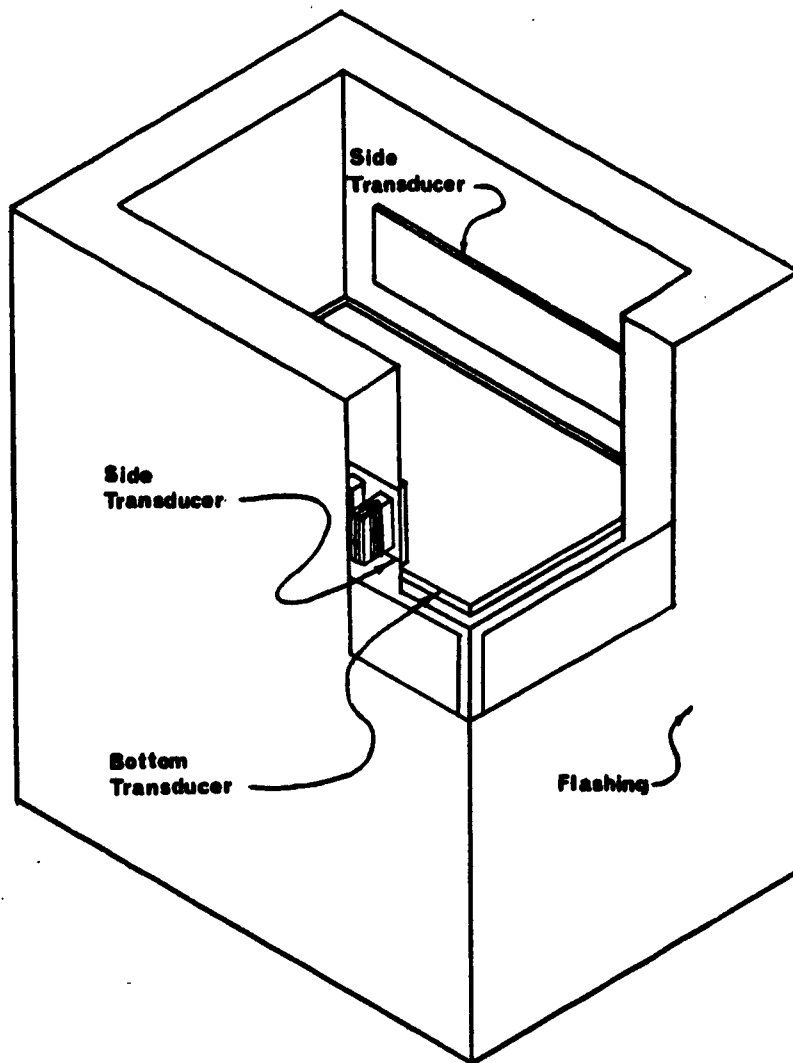Fig. 3. System and Related Instrumentation Schematic.
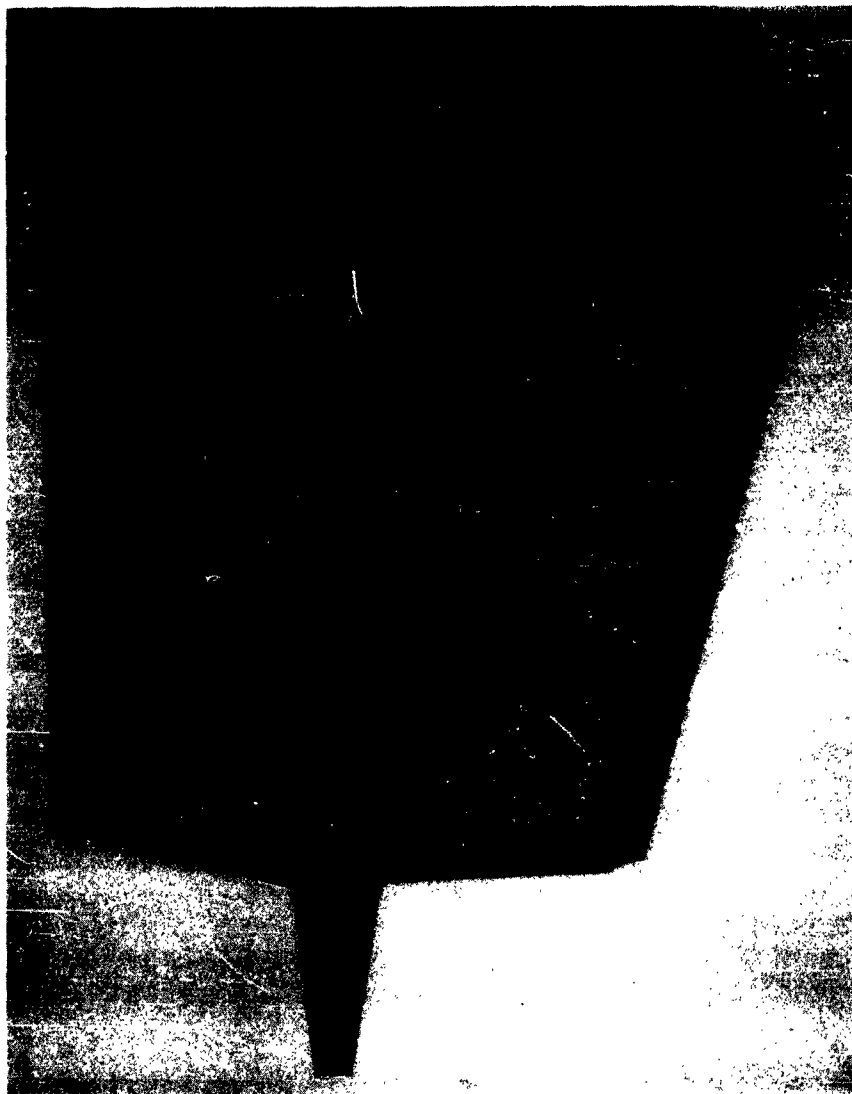
Figure 4: Schematic of Tank and Flashing

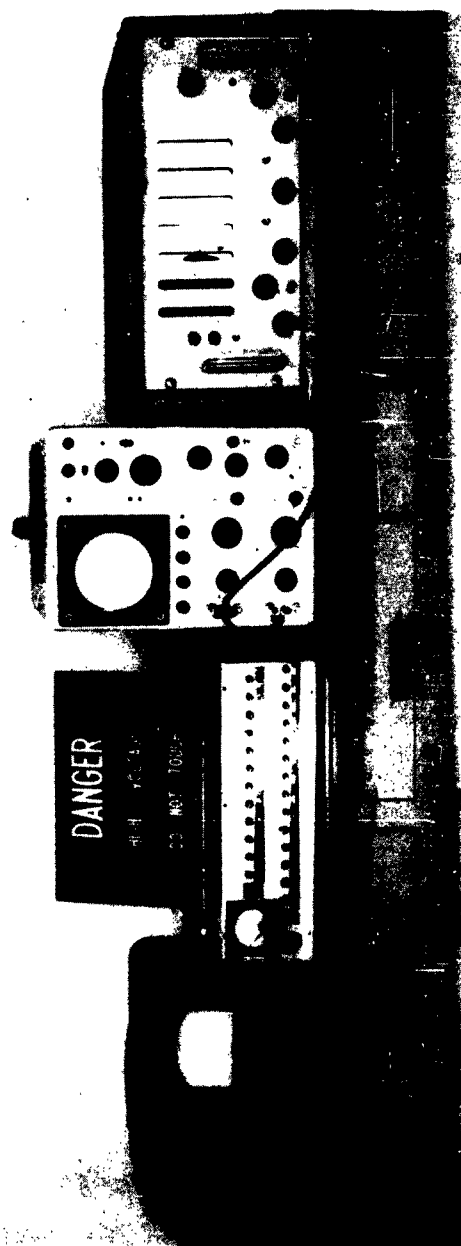Fig. 5. Power Generator

Figure 6   Bottom Plate of Transducers

183

Fig. 7. Related Instrumentation.

DANGER

184

However, only the bottom plate of transducers was utilized in this investigation. A means of controlling the temperature of the liquid was accomplished by installing an immersion heater.

A separate flashing was used to enclose the outside of the tank. providing protection as well as a cooling duct. At normal power levels, no cooling is needed; but at high levels, air cooling can be used.

Procedure

Referring to the schematic of Fig. 3, the power input to the bottom transducers was monitored. Only enough power was used so that vapor bubbles could be detected throughout the liquid.

For reference, the surface was divided into forty-eight smaller areas. These areas and associated position of each transducer are illustrated in Fig. 8.

6	7	18	19	30	31	42	43
5			20	29			44
4			21	28			45
3			22	27			46
2			23	26			47
1	12	13	24	25	36	37	48

Fig. 8. Division of the Surface and Related Transducers.

The intensity at each coordinate, Fig. 9, was obtained by positioning a 0.75 inch diameter immersible transducer with a natural frequency of 5 megacycles in the center of each area and perpendicular to the transducer face, Fig. 10. The pickup transducer was connected to an oscilloscope, Fig. 11, from which the peak-to-peak amplitude was read and recorded.

An example of the signal received at different locations by the oscilloscope is illustrated in Appendix B.

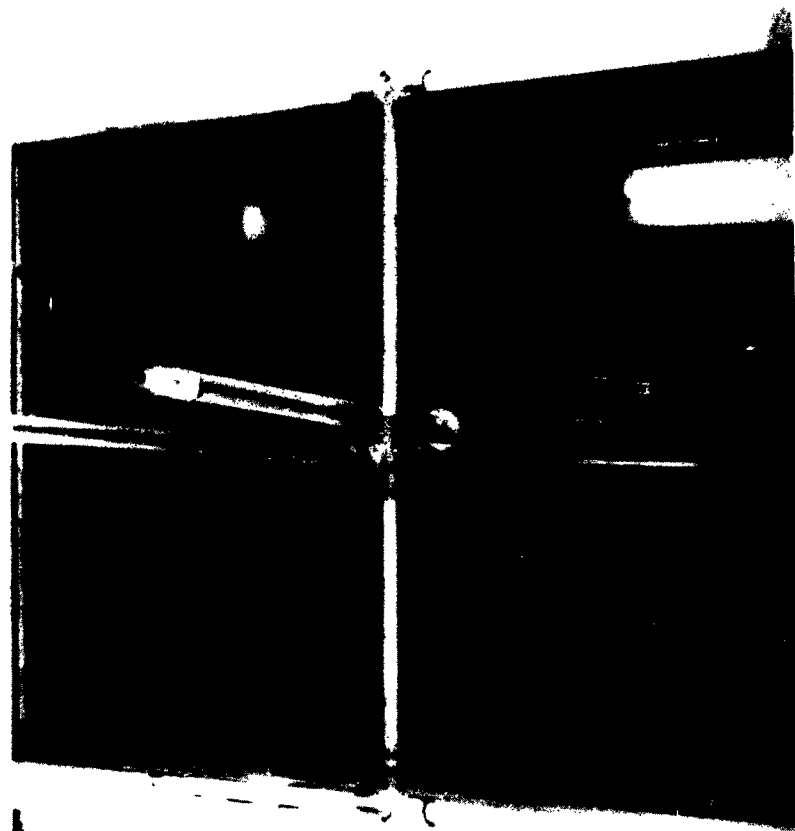| Top |
|---|
| 2.3" |
| 4.6" |
| 6.9" |
| 9.2" |
| Transducer Plate |

Fig. 9. Depth Division.
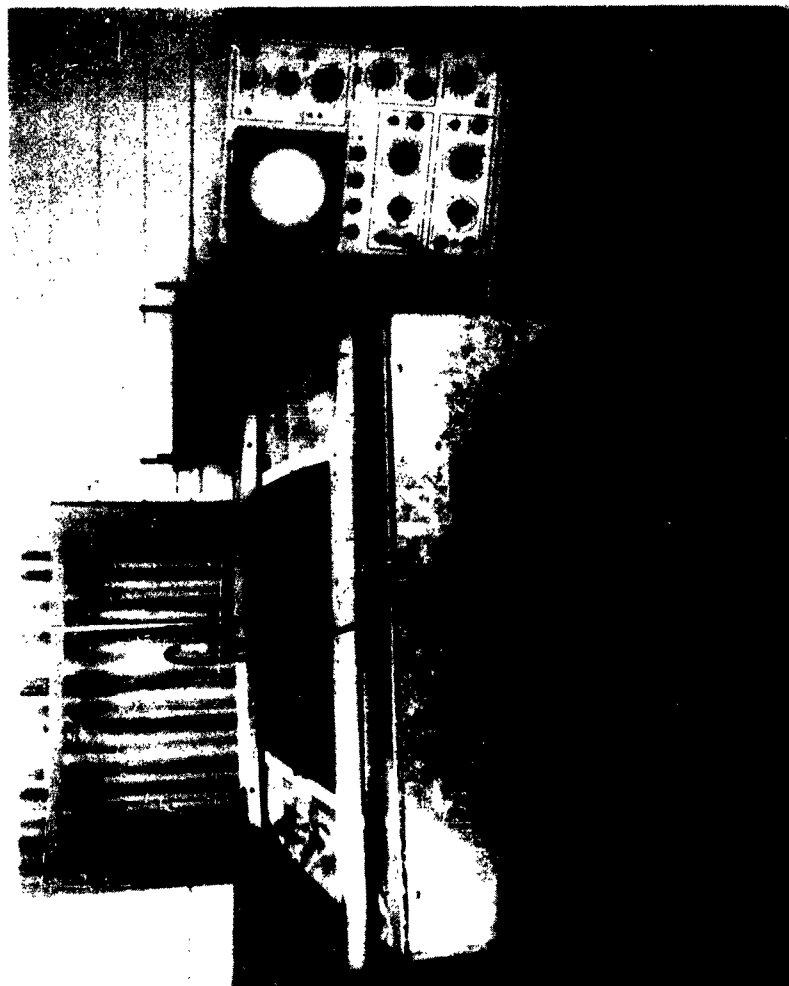
Fig. 10. Positioning of Transducer System.

187

Fig. 11. Transducer System with Oscilloscope.

TABLE 1

NORMALIZED INTENSITY DATA

Cell	Top Layer	2.3" Layer	4.6" Layer	6.9" Layer	9.2" Layer
1	0.710	0.62	0.41	0.50	0.40
2	0.96	1.05	0.68	0.85	0.70
3	1.07	1.25	0.90	0.93	1.04
4	0.77	0.90	0.80	0.85	0.77
5	0.70	0.70	0.69	0.58	0.65
6	0.37	0.55	0.55	0.41	0.51
7	0.43	0.70	0.70	0.71	0.53
8	0.53	0.50	0.95	0.75	0.95
9	0.86	0.52	1.45	1.03	0.95
10	1.10	1.05	1.55	1.00	0.90
11	1.04	1.03	1.45	0.98	1.03
12	0.75	0.70	1.03	0.70	0.83
13	0.84	0.83	0.95	0.80	1.13
14	1.12	1.15	1.43	0.97	1.20
15	1.10	1.17	1.40	1.15	1.03
16	1.10	1.03	1.48	0.91	1.23
17	0.85	0.57	1.15	0.86	1.15
18	0.25	0.35	0.68	0.58	0.56
19	0.30	0.30	0.50	0.45	0.60
20	0.93	0.73	1.45	0.60	1.13
21	1.00	1.23	1.30	0.68	1.40
22	1.25	1.25	1.30	1.11	1.70
23	1.12	1.13	1.30	0.98	1.56
24	0.87	0.85	1.15	0.71	0.90
25	0.93	0.83	1.28	0.70	1.00
26	1.08	0.97	1.20	1.10	1.68
27	1.40	1.23	1.30	1.05	1.70
28	1.16	1.02	1.50	0.68	1.58
29	0.92	0.47	1.55	0.82	1.18
30	0.22	0.30	0.55	0.53	0.77
31	0.20	0.22	0.45	0.35	0.70
32	0.83	0.70	1.13	0.85	1.15
33	1.10	0.90	1.55	0.86	1.15
34	1.40	1.20	1.43	1.06	1.30
35	1.12	1.10	1.45	0.95	1.41
36	1.02	0.92	1.28	0.82	0.76
37	0.75	0.65	0.98	0.40	1.10
38	0.82	0.50	1.41	0.80	0.86
39	1.10	0.75	1.45	0.98	0.95
40	1.05	0.56	1.50	0.75	1.25
41	0.95	0.85	0.60	0.78	1.40
42	0.38	0.48	0.45	0.55	0.65
43	0.40	0.38	0.55	0.52	0.25
44	0.70	0.65	0.80	0.40	0.82
45	1.00	0.85	0.70	0.53	1.18
46	1.15	0.95	1.10	0.70	1.37
47	1.00	0.80	1.00	0.65	1.20
48	0.65	0.70	0.40	0.65	0.55
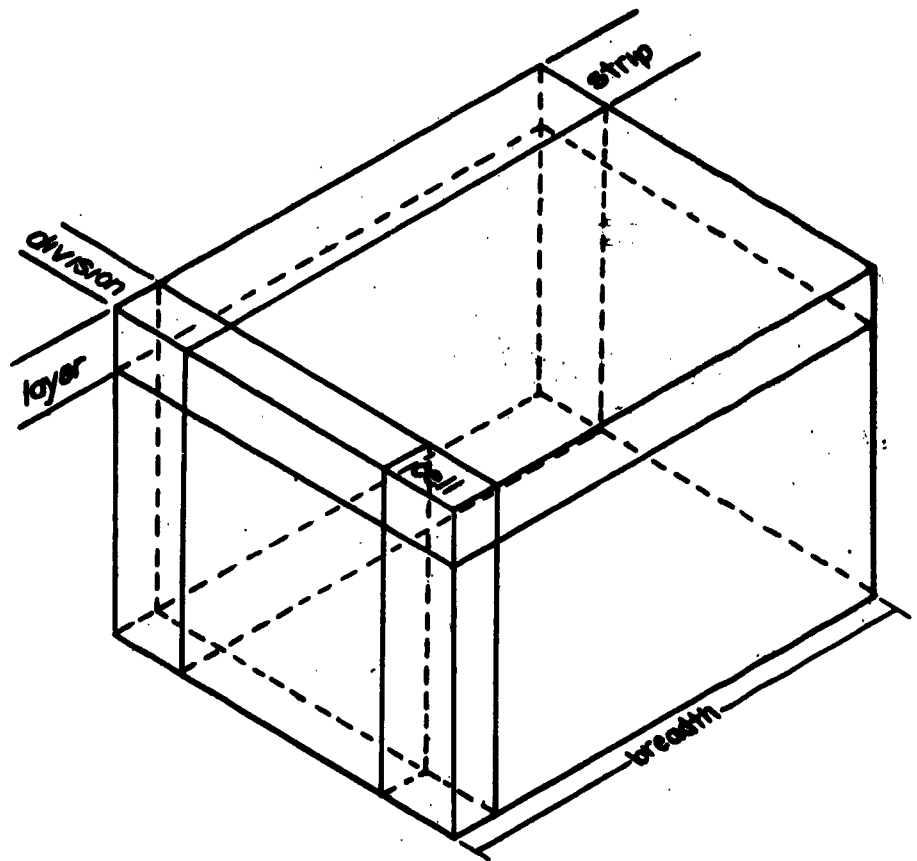
Figure 12. Reference System.
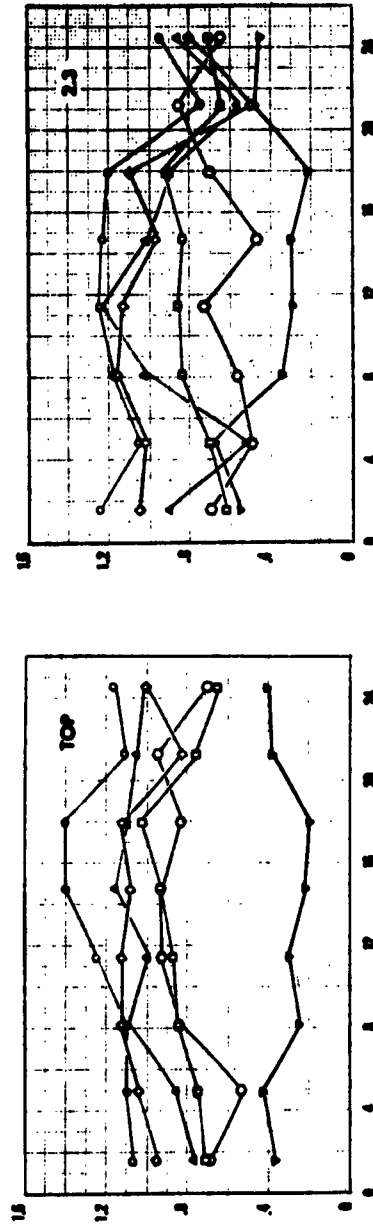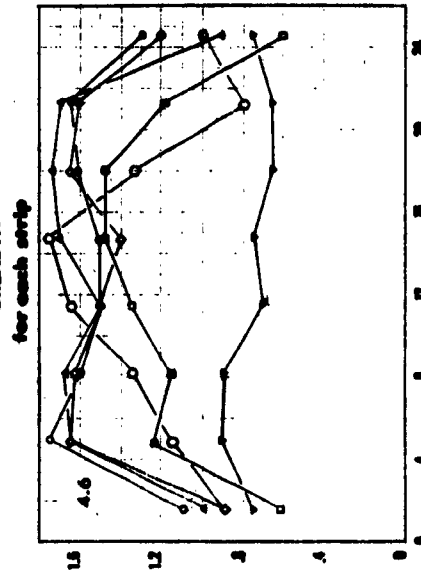
Figure 13.   Intensity Distribution for the Top, 2.3, and 4.6 Layers.
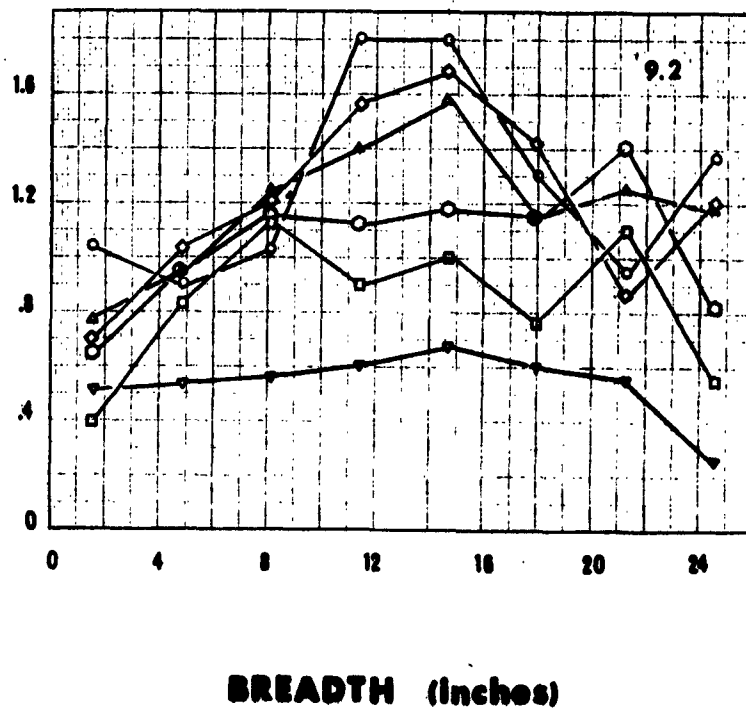
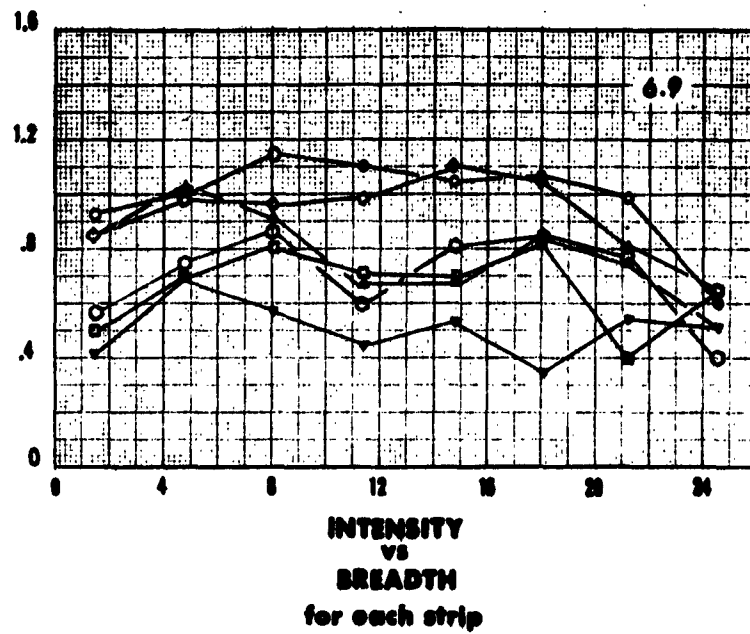BREADTH (inches)

INTENSITY

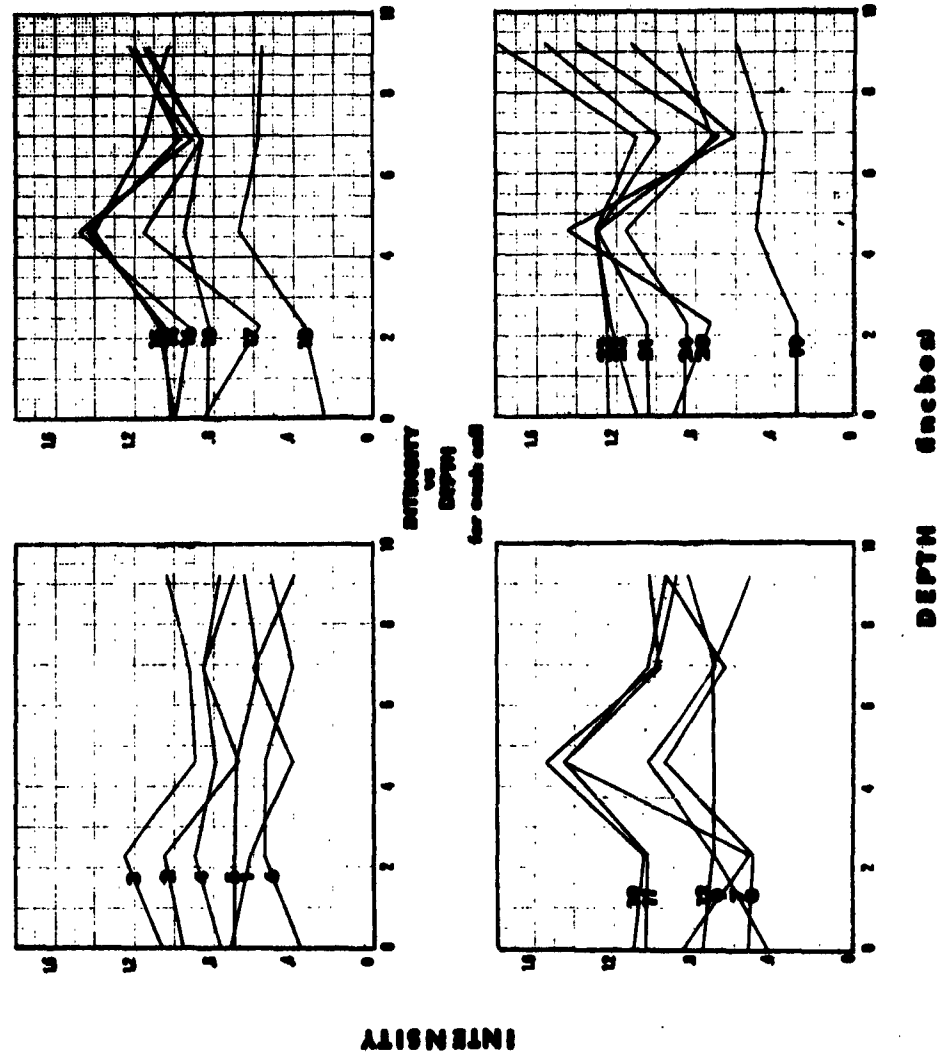Figure 14: Intensity Distribution for the 6.9 and 9.2 Layers.

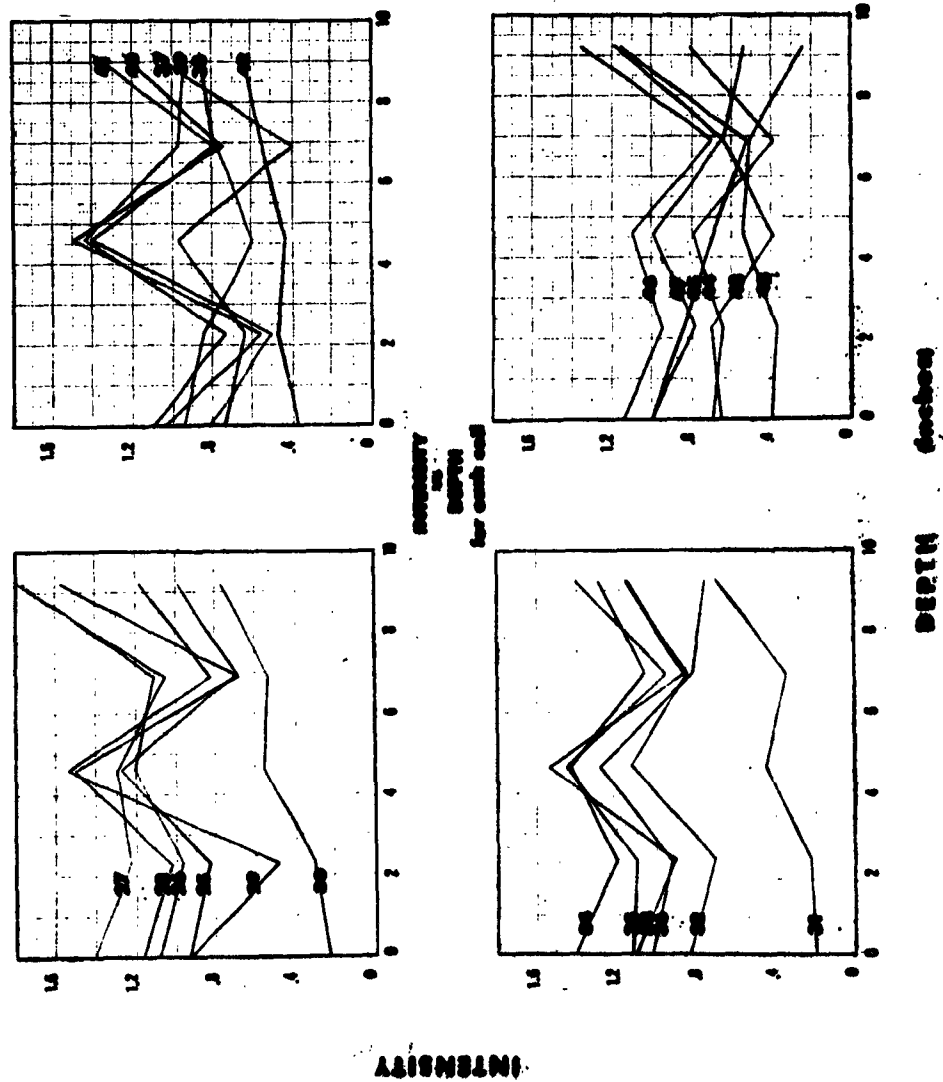Figure 15: Intensity Distribution for Cells 1 thru 24.

193

Figure 16: Intensity Distribution for Cells 25 thru 48.

DISCUSSION OF RESULTS

For this study, the normalized intensity points were joined by straight lines. Since only the relative intensity of one section with respect to another was desired, the normalized intensity instead of the intensity was plotted. To make the discussion of the intensity[2] patterns more meaningful, the volume has been subdivided into cells, layers, divisions, and strips, Fig. 12.

The data, Table 1, represent the average intensity of several different complete test runs, and the results have been presented in two different ways. The first being a plot of the intensity vs the depth level for each strip - Figs. 13 and 14. The second was to plot the intensity vs the depth of each cell - Figs. 15 and 16.

With reference to Figs. 13 and 14, the intensity is noted to follow a general pattern. This pattern is one in which the intensity is lower at the boundaries than in the central area. It was also noticed that at all levels the intensity of cells 6, 7, 8, 18, 19, 30, 31, 42, and 43 was somewhat lower. The cause of this lower intensity was attributed to the reflection, refraction, and absorption of the energy by the immersion heater which lay along this wall. At each level, there is a general band of intensity. In some instances, the band of intensity is almost plane while in others it tends toward a spherical shape. The

---

[2] Hereafter, intensity will be used for normalized intensity unless otherwise stated.

195

wave surfaces mentioned here refer to the two-dimensional case.

The 9.2" layer always had the greatest intensity. This is to be expected since it was the layer closest to the transducer face. However, this layer also had the most spherical shape for its band width of intensity. The 4.6" layer had the next highest intensity and at the same time tended more toward a plane shape than a spherical shape. The remaining layers are all of about the same intensity and are essentially plane, away from the tank boundaries.

With reference to Figs. 15 and 16, it was noted that here again the intensity tended toward a band for each division. It was also noted that the corner cells had lower intensity than the adjacent cells, and the center cells were the most intense of all.

SELECTED BIBLIOGRAPHY

1. Carlin, B., _Ultrasonics_, McGraw-Hill Publishing Co., Inc., New York, 1949.

2. Crawford, A. E., _Ultrasonic Engineering_, Butterworths Scientific Publications, London, 1955.

3. Hueter, T. F., and R. H. Bolt, _Sonics_, John Wiley and Sons, Inc., New York, 1955.

4. Burkhart, M. C., "A Study of Cavitation in Water as Produced with Low Frequency Sound Energy," M.S. Thesis, Oklahoma State University, Stillwater, Oklahoma, 1959.

5. Babikov, O. I., _Ultrasonics and Its Industrial Applications_, Consultants Bureau, New York, 1960.

6. Fay, R. D., R. L. Brown, and O. V. Fortier, "Measurement of Acoustic Impedances of Surfaces in Water," _The Journal of the Acoustical Society of America_, Volume 19, No. 5, 1947.

7. Rayleigh, J. W. S., "Pressure due to Collapse of Bubbles," _Philosophical Magazine_, Volume 34, 1917.

8. Silver, R. S., "Theory of Stress due to Collapse of Vapor Bubbles in a Liquid," _Engineering_, Volume 154, 1942.

APPENDIX A

PRESSURES DEVELOPED BY THE COLLAPSE OF A SPHERICAL BUBBLE

Simplified calculations for the forces developed by the collapse of a spherical bubble are given by Lord Rayleigh (7). With a starting radius, r_o, in a liquid of density, ρ, and under a hydrostatic pressure, P_o, the pressure developed in the liquid rises to a high value as the cavity volume decreases. At any time when the radius has decreased to the value r, the pressure is a maximum in the liquid at a distance $r^{3}\sqrt{4}$ and at this point is equal to

$$P = P_o(4)^{-4/3}(r_o/r)^3.$$

For example, if the bubble is initially empty in water at atmospheric pressure, a decrease to one twentieth of its original diameter will give a pressure of 10,300 atm. The time taken for complete collapse is

$$T = 0.915 r_o(\rho/P_o)^{\frac{1}{2}}$$

when P_o is in dyne/cm^2. In water at ordinary temperatures, a cavity 0.1 mm in diameter requires about 5 microseconds to vanish.

More elaborate calculations have been made by R. S. Silver (8),in which consideration is given to the saturated or unsaturated vapor of the liquid contained in the cavity. Also, since the vapor is heated by the compression, heat is lost to the liquid. The effects of viscosity and pressure of permanent gas in the cavity are not included.

The pressure caused by the collapse of a bubble is given by

$$P_s = KP \frac{V_s}{V_w} \left[1 + \frac{3S}{Pr_o} \left(1 - \frac{V_w}{V_s} \right) \right]^{\frac{1}{2}}$$

where $P = P_e - P_o$ = applied pressure - average saturation pressure

V_w = specific volume of the liquid

V_s = specific volume of the vapor

k = bulk modulus of the liquid

r_o = initial radius

S = surface tension.

The pressure has been calculated for water containing a large number of these bubbles collapsing simultaneously near the boundary of a solid. For example, if the cavities are larger than about 10 cm in diameter, the pressure at the solid is about 1,000 atm. From the above equation, it can be seen that as the radius of the bubble decreases the pressure will increase.

199

APPENDIX B

SAMPLE OF THE SIGNAL

RECEIVED BY THE

OSCILLOSCOPE

Fig. 17. Sample of Signal Received in Areas
of Lower Intensity.

Fig. 18. Sample of Signal Received in Areas
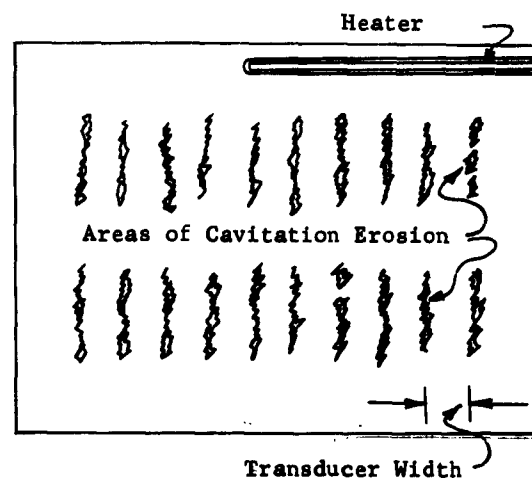of Highest Intensity.

201

APPENDIX C

EROSION PATTERNS IN DRIVER PLATE

Fig. 19. Aluminum Foil Tests Interpretation Schematic.